Urban Wind Power Assessment:
A Study of Winds over the Near Surfaces of Buildings in San Francisco

By

Bethany Kay Kuspa
B.S. (University of California, Davis) 2001

THESIS

Submitted in partial satisfaction of the requirements for the degree of

MASTER OF SCIENCE

in

Mechanical and Aeronautical Engineering

in the

OFFICE OF GRADUATE STUDIES

of the

UNIVERSITY OF CALIFORNIA

DAVIS

Approved:

____

____

____

Committee in Charge

2006

Acknowledgements

The author wishes to thank Cal Broomhead of the San Francisco Department of Energy, Environment Group, for his communications and input, and Chuck Bennett and ESA for allowing access to their models of San Francisco for use in this study's wind-tunnel testing.

Table of Contents

Table of Figures

Table of Tables

Abstract

This project is a preliminary investigation of the wind resource in urban areas. Five buildings in two separate locations within the city of San Francisco were chosen to assess near surface winds on buildings by means of wind-tunnel testing in the Atmospheric Boundary Layer Wind Tunnel at the University of California, Davis. Three buildings, Fox Plaza, the CSAA Building and the Bank of America Building, located near 10th Street and Market Street, were tested for two settings: existing, which includes existing buildings and approved developments in the area, and cumulative, which includes proposed development projects and gives an idea of what the city might look like in the near future. Two buildings near Folsom Street and Main Street were wind-tunnel tested for the existing setting only.

It was shown that the wind over all of the buildings tested near 10th Street and Market Street averaged “good”, over 400 Watts per square meter, or “great”, over 700 Watts per square meter, average wind power density values for both existing and cumulative settings, and the two buildings near Folsom Street and Main Street had average values of 235.07 and 232.73 Watts per square meter.

Executive Summary

Introduction

This project is a preliminary investigation of the wind resource in urban areas. Five buildings in two separate locations within the city of San Francisco were chosen to assess near surface winds on buildings by means of wind-tunnel testing in the Atmospheric Boundary Layer Wind Tunnel at the University of California, Davis. Three buildings, Fox Plaza, the CSAA Building and the Bank of America Building, located near 10th Street and Market Street, were tested for two settings: existing, which includes existing buildings and approved developments in the area, and cumulative, which includes proposed development projects and gives an idea of what the city might look like in the near future. Two buildings near Folsom Street and Main Street were wind-tunnel tested for the existing setting only.

The surfaces of the buildings, including locations spread out over the faces and corners of the building, rooftop perimeters and specific elevations above certain rooftop locations were analyzed and average wind power densities were calculated for each location measured on the building.

Purpose

The need to utilize renewable energy resources is continually growing. California has already enacted an initiative to dramatically increase its use of renewable energy sources, including wind, to 20% of all electric energy usage by 2017. Potential current and future difficulties transmitting energy from the rural locations of many sources of renewable energy make it ideal to find sources of renewable energy close to the areas of maximum usage, which include urban areas. Thus, the utilization of wind energy in urban areas is of rapidly growing interest; but, there is a lot of work left to be done before *wind energy converters*, or WECs, can be successfully integrated into an urban environment.

The purpose of the study is not to evaluate any specific type of WEC; however, power curves from specific WECs are necessary to predict power production and energy capture and are used to obtain preliminary results. Various WECs for urban settings are discussed for informational purposes only.

Project Objectives

The objective of this study is to gain a further understanding of the wind resource in urban environments, thus expanding the possibilities of wind energy utilization in urban areas. This study focuses on a specific city, San Francisco, by examining the wind flow over five buildings at two different sites, measuring wind over various locations near the surfaces, corners, rooftop perimeters and elevated points around the rooftop of each building. All five buildings were assessed with surrounding buildings as they exist today, or including recently approved projects in the city where construction is imminent. In addition, three buildings at one of the sites were also analyzed in a setting that is based off of potential future development plans in the city, showing how the wind, and with it wind power potential, could change with future construction around the site.

Project Outcomes

It was shown that all of the buildings tested near 10th Street and Market Street averaged “good”, over 400 Watts per square meter, or “great”, over 700 Watts per square meter, average wind power density values for both existing and cumulative settings, and the buildings near Folsom Street and Main Street had much lower average values of approximately 234 Watts per square meter. The measurement locations yielding the highest average wind power densities were typically on the perimeter of the rooftops and the space above the roof for all buildings.

Building development in San Francisco around the sites had varying effects on the wind characteristics of each building. In some cases, developments increased the average wind power densities for many measurement locations; in others, is lowered the average wind power density values for many measurement locations. All buildings experienced locations of increasing and decreasing average wind power density values.

Conclusions

Wind-tunnel testing showed that the best place to place WECs is on or above the roof level of a given building. While a few general trends such as this were found, it was also shown that each building had its own specific set of wind characteristics, leading to the conclusion that testing of specific sites should be recommended if it is desired to incorporate WECs into that building's design.

Recommendations

In order to gain a more general understanding of wind over the surface of a building in an urban environment, it is recommended that more buildings be wind-tunnel tested to get a better sampling of possible wind conditions for different kinds of urban cityscapes. With enough information, it may be possible to find ways to further generalize wind characteristics of certain types of cityscapes and building configurations. Other urban areas, besides San Francisco, may also be studied in the wind tunnel to further expand knowledge of wind patterns in an urban environment.

Urban environments have the potential to provide a suitable wind energy resource, provided that turbulence effects, if proven to be a problem with current of future designed WECs, can be mitigated. A closer look into how turbulence can affect urban WECs is advised.

One way to improve the data obtained from wind-tunnel testing in the future is to implement the use of a 3-D probe.

Benefits to California

With a better understanding of winds on the surfaces of buildings in an urban area, more effective WECs can be developed for and therefore utilized in urban areas. This would help California meet its goal of having 20% of its electric energy produced as renewable energy by 2017 and could cut down on transmission problems if utilized effectively.

1.0 Introduction

The need to utilize renewable energy resources is continually growing. California has already enacted an initiative to dramatically increase its use of renewable energy sources, including wind, to 20% by 2017. Thus, the utilization of wind energy in urban areas is of rapidly growing interest; however, there is a lot of work left to be done before *wind energy converters*, or WECs, can be successfully integrated into an urban environment.

The objective of this study is to gain a further understanding of the wind resource in urban environments, thus expanding the possibilities of wind energy utilization in urban areas. This study focuses on a specific city, San Francisco, by examining the wind flow over five buildings at two different sites, measuring wind over various locations near the surfaces, corners, rooftop perimeters and elevated points around the rooftop of each building. All five buildings were assessed with surrounding buildings as they exist today, or including recently approved projects in the city where construction is imminent. In addition, three buildings at one of the sites were also analyzed in a setting that is based off of potential future development plans in the city, showing how the wind, and with it wind power potential, could change with future construction around the site.

This report covers the findings in the wind-tunnel study conducted in the Atmospheric Boundary Layer Wind Tunnel at the University of California, Davis. Results include average wind power density calculations for each measured location based on San Francisco's wind data, and potential power output calculations for various types of WECs. From this information, recommendations on where to site anemometers around the sites in this study are made.

The purpose of the study is not to evaluate any specific type of WEC; however, power curves from specific WECs are necessary to predict power production and energy capture and are used to obtain preliminary results. Various WECs for urban settings are discussed for informational purposes only. Please note that large tables and figures, as referred to in the text of this study, are located at the end of their respective sections or sub-sections.

1.1 Background on Urban Wind Energy Converters

Great interest in wind energy has led to much advancement, however most wind energy production occurs in rural areas, where energy transmission can be difficult and costly. It may be possible for some of these issues to be mitigated by placing WECs at the site of demand, which would include urban areas. Unfortunately, other issues may be created by locating WECs in an urban environment, most of which are not yet fully evaluated. These issues may include noise, visual impacts, electromagnetic interferences and various safety concerns. While there are not many studies as to these impacts in an urban area, studies conducted regarding rural areas can be analyzed and related to potential urban impacts. The objective of this study is not to fully assess the effects WECs may have on their surrounding environments; however, it is important to be aware that the wind resource is not the only issue affecting the choice of site for a WEC in an urban environment.

One way of siting potential WECs is by utilizing a wind tunnel to survey sites in cities. The wind tunnel will allow for data collection in a compressed time, as well as a future look into the changes that will occur as the urban area changes.

1.1.1 Typical Horizontal Axis Turbines in an Urban Environment

While horizontal axis turbines are the predominant WEC here in the United States, most are placed in rural areas. Some of the effects of these wind turbines on their environment include visual impacts, seismic issues, electromagnetic interference, noise impacts and disturbance to avian life. Locating large horizontal axis turbines away from the population significantly lowers the weight of these effects, while locating these devices near an urban area may require significant mitigation of these issues.

Visual Impacts

The visual impact of a wind turbine or farm is the most difficult to quantify because it is the most subjective impact on the environment. There have been several studies on the design aspect of wind turbines that lead to many design ideas that could aid in the reduction of visual disturbance caused by wind energy systems (Manwell 2003). One of the major advantages of placing wind turbines in urbanized areas, however, is that the WECs would not intrude on naturally visually pristine areas. This does not mean that the visual impact is negligible; more people will be subjected to the visual impact of an urban wind farm simply due to its proximity to people. It may be possible, however, to blend technology into a building's architecture, making it aesthetically pleasing and interesting.

One of the more interesting issues that causes a visual disruption are the opposite spinning of rotors, and it is suggested that wind turbines be sectioned by spin direction. Light pollution is also a concern, and lights on turbines should be restricted to aircraft safety. Running power cables and transmission lines underground or coupling them with roads will minimize visual obstructions in rural areas (Manwell 2003). Luckily, most of these issues do not appear to be as significant in an urban area due to the many light sources and power lines already in existence. The movement patterns of a WEC will still need deeper considerations and studies.

While flickering shadows caused by the rotating blades can be a source of annoyance, it will only occur for a few minutes at a time and only at certain times of the day. Manfred (1991) suggests that residents close their blinds when affected. It is difficult to say whether residents will even entertain this suggestion, however; any infraction into residents' daily lives is usually met with severe resistance, supporting the need for further studies into visual impact issues in residential/urban areas.

Seismic Issues

Buildings are constantly undergoing seismic analyses, and the addition of a WEC to an existing building may meet with concern. An analytical study was done on wind turbines being placed on building rooftops, showing that a time domain analysis for seismic issues can yield significant benefits over sole analysis in the frequency domain.

Witcher (2004) states that by correctly applying earthquake analysis from buildings to wind turbines and performing that analysis in the time domain, the "aeroelastic interaction of the dynamic motion of the wind turbine structure with both the wind loading action on the rotor blades and the response of the turbine controller can be modeled." It also is shown that, for a parked turbine, the combination of a high wind speed and a seismic event may cause loads higher than if the turbine were operating. A study consisting only of a frequency domain analysis would not have shown this due to the incorrect modeling of the damping of the turbine (Witcher 2004).

Yet another advantage is that the safety system and controller's influence are modeled correctly in the time domain. If nacelle acceleration causes the turbine to shut down, the effects of the shutdown, from operation to idle or parked status, can be correctly modeled. It is important to note that analyses done in the time domain have yielded results similar to those from a frequency domain analysis (Witcher 2004). If a wind turbine is to be placed on top of a building, it should be possible to model seismic events effectively.

Electromagnetic Interference

Electromagnetic interferences may be of significant concern in an urban area. While such interference can already be disruptive in a rural area, the disturbance does not affect many people. When moving to an urban environment, however, the number of signals jumps up dramatically. Just how electromagnetic wave transmission will be affected in such a complex area is not yet fully understood. Studies in rural areas, however, shed some light on some issues expected to occur in urbanized areas, though most studies have also been conducted solely on wind turbines, and may not apply to other WECs.

Many of the actual or potential effects of wind turbines on electromagnetic waves have either been observed in the field or in a laboratory, or have been worked on analytically. Broadcast television interference has been reported as a slight wiggle of the picture in frequency with the passing of each blade through the signal at every rotation (Manwell 2003). This effect may be exaggerated by the use of metal blades, and may be minimized by current fiberglass technology. FM interference has only been observed in laboratories, and is characterized by a background hiss. This interference was determined to occur within tens of meters from the turbine, which might not be a large affect in a rural wind farm, yet could be a significant problem for an urbanized wind farm (Manwell 2003).

Certain aircraft navigation and landing systems, such as VOR (VHF omni directional ranging) are affected by stopped wind turbines, yet are relatively unaffected by operating turbines; as a result, wind turbines (and other structures of similar size) have been disallowed within one kilometer of a VOR station. Analytical studies have shown a significant effect of wind turbines on microwave links, where the turbine interferes with the microwave's modulation. Cellular phones are expected to be minimally affected due to their already mobile nature, and satellite signals should not be affected due to their elevation and antenna gain (Manwell 2003).

Since the problem of electromagnetic interference is so complex, each wind site will require its own evaluation. A typical evaluation includes locating radio and television (or other) transmitters and receivers in the general vicinity of the turbine, which can be difficult since it is rare for a central registry of all transmitters in an area to exist. Mobile transmitters and part-time transmitters must also be accounted for, as well as emergency services and air craft transmitters. Interference zones must then be identified, and if the turbine is set to be located inside an interference zone, further study will need to be conducted. Some solutions to interference are to better direct the antenna, reduce the effect of the wind turbine through design compromises, and maximize the distance from the wind turbine to the receiver (Manwell 2003). This will be difficult if it is desired that turbines be located near residences.

Again, most of these studies discussed are located in rural environments. This problem will most likely require studies in an urban environment, however, due to a significant increase in receivers, in addition to a more complex terrain, including buildings and other man-made structures. If a wind turbine is designed for placement on the top of a building, this could create even more problems since it is also where the building’s antenna is usually located. In this case, it may be necessary to evaluate certain trade-offs, or consider the use of non-classical WECs. One consideration, however, is the growing use of cable as opposed to antenna transmission. It is unclear if and how wind turbine operation affects cable reception, but, intuitively, it would seem that cable television should remain relatively undisturbed.

Noise

Noise effects are similar to visual effects because quantification of disturbances is usually subjective. Different people are more or less perceptive to different sound sources, depending on frequency, intensity, patterns and pitch, making it difficult to quantify when certain noises become problematic (Manwell 2003). Low frequency vibrations from rooftop WECs are transmitted to a building's structure and can be problematic for residents, but maybe tolerated for industrial buildings (Manfred, 1991). Again, most studies have been done with respect to wind turbines, and may not be applicable to the noise effects of other WECs.

Noise perception can be broken down into three basic categories: subjective, where it is a minor annoyance; interfering, where it interferes with daily activities such as talking, sleeping and possibly learning; physiological, where it can have lasting, physical effects such as anxiety, hearing loss or can cause ringing in the ear (Manwell 2003).

Since wind turbines run when the wind is blowing, much of the noise is masked by the naturally occurring noise of the wind (Manwell 2003). The greatest noise inconvenience occurs at low speeds because at higher speeds, the noise of the wind itself surpasses the noise of the WEC (at about 7 meters per second) (Manfred, 1991). One suggestion might be to have a higher startup wind speed for turbines, but this could significantly decrease the total energy availability of a turbine, and is unpractical, especially in an urban environment where lower speeds are prevalent. Advances in technology also may eliminate this problem all together (Manwell 2003).

If it is desired that a wind farm be located near an urban area, distances between WECs and buildings were determined to satisfy noise policies in Germany, ranging from 100 to 1000 meters for a residential area and 20 to 250 meters for a commercial area (Manfred 1991). If the tower is 20 meter above the roof this could be satisfied. However, most buildings do not have devices with a height above the roof of more than 10 meters.

Noise from wind turbines is transmitted either through the air or through the turbine's structure (Manwell 2003). This may be problematic for placing WECs on rooftops unless there is a way to isolate the vibrations of a WEC that may be transmitted and amplified through the building, causing further annoyance and discomfort.

The four different types of noise created by wind turbine operations are categorized as follows:

- Tonal: discrete frequency noise caused by meshing gears, the yaw drive, rotational frequencies of the shafts and generators, non-linear instabilities affecting the rotor blade surface, blunt-trailing edge vortex shedding and/or unstable flows over slits and holes. It is possible for the hub, rotor and tower to amplify and transmit mechanical noises (Manwell 2003). Again, this could be a major issue for wind turbines placed on buildings since noise could be transmitted through the tower to the building; one idea is to integrate wind power into a building's design and conduct the noise away from the structure.
- Broadband: continuous sound pressure distribution with frequencies over 100Hz, usually caused by atmospheric turbulence interfering with the blades, creating a

‘whooshing’ or ‘swishing’ sounds. The higher the tip speed or tip speed ratio, the louder the noise (Manwell 2003).

- Low-frequency: noise from 20-100Hz that is usually detected downwind of a turbine, caused wake shedding from blades or the interference of the tower with the flow over a blade such that every time a blade passes by the tower, noise is created (Manwell 2003).
- Impulsive: short thumps varying in amplitude with time, which may be caused by a disturbance of the flow around a tower or downwind machine and its interaction with the turbine blades, but could also be caused by sudden aerodynamic changes in the blades such as the deployment of actuators or breaks (Manwell 2003).

Fortunately, there are many ways to mitigate noise from a turbine and even retrofit older turbines to be noise compliant: gear teeth can be fabricated with a special finish, low-speed cooling fans can be used, components can be mounted in the nacelle as opposed to the ground, acoustic insulation and baffles can be added to the nacelle, vibration isolators and soft mounts can be utilized in addition to designing new turbines with noise minimization as a priority (Manwell 2003).

While there are no international standards governing noise regulation (and there is no formal federal noise regulation within the United States, only guidelines from the EPA exist), the table below compares noise standards of several different countries; note that all values are in decibels (Manwell 2003):

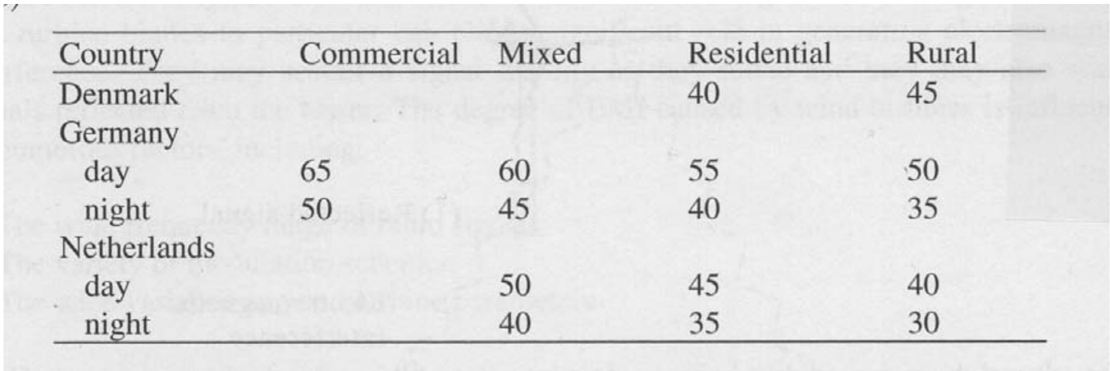

Country	Commercial	Mixed	Residential	Rural
Denmark			40	45
Germany				
day	65	60	55	50
night	50	45	40	35
Netherlands				
day		50	45	40
night		40	35	30

Figure 1. Noise standards (in decibels) for several European countries (Manwell 2003).

In addition, it is not unusual for tonal noises to suffer a deduction in allowable levels, usually around 5 decibels (Manwell 2003). It does not appear that many studies have been done on how the noise from wind turbines might affect animals such as house pets. Animals have much more acute hearing compared with humans, and frequencies that might not bother people could in fact be very disruptive to animals.

Avian Issues

In the late 1980s, it was found that many golden eagles and red-tailed hawks, which are federally protected species, were being killed at Altamont Pass by some interaction with the wind turbines or high voltage lines in the wind farm. Bird migration through wind farms is also an issue due to possible violations of the Migratory Bird Treaty Act, in addition to the Endangered Species Act. There have been major bird kill reports in the United States as well as in some wind farms across Europe (Manwell 2003).

Adverse effects on avian life are listed as follows (Manwell 2003):

- Bird electrocution and collision

- Changes to foraging, nesting and breeding habits
- Migratory alterations
- Reduction of available habitat

Positive effects on avian life, however, include the protection of the environment, which means less available habitat loss due to pollution. Wind farms might also be able to provide perch and nest sites on towers, and offer further protection from predators (Manwell 2003).

Some mitigation concepts include the avoidance of siting wind turbines in areas of high bird population or migratory paths, using fewer and larger turbines to reduce the general air space used by wind farms in order to number of impacts, alternate tower designs with less perches and unguyed structures, relocation of nests from a wind farm to a more suitable habitat, prey base management with live traps to rid the wind farm of undesired prey, buried electrical lines to reduce electrocution and, of course, site specific studies of a wind farms affects on avian life (Manwell 2003).

Unfortunately, good wind sites are often areas that attract birds (Manwell 2003). Fortunately, however, it seems less likely that a flock of birds will migrate over a city, making the placement of WECs in urban areas an ideal choice to help lower bird kills due to WECs. Studies on migration patterns of birds around urban areas can be utilized to better assess this risk. However, birds already face many other hazards in an urbanized area, such as building ventilation fans, windows and electrocution.

Land Use

The one fortuitous aspect of utilizing wind power within an urban environment is that placing wind turbines on building roofs may virtually eliminate many land-use issues. Major land-use issues include the amount of land required to create enough energy to be useful, rural preservation, placement of access roads and erosion. Usually, however, wind farms are placed within agricultural areas, allowing for agricultural and wind farming (Manwell 2003). Placing a farm of WECs (WECs distributed over an urban environment, such as the surfaces of a building or group of buildings) further expands on the idea of utilizing land for multiple uses.

Safety Concerns

Mechanical safety is the greatest source of concern. A study has shown, however, that the chances of blade that breaks off actually hitting a person is 2%, though it's chances of breaking off are considerably less such that it is possible to have a wind plant in an urban area without needing a security perimeter (Manfred 1991). As the population density of an urban development increases, however, the chances of a person being hit by a thrown blade can go up, so the only way a safety evaluation should be assessed is by looking at the probability of a blade breakage. Some useful studies to correlate results with would be heliport safety studies for that area.

Unfortunately for potential urban wind sites, many permitting agencies have required a buffer zone between the turbine and residential areas and public travel ways to mitigate the event of a blade throw (Manwell 2003). Again, however, this currently only applies to certain forms of WECs, such as horizontal axis turbines, not all WECs; further studies of the safety effects of urban WECs requires further consideration.

Some safety concerns that can adversely affect an urban area concern falling or thrown ice (either due to accumulated ice melting, or the start of a turbine whose blades have iced over), collapse of the tower or any other part of the turbine, fire and maintenance hazard, and health effects due to the electromagnetic fields produced by the turbine itself (Manwell 2003).

1.1.2 Urban Wind Energy Converter Survey

While there are not many readily available WECs for current use in urban areas, technology is quickly advancing and some ideas are being developed and, in some cases, implemented around the world. The Aeolian Roof Wind Energy System™ (Tyler 2002), Aeolian Towers™ (Tyler 2002), the Vawtex (ASHRAE 2003) and Architectural Wind^R (AeroVironment 2004) are a few examples of developing or currently used technologies to utilize wind energy in urban environments.

Tyler proposes that building rooftops be integrated with an Aeolian Roof Wind Energy System™. This design requires a properly oriented building and a roof built with specifications that take advantage of aerodynamics over rooftops. But cross flow turbines capture a relatively wide selection of wind angles, even though they are static concentrators (Tyler 2002). This is a good idea for an area where the wind blows predominately from one direction, but can result in a significant drop in energy capture for areas with many contributing wind sectors.

Such a system will limit visual appearance, and the small diameter turbine does not require the use of a gearbox, cutting down on noise (Tyler 2002). The simplicity of this design may cut down on maintenance and overall cost. This system's design also provides a simple way to integrate solar and wind power (Tyler 2002). While this system appears to work best with long, relatively low and narrow buildings, it will probably not work in an urban city with a tall skyline.

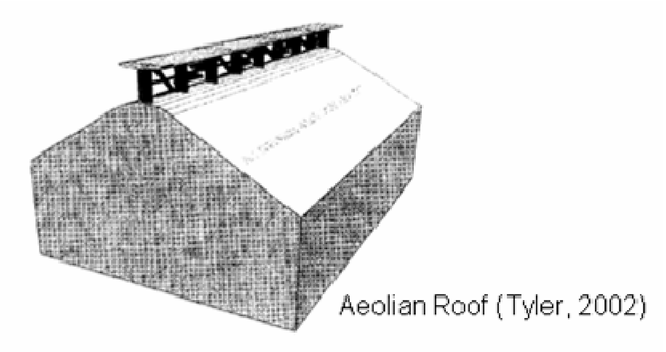

Figure 2. Aeolian Roof concept.

The Aeolian Towers™ concept employs the use of a device attached to a tower, and due to corner attachment can be acoustically insulated (Tyler 2002). This shows that noise issues may be effectively mitigated. Another advantage to both designs is that they can be placed in areas with little or no power transmission lines (Tyler 2002).

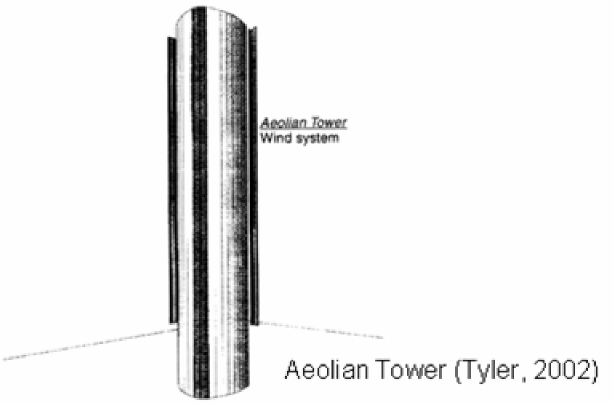

Figure 3. Aeolian Tower concept.

Two other examples of developing urban wind energy converters are the Vawtex, or Vertical Axis Wind Turbine Extractor, and the Architectural Wind^{R} system. The Vawtex, designed by the Harare engineering firm, Ove Arup, utilizes the wind to cool buildings in Zimbabwe. It is a vertical axis turbine, supposedly allowing it to capture more wind power than a horizontal axis turbine as the wind changes directions. In addition, the Vawtex can be constructed out of local materials, making it an environmentally friendly and viable alternative for poorer areas (ASHRAE 2003). Architectural Wind^{R}, designed by AeroVironment, is an easily installable set of horizontal axis wind turbines with cages around them (for blade safety issues) that can sit on the top of an architectural wall of a building. It is unobtrusive and can generate up to 2.4 kW in an area of approximately 9.3 square meters (100 square feet), yielding an average power density of 240 Watts per square meter (AeroVironment 2005).

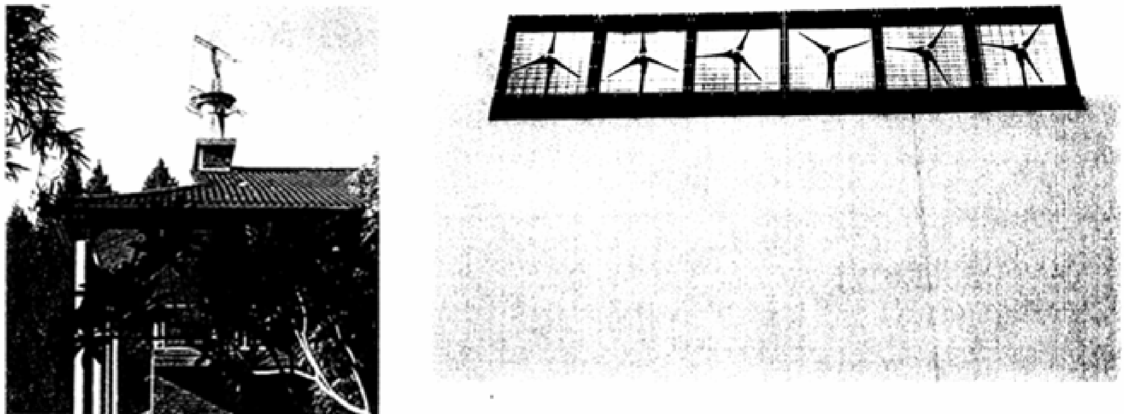

Wind turbine in Zimbabwe.

Figure 1 – 2.4 kW demonstration system (approximately 4' tall by 25' long)

Vawtex
(ASHRAE, 2003)

Architectural Wind^{R}
(AeroVironment, 2004)

Figure 4. Vawtex and Architectural Wind^{R} pictures.

Another company, Aerotecture International, Inc., has an urban WEC and has reported actual production of the Aeroturbine, and currently claims to have already made several sales of this device. The website for this company gives a power curve for the turbine, along with a conceptual drawing (shown left) and picture (shown right), in Figure 5 (Aerotecture 2006).

Figure 5. Concept drawing of an Aerotecture Aeroturbine and vertical mounting on a rooftop.

Since this was the only WEC designed specifically for urban use that had substantial information reported, such as a power curve and reported actual sales, the Aeroturbine was chosen for comparative power production analysis to be displayed in the Results section of this report.

Other urban WECs were revealed during the CWEC forum held in San Diego from December 12 to December 14, 2005, but substantive information has yet to be obtained about these devices. More information on the proceedings of the forum can be found at http://cwec.ucdavis.edu/forum2005/proceedings.

2.0 Methods

Several steps were implemented in the analysis for this study: wind-tunnel testing was used to acquire data; San Francisco wind records were digitized and compiled into useful hourly wind information; various computer codes and applications were used to reduce the raw data acquired through wind-tunnel testing.

2.1 Wind-tunnel Testing

Wind-tunnel testing was the method used to gather data for this study. The Atmospheric Boundary Layer Wind Tunnel was used to perform all testing due to the extensive testing of pedestrian-level winds in San Francisco previously conducted there. The wind tunnel itself, along with methods for setup of the tests, is described in detail in the next few sections. Validation of wind-tunnel testing has been conducted on numerous occasions and is not a part of this thesis study; thus it will only be recapped in this section. A more thorough investigation into the validation of wind-tunnel studies is conducted in Appendices C and D (modified from Coquilla 2002).

In order to obtain flow similarity between wind-tunnel and full-scale flows, flow similarity parameters must be defined. Using the conservation of mass, momentum and energy equations for turbulent flow, applying the Boussinesq density approximation, defining non-dimensional quantities and substituting into these equations will yield several dimensionless equations: continuity, momentum and turbulent energy equations. From these equations, the following non-dimensional parameters are observed (Coquilla 2002):

- Rossby number: $\mathrm{Ro} \equiv \dfrac{U_0}{L_0 \Omega_0}$
- Densimetric Froude number: $Fr \equiv \dfrac{U_0}{(g L_0 \delta T_0 / T_0)^{1/2}}$
- Prandtl number: $\mathrm{Pr} \equiv \dfrac{\rho_0 c_{p0} \nu_0}{\kappa_0}$
- Eckert number: $\mathrm{Ec} \equiv \dfrac{U_0^2}{c_{p0} \delta T_0}$
- Reynolds number: $\mathrm{Re} \equiv \dfrac{U_0 L_0}{\nu_0}$

where U is the speed of the fluid, L is the length in question, Ω is the angular rotation, g is gravity, T is temperature (Kelvin), ρ is the density of the fluid, c_P is the heat capacity of the fluid, ν is the kinematic viscosity and κ is the thermal conductivity of the fluid.

The Rossby number shows the magnitude of the Coriolis effect. Typically, if the modeled area is less than 5 kilometers in length or if measurements are confined to a height below the boundary layer, as was the case in this study, this effect is negligible and the Rossby number is ignored (Coquilla 2002).

The densimetric Froude number is the ratio of the fluid’s inertial to buoyant forces. Since the wind tunnel simulates a neutrally stable atmospheric condition, buoyant forces are negligible and the Froude number goes toward infinity, and can be disregarded in this analysis (Coquilla 2002).

The Prandtl number is matched between the wind-tunnel and full-scale measurements since the fluid, air, is the same. The Eckert number concerns compressible flow, and since the speed of the air in the wind tunnel, as well as the speed of the air at full-scale, is low, this number is negligible (Coquilla 2002).

The involvement of the Reynolds number is very important in this study. It would be unrealistic to try and try and match the full-scale Reynolds number in this wind-tunnel study due to the geometric downsizing of the model. Instead of matching the wind-tunnel Reynolds number with the full-scale value, Reynolds number independence was obtained. According to Sutton (1949), if the roughness Reynolds number, $\mathrm{Re}_z = \frac{u_* z_0}{\nu}$, is less than or equal to 2.5, where u_* is the friction speed of the fluid and z_0 is the roughness height, Reynolds number independence is achieved, and the large scale turbulence occurring in full-scale is properly simulated in the wind tunnel. Using a free stream velocity of approximately 3.8 meters per second yields a friction speed of 0.24 meters per second and a roughness height of 0.0025 meters, the wind-tunnel tests conducted in this study satisfy this condition (Coquilla 2002).

Other conditions that need to be satisfied are the matching of the power-law, Jensen's length scale criterion, matching H/δ if H/δ is greater than 20 percent (H is the height at which the measurement is made in the wind tunnel), otherwise just satisfying H/δ is less than 0.2 is sufficient for the lower 20% of the boundary layer (it does not have to match under this condition), and limiting the cross-sectional area of the test section in the wind tunnel blocked by the model to less than 5%-15% of the total cross-sectional area (this is satisfied by choosing a small enough model, as done in this study) to assures that the simulated flow will not be affected by any stream wise pressure gradients (Coquilla 2002).

The power law, $\frac{U}{U_\infty} = \left(\frac{H}{\delta}\right)^\alpha$, where α is the power-law exponent, U is the velocity at height H, U_∞ is the mean-free velocity of the wind above the boundary layer of height δ and z is again the roughness height (Coquilla 2002), is matched in the wind tunnel by arranging the roughness elements, which are 2 inch by 4 inch wooden blocks, 12 inches in length, laid out on the floor upwind of the test section, in a manner previously determined to give that value. For San Francisco, the typical value for α is 0.3, which was closely matched in the wind tunnel for this study.

Jensen's length scale criterion requires matching of the ratio of the roughness height to the building height, or z_0/H, between wind-tunnel and full-scale simulations (Coquilla 2005). Since this study geometrically scaled the model and roughness height, this criterion is satisfied.

Due to the law-of-the-wall, the condition of keeping H/δ less than 0.2 for the lower 20% of the boundary layer, meaning that if H/δ in full-scale is less than 0.2, the full-scale value does not have to be matched in the wind-tunnel simulation, H/δ for the wind tunnel needs only to be less than 0.2, is met (Coquilla 2002). Since the boundary layer height in the ABLWT is approximately 1 meter, limiting the height at which measurements are taken to no more than 20 centimeters unless H/δ is matched above that height. Fortunately, due to the tall buildings' obstruction of the Ekman spiral, it is possible to obtain good data for a measurement height above 20 centimeters.

2.1.1 The Atmospheric Boundary Layer Wind Tunnel

The Atmospheric Boundary Layer Wind Tunnel, or *ABLWT*, shown in Figure 6, is located at the University of California, Davis and simulates flow under the earth's turbulent boundary layer. The ABLWT consists of three main sections: the flow development section, the test section and the diffuser section (Coquilla 2002). Flow enters through the inlet, passing through flow straighteners and spires, then travels over a long fetch of roughness elements, blocks of wood no taller than 2 inches arranged in a specific pattern to simulate the proper flow profile, in the flow development section (Coquilla 2002). The flow has the proper turbulence characteristics by the time it reaches the test section, which has a Plexiglas window on either side for visibility. The flow then exits after passing through the diffuser section, flow straighteners and the fan (Coquilla 2002). More detailed specifications of the wind tunnel are located in Appendix A.

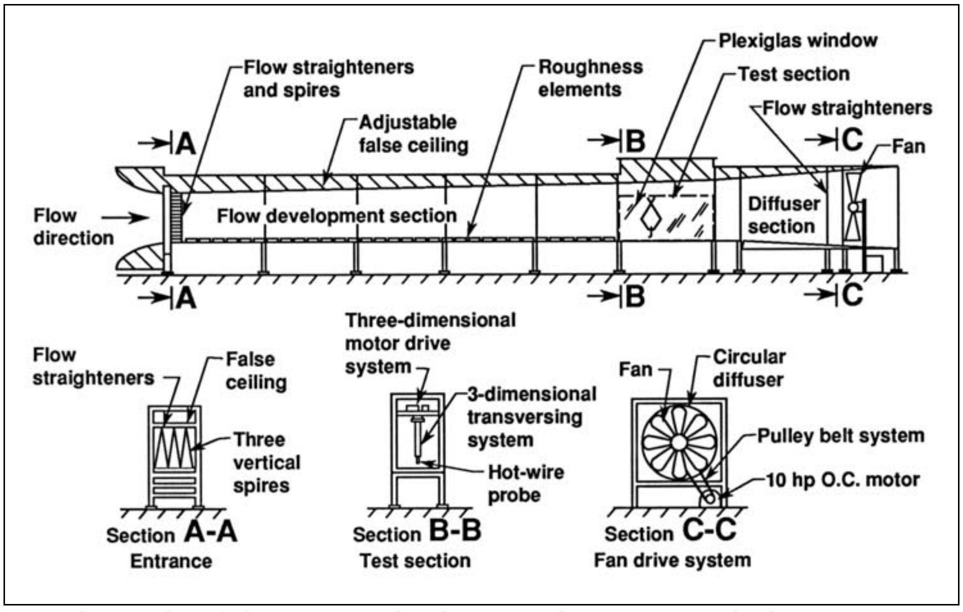

Figure 6. Schematic of the Atmospheric Boundary Layer Wind Tunnel at UC Davis (Coquilla 2005).

2.1.2 Wind Tunnel Setup

A model of the financial district, and surrounding areas as needed, of San Francisco was used for all wind-tunnel testing. The model scale was 1:600, or one inch (0.0254 meters) in the wind tunnel equals fifty feet (15.24 meters) in full-scale. This model is broken up into blocks, not necessarily corresponding to city blocks, and piece together like a puzzle to create the area of downtown shown in Figure 7.

Once a wind direction is chosen for testing, the test building's model block is centered in the test section of the wind tunnel, and surrounding blocks are placed around it to fill up the entire test section with model blocks. Model blocks are included far enough upwind (typically 600 meters or 1970 feet, full-scale) of the test building to ensure proper simulation of the effects of these buildings on the wind flow as it travels to the test building, just as they would in the city. Any model blocks that would only partially fit into the wind tunnel were simulated with wooden blocks of approximate size to replicate any buildings that would otherwise be missing because those blocks do not fit. Once testing of the wind direction is finished, the model blocks can be rotated to simulate a new wind direction (of course, some model blocks will rotate out of the test section and some new ones will have to fill in areas where there are none). Any area of the city or wind direction can be simulated by rotating the model blocks or changing them out for other model blocks, making it relatively simple to test as many wind directions as needed in a compressed amount of time when compared to full-scale testing.

Figure 7.Configuration of San Francisco wind tunnel model blocks (modified from ESA 2006).

Building Selection

There are many tall buildings suitable for study in downtown San Francisco. The buildings that were chosen for analysis met several subjective criteria: each building is taller than the average building height of its respective local area; each building's height meets or exceeds 76 meters (approximately 250 feet); each building or tower of the building is of relatively conventional shape, meaning rectangular without extra architectural detail.

Two specific areas of downtown San Francisco were considered for analysis. The first area, near 10th Street and Market Street, is well known for having high winds and has several tall buildings in its vicinity. The buildings chosen at this location are the California State Automobile Association (CSAA) Building, on the northeast corner of Fell Street and Van Ness Avenue; the Bank of America building, on the southwest corner of 11th and Market Streets, and the Fox Plaza building, on the northeast corner of Polk and Market Streets. The second area, Folsom Street and Main Street, was selected due to its proximity to the bay, where downwind conditions are unlikely to change due to lack of land. The two buildings at this locations are not yet built, but are have been approved and are scheduled to replace two parking lots, which are just south of Folsom Street and are separated by Main Street. The building to the west of Main Street is labeled Folsom and Main West, and the building to the east of Main Street is labeled Folsom and Main East. Though each building has two towers, only one tower was analyzed for each building. The towers studied in this project were both the western most towers.

While every attempt was made to ensure model correctness at the time of testing, the city itself is in a constant state of change. Two settings were tested for the 10th and Market area buildings: *existing setting*, which means that buildings included in the model are buildings that existed at the time of testing, but also includes buildings that have been approved for construction by the city and are scheduled to be built within the next few years; and *cumulative setting*, which includes building developments that are going through the city's approval process, and may or may not be built in the future, either replacing existing buildings or empty lots. The two buildings at Folsom Street and Main Street were tested for the existing setting only due to limited information on the area’s development.

Figures 8 and 9 show the differences between the existing and cumulative settings for the Fox Plaza, CSAA and Bank of America Buildings. Figures 10 and 11 show how this area was set up in the wind tunnel for testing. All of the buildings near 10th Street and Market Street, Fox Plaza, the CSAA and Bank of America Buildings, were tested for the same wind-tunnel setup since their model blocks all fit in the wind tunnel at once. An overview of the surrounding area of the Folsom and Main Street buildings is illustrated in Figure 13. Folsom and Main East and West buildings were tested in another wind-tunnel setup. All pictures were taken as angled overviews, where up is the upwind direction, or the direction from which the wind is coming (i.e., the wind is going from top to bottom in the picture). While Folsom and Main East and Folsom and Main West buildings are not shown for the west wind direction due to camera issues during testing, the setup can be pieced together by looking at Figure 12, which shows the southwest wind direction wind-tunnel setup and the west-northwest wind direction wind-tunnel setup. The most important information about that wind direction is that the heights of the buildings upwind are relatively shorter than for the other wind directions.

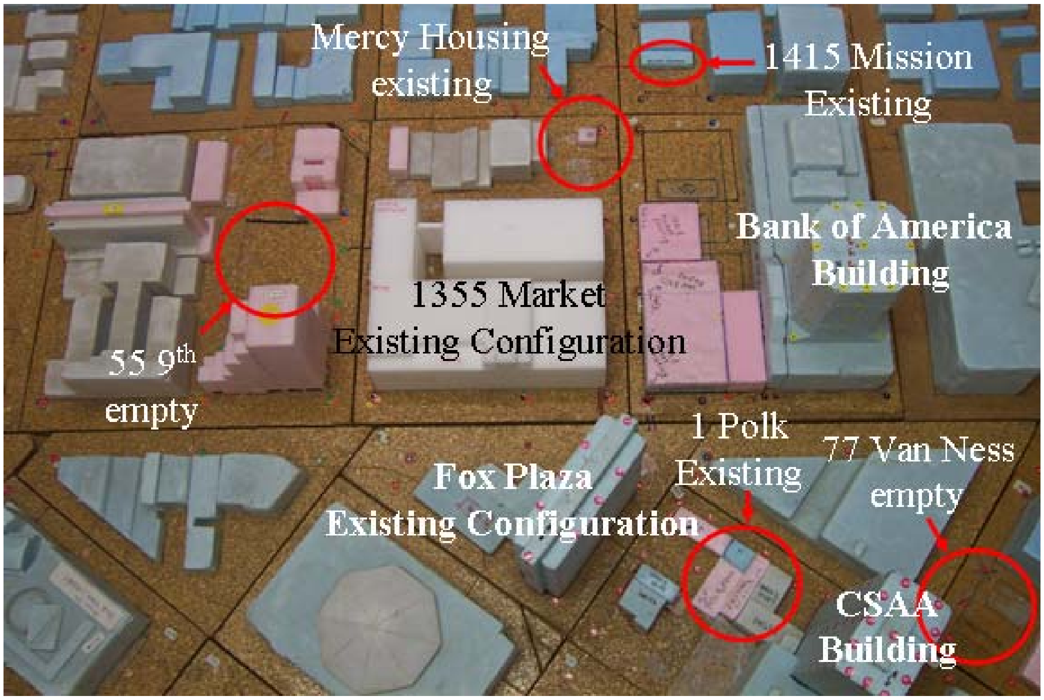

Figure 8. Overview of 10th and Market Street buildings, existing setting.

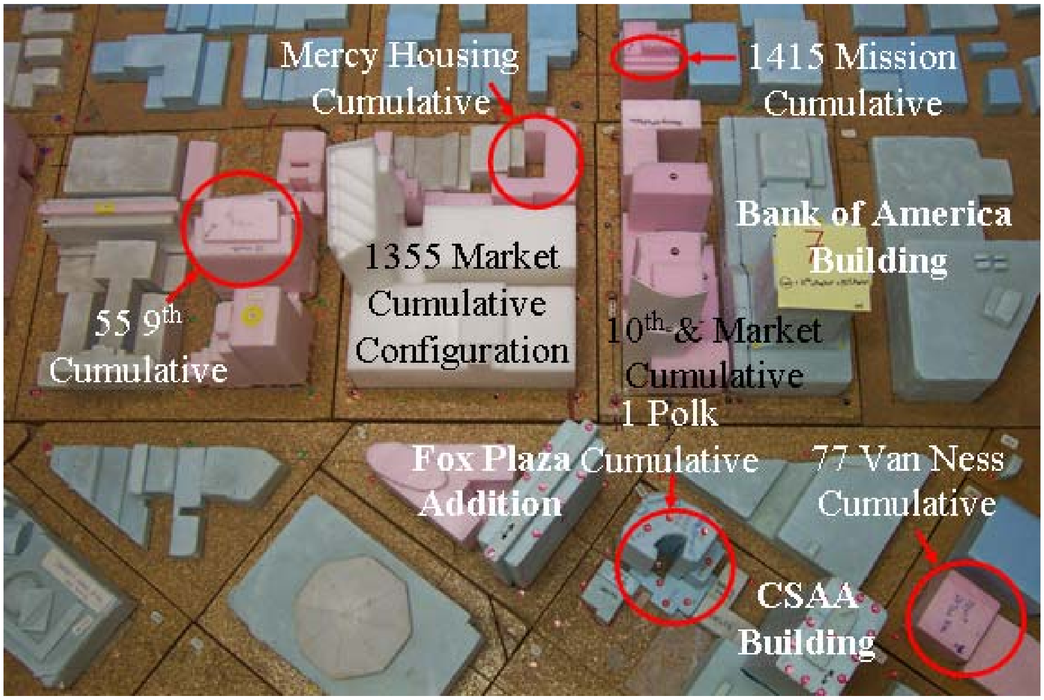

Figure 9. Overview of 10th and Market Street buildings, cumulative setting.

Figure 10. 10th and Market Street buildings, northwest, west-northwest, west and southwest wind directions, shown left-to-right, for the existing setting (winds blow from top to bottom).

Figure 11. 10th and Market Street buildings, northwest, west-northwest, west and southwest wind directions, shown left-to-right, for the cumulative setting (winds blow from top to bottom).

Figure 12. Folsom and Main East and West buildings, northwest, west-northwest and southwest wind directions, shown left-to-right, for the existing setting (winds blow from top to bottom).

Figure 13. Overview of the Folsom and Main East and West buildings.

Measurement Locations

Measurement locations, also referred to as *points*, were chosen to be near the surface of the buildings, including measurements starting at the base and continuing up the centers of the faces or corners of the building in increments of 15.24 meters (50 feet) until the top edge of the building is reached. The numbering scheme for each building is illustrated in Figure 14 through Figure 18, and is described in Table 1 through Table 5, which give the heights of each point. If the building has a tower and base architecture, as is the case with the Bank of America building and the Folsom East and West buildings, the base is ignored in the study. Points that would be covered by adjacent buildings or structures are also ignored.

All measurement positions are correct within a full-scale radius of 1.5 meters (5 feet) in any direction due to measurement position uncertainty. While attempts were made to place the hotwire as close to the surface of the building without touching it, since neither the probe’s support nor the buildings were completely straight, there were a few instances where there was an angle between the probe’s support and the building, leading to a distance away from the building of up to 3 meters (10 feet) in full-scale.

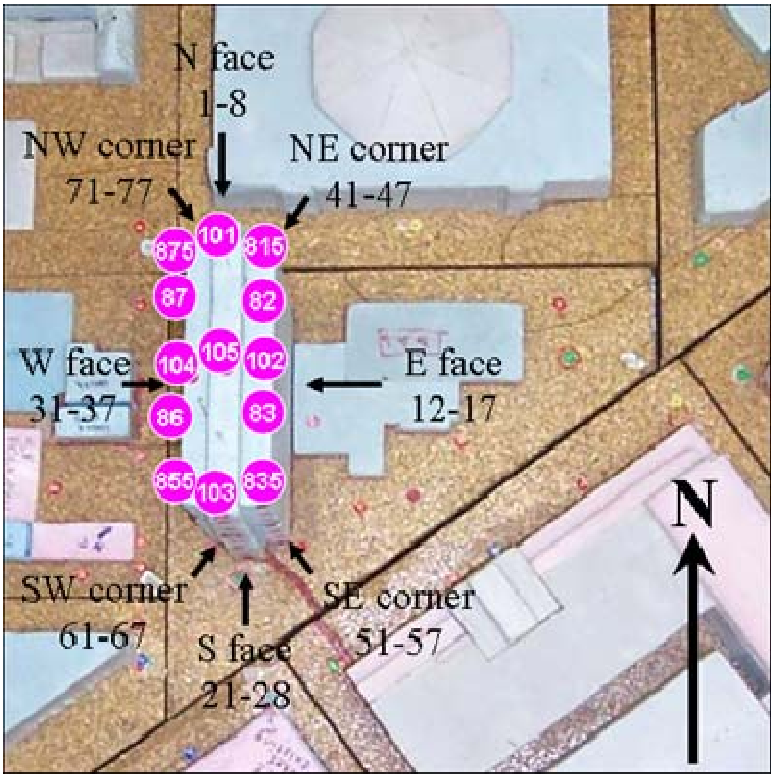

Figure 14. Fox Plaza point locations (rooftop locations are highlighted).

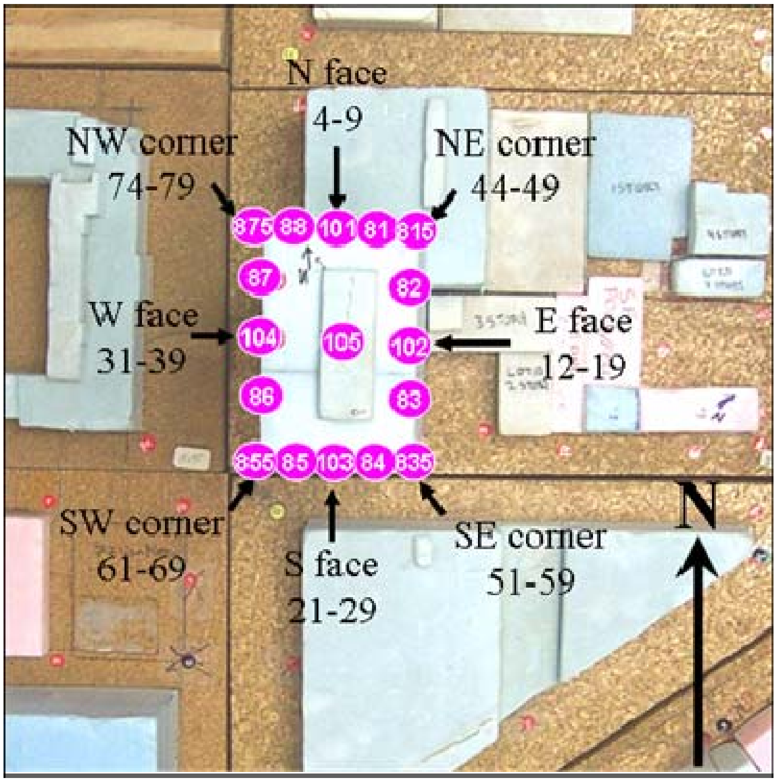

Figure 15. CSAA Building point locations (rooftop locations are highlighted).

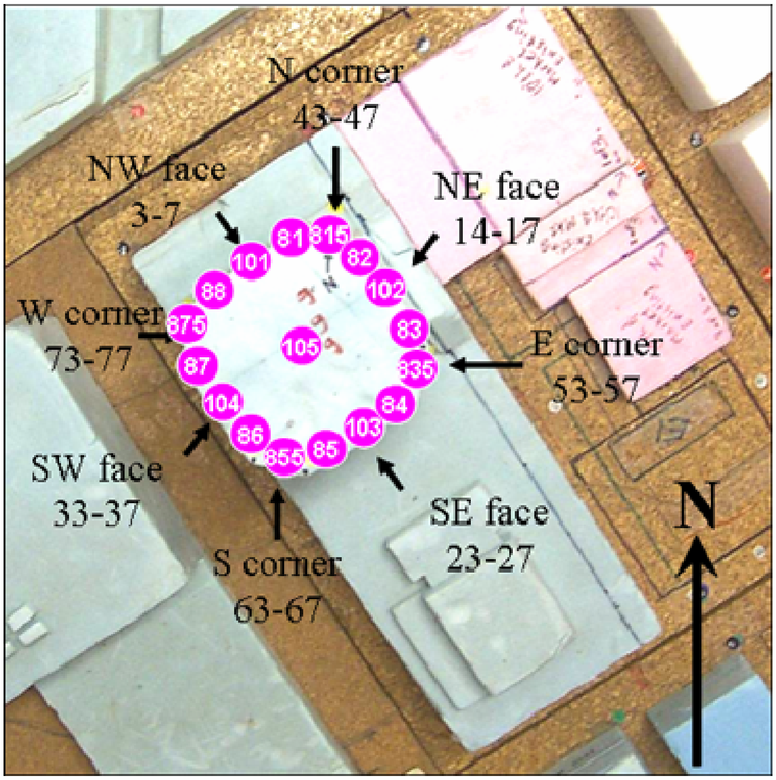

Figure 16. Bank of America Building point locations (rooftop locations are highlighted).

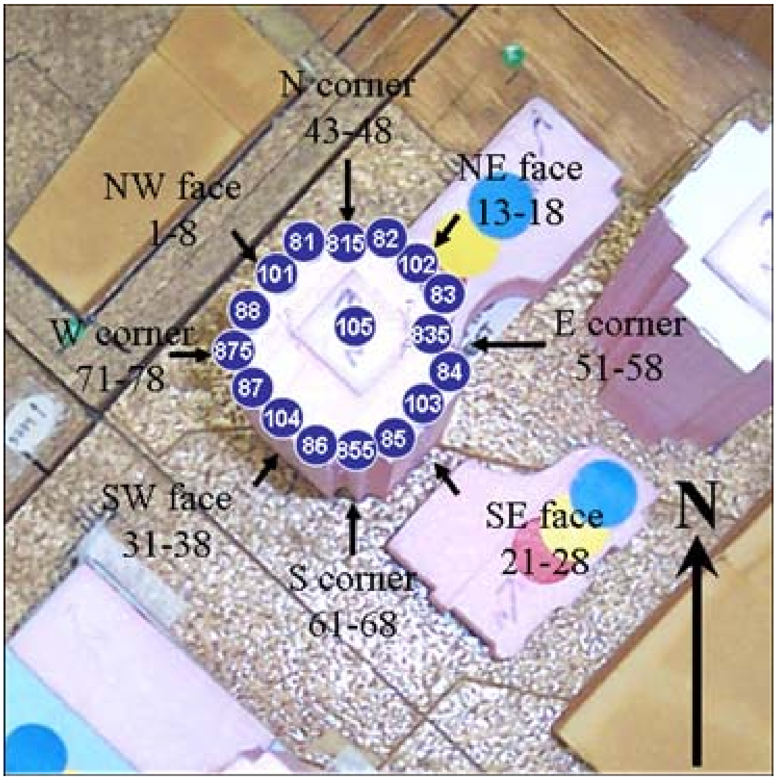

Figure 17. Folsom and Main East point locations (rooftop locations are highlighted).

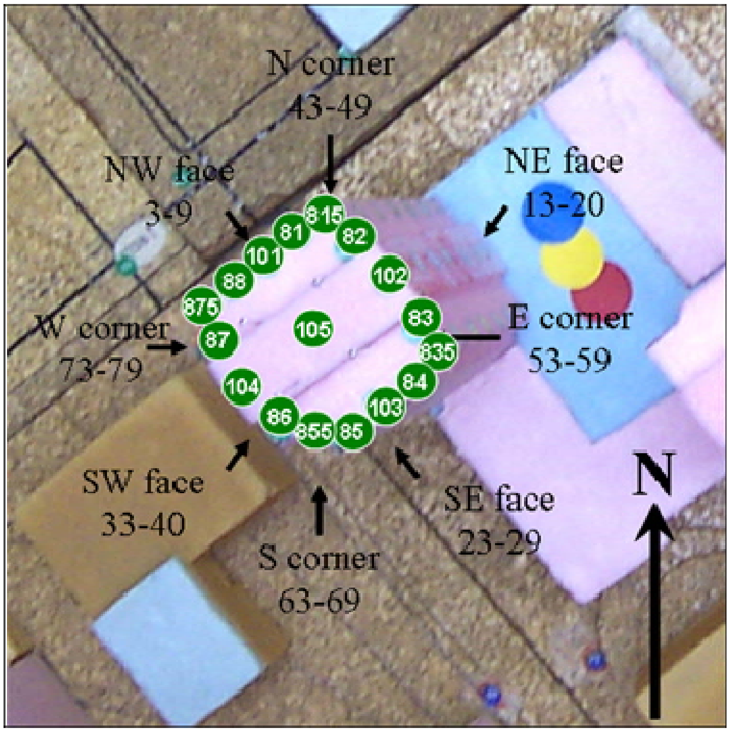

Figure 18. Folsom and Main West point locations (rooftop locations are highlighted).

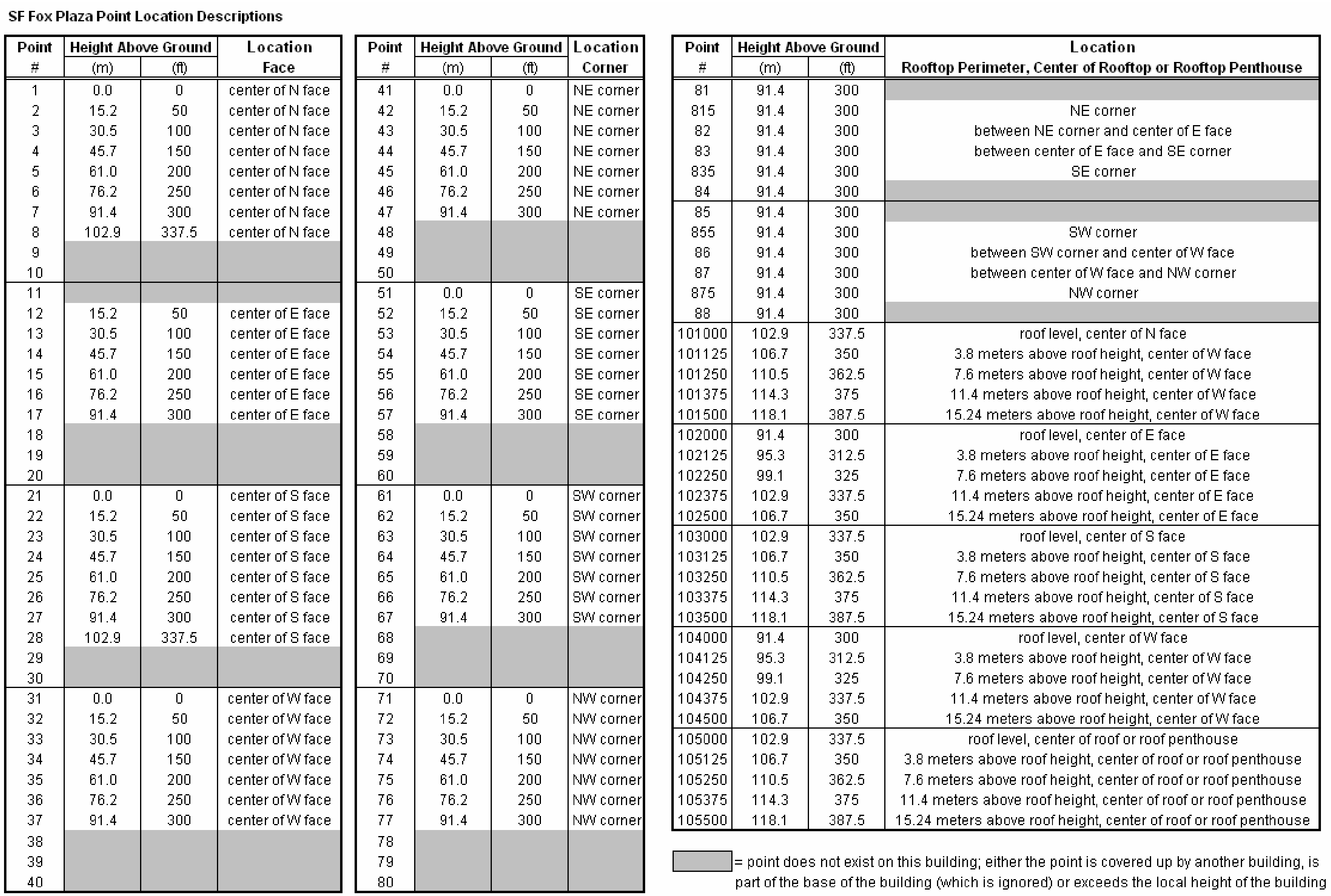

SF Fox Plaza Point Location Descriptions

Point	Height Above Ground		Location
#	(m)	(ft)	Face
1	0.0	0	center of N face
2	15.2	50	center of N face
3	30.5	100	center of N face
4	45.7	150	center of N face
5	61.0	200	center of N face
6	76.2	250	center of N face
7	91.4	300	center of N face
8	102.9	337.5	center of N face
9	▨	▨	▨
10	▨	▨	▨
11	▨	▨	▨
12	15.2	50	center of E face
13	30.5	100	center of E face
14	45.7	150	center of E face
15	61.0	200	center of E face
16	76.2	250	center of E face
17	91.4	300	center of E face
18	▨	▨	▨
19	▨	▨	▨
20	▨	▨	▨
21	0.0	0	center of S face
22	15.2	50	center of S face
23	30.5	100	center of S face
24	45.7	150	center of S face
25	61.0	200	center of S face
26	76.2	250	center of S face
27	91.4	300	center of S face
28	102.9	337.5	center of S face
29	▨	▨	▨
30	▨	▨	▨
31	0.0	0	center of W face
32	15.2	50	center of W face
33	30.5	100	center of W face
34	45.7	150	center of W face
35	61.0	200	center of W face
36	76.2	250	center of W face
37	91.4	300	center of W face
38	▨	▨	▨
39	▨	▨	▨
40	▨	▨	▨

Point	Height Above Ground		Location
#	(m)	(ft)	Corner
41	0.0	0	NE corner
42	15.2	50	NE corner
43	30.5	100	NE corner
44	45.7	150	NE corner
45	61.0	200	NE corner
46	76.2	250	NE corner
47	91.4	300	NE corner
48	▨	▨	▨
49	▨	▨	▨
50	▨	▨	▨
51	0.0	0	SE corner
52	15.2	50	SE corner
53	30.5	100	SE corner
54	45.7	150	SE corner
55	61.0	200	SE corner
56	76.2	250	SE corner
57	91.4	300	SE corner
58	▨	▨	▨
59	▨	▨	▨
60	▨	▨	▨
61	0.0	0	SW corner
62	15.2	50	SW corner
63	30.5	100	SW corner
64	45.7	150	SW corner
65	61.0	200	SW corner
66	76.2	250	SW corner
67	91.4	300	SW corner
68	▨	▨	▨
69	▨	▨	▨
70	▨	▨	▨
71	0.0	0	NW corner
72	15.2	50	NW corner
73	30.5	100	NW corner
74	45.7	150	NW corner
75	61.0	200	NW corner
76	76.2	250	NW corner
77	91.4	300	NW corner
78	▨	▨	▨
79	▨	▨	▨
80	▨	▨	▨

Point	Height Above Ground		Location
#	(m)	(ft)	Rooftop Perimeter, Center of Rooftop or Rooftop Penthouse
81	91.4	300	▨
815	91.4	300	NE corner
82	91.4	300	between NE corner and center of E face
83	91.4	300	between center of E face and SE corner
835	91.4	300	SE corner
84	91.4	300	▨
85	91.4	300	▨
855	91.4	300	SW corner
86	91.4	300	between SW corner and center of W face
87	91.4	300	between center of W face and NW corner
875	91.4	300	NW corner
88	91.4	300	▨
101000	102.9	337.5	roof level, center of N face
101125	106.7	350	3.8 meters above roof height, center of W face
101250	110.5	362.5	7.6 meters above roof height, center of W face
101375	114.3	375	11.4 meters above roof height, center of W face
101500	118.1	387.5	15.24 meters above roof height, center of W face
102000	91.4	300	roof level, center of E face
102125	95.3	312.5	3.8 meters above roof height, center of E face
102250	99.1	325	7.6 meters above roof height, center of E face
102375	102.9	337.5	11.4 meters above roof height, center of E face
102500	106.7	350	15.24 meters above roof height, center of E face
103000	102.9	337.5	roof level, center of S face
103125	106.7	350	3.8 meters above roof height, center of S face
103250	110.5	362.5	7.6 meters above roof height, center of S face
103375	114.3	375	11.4 meters above roof height, center of S face
103500	118.1	387.5	15.24 meters above roof height, center of S face
104000	91.4	300	roof level, center of W face
104125	95.3	312.5	3.8 meters above roof height, center of W face
104250	99.1	325	7.6 meters above roof height, center of W face
104375	102.9	337.5	11.4 meters above roof height, center of W face
104500	106.7	350	15.24 meters above roof height, center of W face
105000	102.9	337.5	roof level, center of roof or roof penthouse
105125	106.7	350	3.8 meters above roof height, center of roof or roof penthouse
105250	110.5	362.5	7.6 meters above roof height, center of roof or roof penthouse
105375	114.3	375	11.4 meters above roof height, center of roof or roof penthouse
105500	118.1	387.5	15.24 meters above roof height, center of roof or roof penthouse

▨ = point does not exist on this building; either the point is covered up by another building, is part of the base of the building (which is ignored) or exceeds the local height of the building

Table 1. Fox Plaza point location descriptions.

Table 2. CSAA Building point location descriptions.

SF CSAA Building Point Location Descriptions

Point	Height Above Ground		Location
#	(m)	(ft)	Face
1	0.0	0	▨
2	15.2	50	▨
3	30.5	100	▨
4	45.7	150	center of N face
5	61.0	200	center of N face
6	76.2	250	center of N face
7	91.4	300	center of N face
8	106.7	350	center of N face
9	125.7	412.5	center of N face
10	▨	▨	▨
11	▨	▨	▨
12	15.2	50	center of E face
13	30.5	100	center of E face
14	45.7	150	center of E face
15	61.0	200	center of E face
16	76.2	250	center of E face
17	91.4	300	center of E face
18	106.7	350	center of E face
19	125.7	412.5	center of E face
20	▨	▨	▨
21	0.0	0	center of S face
22	15.2	50	center of S face
23	30.5	100	center of S face
24	45.7	150	center of S face
25	61.0	200	center of S face
26	76.2	250	center of S face
27	91.4	300	center of S face
28	106.7	350	center of S face
29	125.7	412.5	center of S face
30	▨	▨	▨
31	0.0	0	center of W face
32	15.2	50	center of W face
33	30.5	100	center of W face
34	45.7	150	center of W face
35	61.0	200	center of W face
36	76.2	250	center of W face
37	91.4	300	center of W face
38	106.7	350	center of W face
39	125.7	412.5	center of W face
40	▨	▨	▨

Point	Height Above Ground		Location
#	(m)	(ft)	Corner
41	▨	▨	▨
42	▨	▨	▨
43	▨	▨	▨
44	45.7	150	NE corner
45	61.0	200	NE corner
46	76.2	250	NE corner
47	91.4	300	NE corner
48	106.7	350	NE corner
49	125.7	412.5	NE corner
50	▨	▨	▨
51	0.0	0	SE corner
52	15.2	50	SE corner
53	30.5	100	SE corner
54	45.7	150	SE corner
55	61.0	200	SE corner
56	76.2	250	SE corner
57	91.4	300	SE corner
58	106.7	350	SE corner
59	125.7	412.5	SE corner
60	▨	▨	▨
61	0.0	0	SW corner
62	15.2	50	SW corner
63	30.5	100	SW corner
64	45.7	150	SW corner
65	61.0	200	SW corner
66	76.2	250	SW corner
67	91.4	300	SW corner
68	106.7	350	SW corner
69	125.7	412.5	SW corner
70	▨	▨	▨
71	▨	▨	▨
72	▨	▨	▨
73	▨	▨	▨
74	45.7	150	NW corner
75	61.0	200	NW corner
76	76.2	250	NW corner
77	91.4	300	NW corner
78	106.7	350	NW corner
79	125.7	412.5	NW corner
80	▨	▨	▨

Point	Height Above Ground		Location
#	(m)	(ft)	Rooftop Perimeter, Center of Rooftop or Rooftop Penthouse
81	125.7	412.5	between center of N face and NE corner
815	125.7	412.5	NE corner
82	125.7	412.5	between NE corner and center of E face
83	125.7	412.5	between center of E face and SE corner
835	125.7	412.5	SE corner
84	125.7	412.5	between SE corner and center of S face
85	125.7	412.5	between center of S face and SW corner
855	125.7	412.5	SW corner
86	125.7	412.5	between SW corner and center of W face
87	125.7	412.5	between center of W face and NW corner
875	125.7	412.5	NW corner
88	125.7	412.5	between NW corner and center of N face
101000	125.7	412.5	roof level, center of N face
101125	129.5	425	3.8 meters above roof height, center of W face
101250	133.4	437.5	7.6 meters above roof height, center of W face
101375	137.2	450	11.4 meters above roof height, center of W face
101500	141.0	462.5	15.24 meters above roof height, center of W face
102000	125.7	412.5	roof level, center of E face
102125	129.5	425	3.8 meters above roof height, center of E face
102250	133.4	437.5	7.6 meters above roof height, center of E face
102375	137.2	450	11.4 meters above roof height, center of E face
102500	141.0	462.5	15.24 meters above roof height, center of E face
103000	125.7	412.5	roof level, center of S face
103125	129.5	425	3.8 meters above roof height, center of S face
103250	133.4	437.5	7.6 meters above roof height, center of S face
103375	137.2	450	11.4 meters above roof height, center of S face
103500	141.0	462.5	15.24 meters above roof height, center of S face
104000	125.7	412.5	roof level, center of W face
104125	129.5	425	3.8 meters above roof height, center of W face
104250	133.4	437.5	7.6 meters above roof height, center of W face
104375	137.2	450	11.4 meters above roof height, center of W face
104500	141.0	462.5	15.24 meters above roof height, center of W face
105000	129.5	425	roof level, center of roof or roof penthouse
105125	133.4	437.5	3.8 meters above roof height, center of roof or roof penthouse
105250	137.2	450	7.6 meters above roof height, center of roof or roof penthouse
105375	141.0	462.5	11.4 meters above roof height, center of roof or roof penthouse
105500	144.8	475	15.24 meters above roof height, center of roof or roof penthouse

▨ = point does not exist on this building; either the point is covered up by another building, is part of the base of the building (which is ignored) or exceeds the local height of the building

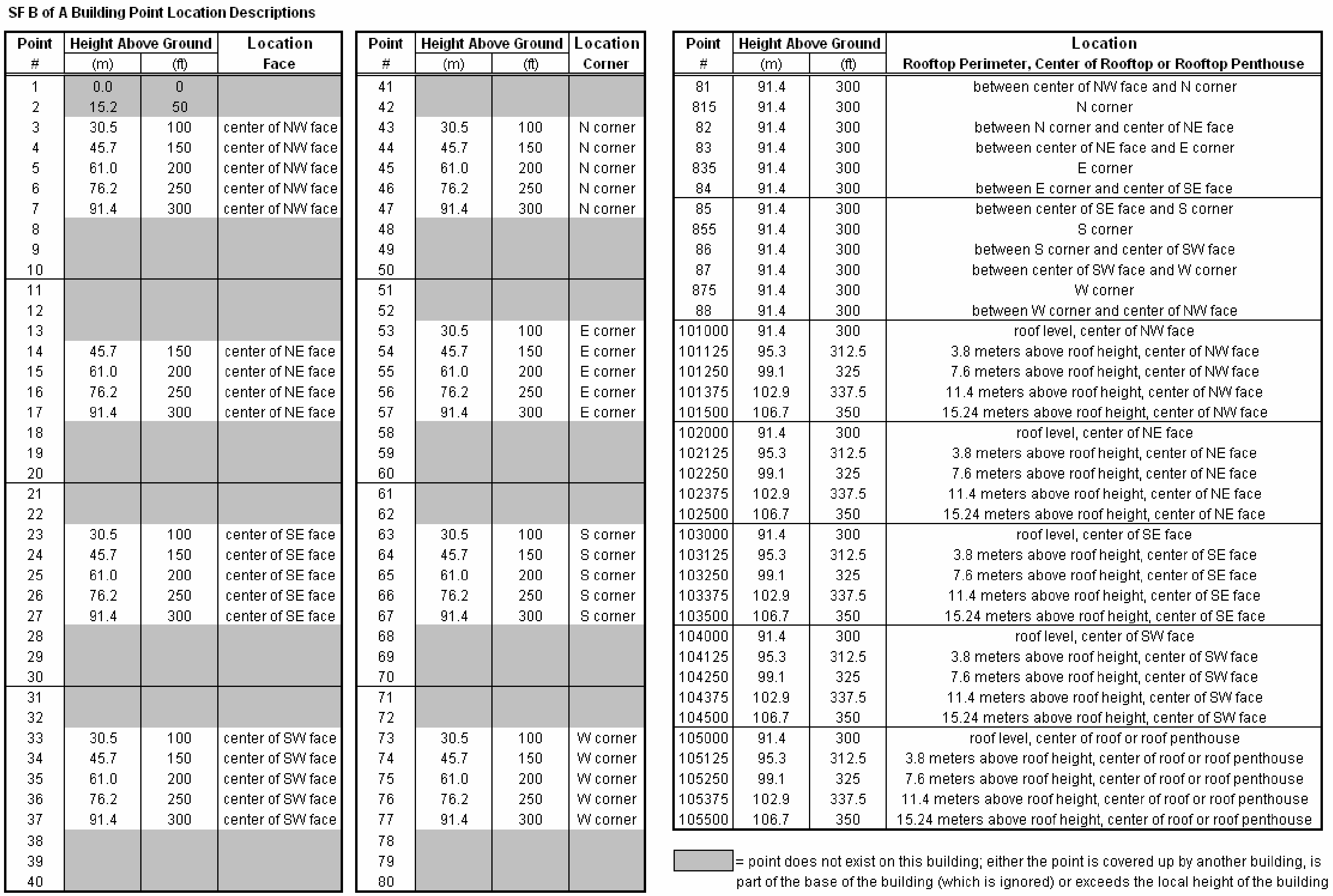

SF B of A Building Point Location Descriptions

Point	Height Above Ground		Location
#	(m)	(ft)	Face
1	0.0	0	▨
2	15.2	50	▨
3	30.5	100	center of NW face
4	45.7	150	center of NW face
5	61.0	200	center of NW face
6	76.2	250	center of NW face
7	91.4	300	center of NW face
8	▨	▨	▨
9	▨	▨	▨
10	▨	▨	▨
11	▨	▨	▨
12	▨	▨	▨
13	▨	▨	▨
14	45.7	150	center of NE face
15	61.0	200	center of NE face
16	76.2	250	center of NE face
17	91.4	300	center of NE face
18	▨	▨	▨
19	▨	▨	▨
20	▨	▨	▨
21	▨	▨	▨
22	▨	▨	▨
23	30.5	100	center of SE face
24	45.7	150	center of SE face
25	61.0	200	center of SE face
26	76.2	250	center of SE face
27	91.4	300	center of SE face
28	▨	▨	▨
29	▨	▨	▨
30	▨	▨	▨
31	▨	▨	▨
32	▨	▨	▨
33	30.5	100	center of SW face
34	45.7	150	center of SW face
35	61.0	200	center of SW face
36	76.2	250	center of SW face
37	91.4	300	center of SW face
38	▨	▨	▨
39	▨	▨	▨
40	▨	▨	▨

Point	Height Above Ground		Location
#	(m)	(ft)	Corner
41	▨	▨	▨
42	▨	▨	▨
43	30.5	100	N corner
44	45.7	150	N corner
45	61.0	200	N corner
46	76.2	250	N corner
47	91.4	300	N corner
48	▨	▨	▨
49	▨	▨	▨
50	▨	▨	▨
51	▨	▨	▨
52	▨	▨	▨
53	30.5	100	E corner
54	45.7	150	E corner
55	61.0	200	E corner
56	76.2	250	E corner
57	91.4	300	E corner
58	▨	▨	▨
59	▨	▨	▨
60	▨	▨	▨
61	▨	▨	▨
62	▨	▨	▨
63	30.5	100	S corner
64	45.7	150	S corner
65	61.0	200	S corner
66	76.2	250	S corner
67	91.4	300	S corner
68	▨	▨	▨
69	▨	▨	▨
70	▨	▨	▨
71	▨	▨	▨
72	▨	▨	▨
73	30.5	100	W corner
74	45.7	150	W corner
75	61.0	200	W corner
76	76.2	250	W corner
77	91.4	300	W corner
78	▨	▨	▨
79	▨	▨	▨
80	▨	▨	▨

Point	Height Above Ground		Location
#	(m)	(ft)	Rooftop Perimeter, Center of Rooftop or Rooftop Penthouse
81	91.4	300	between center of NW face and N corner
815	91.4	300	N corner
82	91.4	300	between N corner and center of NE face
83	91.4	300	between center of NE face and E corner
835	91.4	300	E corner
84	91.4	300	between E corner and center of SE face
85	91.4	300	between center of SE face and S corner
855	91.4	300	S corner
86	91.4	300	between S corner and center of SW face
87	91.4	300	between center of SW face and W corner
875	91.4	300	W corner
88	91.4	300	between W corner and center of NW face
101000	91.4	300	roof level, center of NW face
101125	95.3	312.5	3.8 meters above roof height, center of NW face
101250	99.1	325	7.6 meters above roof height, center of NW face
101375	102.9	337.5	11.4 meters above roof height, center of NW face
101500	106.7	350	15.24 meters above roof height, center of NW face
102000	91.4	300	roof level, center of NE face
102125	95.3	312.5	3.8 meters above roof height, center of NE face
102250	99.1	325	7.6 meters above roof height, center of NE face
102375	102.9	337.5	11.4 meters above roof height, center of NE face
102500	106.7	350	15.24 meters above roof height, center of NE face
103000	91.4	300	roof level, center of SE face
103125	95.3	312.5	3.8 meters above roof height, center of SE face
103250	99.1	325	7.6 meters above roof height, center of SE face
103375	102.9	337.5	11.4 meters above roof height, center of SE face
103500	106.7	350	15.24 meters above roof height, center of SE face
104000	91.4	300	roof level, center of SW face
104125	95.3	312.5	3.8 meters above roof height, center of SW face
104250	99.1	325	7.6 meters above roof height, center of SW face
104375	102.9	337.5	11.4 meters above roof height, center of SW face
104500	106.7	350	15.24 meters above roof height, center of SW face
105000	91.4	300	roof level, center of roof or roof penthouse
105125	95.3	312.5	3.8 meters above roof height, center of roof or roof penthouse
105250	99.1	325	7.6 meters above roof height, center of roof or roof penthouse
105375	102.9	337.5	11.4 meters above roof height, center of roof or roof penthouse
105500	106.7	350	15.24 meters above roof height, center of roof or roof penthouse

▨ = point does not exist on this building; either the point is covered up by another building, is part of the base of the building (which is ignored) or exceeds the local height of the building

Table 3. Bank of America Building point location descriptions.

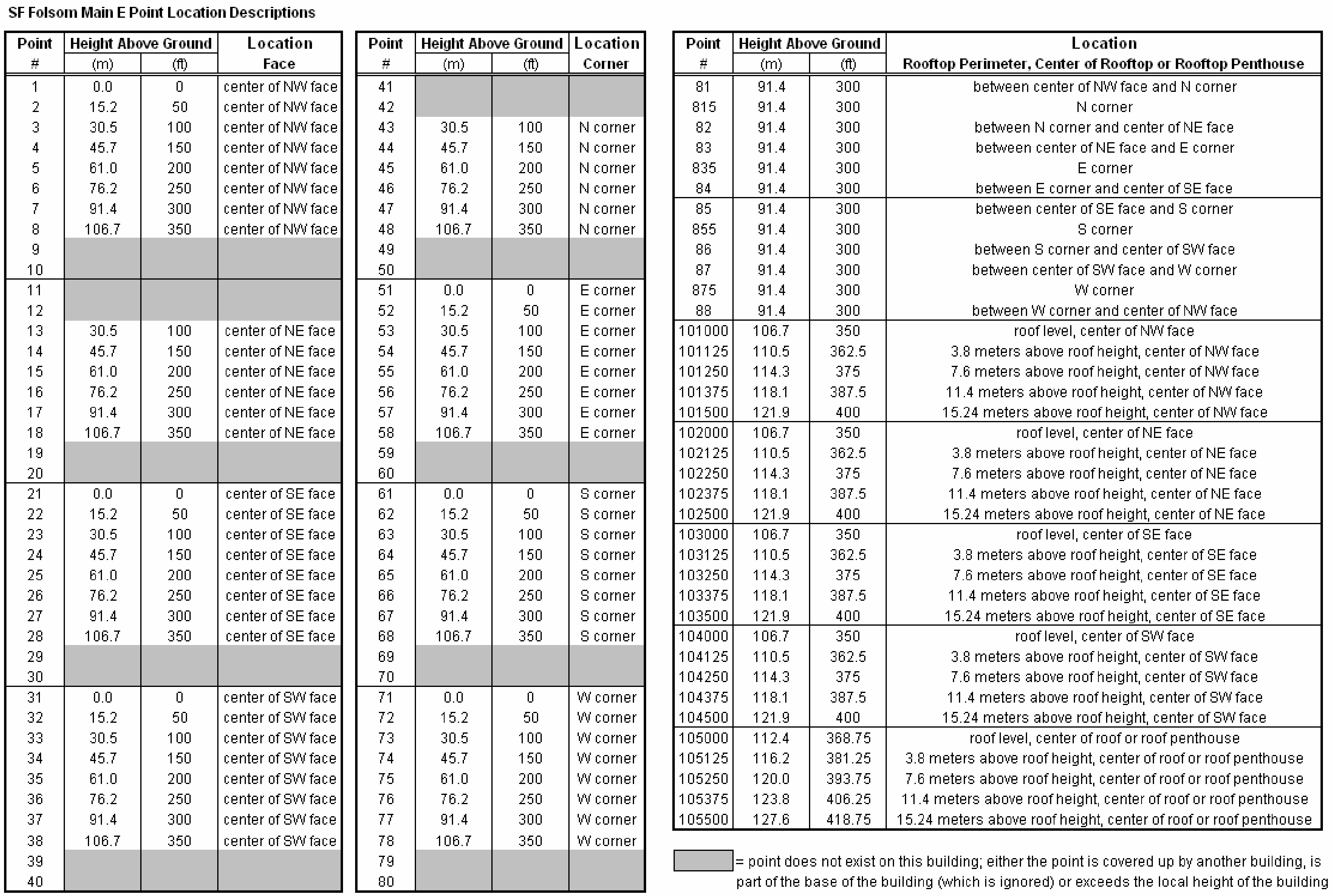

SF Folsom Main E Point Location Descriptions

Point	Height Above Ground		Location
#	(m)	(ft)	Face
1	0.0	0	center of NW face
2	15.2	50	center of NW face
3	30.5	100	center of NW face
4	45.7	150	center of NW face
5	61.0	200	center of NW face
6	76.2	250	center of NW face
7	91.4	300	center of NW face
8	106.7	350	center of NW face
9			
10			
11			
12			
13	30.5	100	center of NE face
14	45.7	150	center of NE face
15	61.0	200	center of NE face
16	76.2	250	center of NE face
17	91.4	300	center of NE face
18	106.7	350	center of NE face
19			
20			
21	0.0	0	center of SE face
22	15.2	50	center of SE face
23	30.5	100	center of SE face
24	45.7	150	center of SE face
25	61.0	200	center of SE face
26	76.2	250	center of SE face
27	91.4	300	center of SE face
28	106.7	350	center of SE face
29			
30			
31	0.0	0	center of SW face
32	15.2	50	center of SW face
33	30.5	100	center of SW face
34	45.7	150	center of SW face
35	61.0	200	center of SW face
36	76.2	250	center of SW face
37	91.4	300	center of SW face
38	106.7	350	center of SW face
39			
40			

Point	Height Above Ground		Location
#	(m)	(ft)	Corner
41			
42			
43	30.5	100	N corner
44	45.7	150	N corner
45	61.0	200	N corner
46	76.2	250	N corner
47	91.4	300	N corner
48	106.7	350	N corner
49			
50			
51	0.0	0	E corner
52	15.2	50	E corner
53	30.5	100	E corner
54	45.7	150	E corner
55	61.0	200	E corner
56	76.2	250	E corner
57	91.4	300	E corner
58	106.7	350	E corner
59			
60			
61	0.0	0	S corner
62	15.2	50	S corner
63	30.5	100	S corner
64	45.7	150	S corner
65	61.0	200	S corner
66	76.2	250	S corner
67	91.4	300	S corner
68	106.7	350	S corner
69			
70			
71	0.0	0	W corner
72	15.2	50	W corner
73	30.5	100	W corner
74	45.7	150	W corner
75	61.0	200	W corner
76	76.2	250	W corner
77	91.4	300	W corner
78	106.7	350	W corner
79			
80			

Point	Height Above Ground		Location
#	(m)	(ft)	Rooftop Perimeter, Center of Rooftop or Rooftop Penthouse
81	91.4	300	between center of NW face and N corner
815	91.4	300	N corner
82	91.4	300	between N corner and center of NE face
83	91.4	300	between center of NE face and E corner
835	91.4	300	E corner
84	91.4	300	between E corner and center of SE face
85	91.4	300	between center of SE face and S corner
855	91.4	300	S corner
86	91.4	300	between S corner and center of SW face
87	91.4	300	between center of SW face and W corner
875	91.4	300	W corner
88	91.4	300	between W corner and center of NW face
101000	106.7	350	roof level, center of NW face
101125	110.5	362.5	3.8 meters above roof height, center of NW face
101250	114.3	375	7.6 meters above roof height, center of NW face
101375	118.1	387.5	11.4 meters above roof height, center of NW face
101500	121.9	400	15.24 meters above roof height, center of NW face
102000	106.7	350	roof level, center of NE face
102125	110.5	362.5	3.8 meters above roof height, center of NE face
102250	114.3	375	7.6 meters above roof height, center of NE face
102375	118.1	387.5	11.4 meters above roof height, center of NE face
102500	121.9	400	15.24 meters above roof height, center of NE face
103000	106.7	350	roof level, center of SE face
103125	110.5	362.5	3.8 meters above roof height, center of SE face
103250	114.3	375	7.6 meters above roof height, center of SE face
103375	118.1	387.5	11.4 meters above roof height, center of SE face
103500	121.9	400	15.24 meters above roof height, center of SE face
104000	106.7	350	roof level, center of SW face
104125	110.5	362.5	3.8 meters above roof height, center of SW face
104250	114.3	375	7.6 meters above roof height, center of SW face
104375	118.1	387.5	11.4 meters above roof height, center of SW face
104500	121.9	400	15.24 meters above roof height, center of SW face
105000	112.4	368.75	roof level, center of roof or roof penthouse
105125	116.2	381.25	3.8 meters above roof height, center of roof or roof penthouse
105250	120.0	393.75	7.6 meters above roof height, center of roof or roof penthouse
105375	123.8	406.25	11.4 meters above roof height, center of roof or roof penthouse
105500	127.6	418.75	15.24 meters above roof height, center of roof or roof penthouse

▨ = point does not exist on this building; either the point is covered up by another building, is part of the base of the building (which is ignored) or exceeds the local height of the building

Table 4. Folsom and Main East point location descriptions.
]

SF Folsom Main W Point Location Descriptions

Point	Height Above Ground		Location
#	(m)	(ft)	Face
1	▨	▨	▨
2	▨	▨	▨
3	30.5	100	center of NW face
4	45.7	150	center of NW face
5	61.0	200	center of NW face
6	76.2	250	center of NW face
7	91.4	300	center of NW face
8	106.7	350	center of NW face
9	121.9	400	center of NW face
10	129.5	425	▨
11	▨	▨	▨
12	▨	▨	▨
13	30.5	100	center of NE face
14	45.7	150	center of NE face
15	61.0	200	center of NE face
16	76.2	250	center of NE face
17	91.4	300	center of NE face
18	106.7	350	center of NE face
19	121.9	400	center of NE face
20	129.5	425	center of NE face
21	▨	▨	▨
22	▨	▨	▨
23	30.5	100	center of SE face
24	45.7	150	center of SE face
25	61.0	200	center of SE face
26	76.2	250	center of SE face
27	91.4	300	center of SE face
28	106.7	350	center of SE face
29	121.9	400	center of SE face
30	▨	▨	▨
31	▨	▨	▨
32	▨	▨	▨
33	30.5	100	center of SW face
34	45.7	150	center of SW face
35	61.0	200	center of SW face
36	76.2	250	center of SW face
37	91.4	300	center of SW face
38	106.7	350	center of SW face
39	121.9	400	center of SW face
40	129.5	425	center of SW face

Point	Height Above Ground		Location
#	(m)	(ft)	Corner
41	▨	▨	▨
42	▨	▨	▨
43	30.5	100	N corner
44	45.7	150	N corner
45	61.0	200	N corner
46	76.2	250	N corner
47	91.4	300	N corner
48	106.7	350	N corner
49	121.9	400	N corner
50	▨	▨	▨
51	▨	▨	▨
52	▨	▨	▨
53	30.5	100	E corner
54	45.7	150	E corner
55	61.0	200	E corner
56	76.2	250	E corner
57	91.4	300	E corner
58	106.7	350	E corner
59	121.9	400	E corner
60	▨	▨	▨
61	▨	▨	▨
62	▨	▨	▨
63	30.5	100	S corner
64	45.7	150	S corner
65	61.0	200	S corner
66	76.2	250	S corner
67	91.4	300	S corner
68	106.7	350	S corner
69	121.9	400	S corner
70	▨	▨	▨
71	▨	▨	▨
72	▨	▨	▨
73	30.5	100	W corner
74	45.7	150	W corner
75	61.0	200	W corner
76	76.2	250	W corner
77	91.4	300	W corner
78	106.7	350	W corner
79	121.9	400	W corner
80	▨	▨	▨

Point	Height Above Ground		Location
#	(m)	(ft)	Rooftop Perimeter, Center of Rooftop or Rooftop Penthouse
81	91.4	300	between center of NW face and N corner
815	91.4	300	N corner
82	91.4	300	between N corner and center of NE face
83	91.4	300	between center of NE face and E corner
835	91.4	300	E corner
84	91.4	300	between E corner and center of SE face
85	91.4	300	between center of SE face and S corner
855	91.4	300	S corner
86	91.4	300	between S corner and center of SW face
87	91.4	300	between center of SW face and W corner
875	91.4	300	W corner
88	91.4	300	between W corner and center of NW face
101000	121.9	400	roof level, center of NW face
101125	125.7	412.5	3.8 meters above roof height, center of NW face
101250	129.5	425	7.6 meters above roof height, center of NW face
101375	133.4	437.5	11.4 meters above roof height, center of NW face
101500	137.2	450	15.24 meters above roof height, center of NW face
102000	129.5	425	roof level, center of NE face
102125	133.4	437.5	3.8 meters above roof height, center of NE face
102250	137.2	450	7.6 meters above roof height, center of NE face
102375	141.0	462.5	11.4 meters above roof height, center of NE face
102500	144.8	475	15.24 meters above roof height, center of NE face
103000	121.9	400	roof level, center of SE face
103125	125.7	412.5	3.8 meters above roof height, center of SE face
103250	129.5	425	7.6 meters above roof height, center of SE face
103375	133.4	437.5	11.4 meters above roof height, center of SE face
103500	137.2	450	15.24 meters above roof height, center of SE face
104000	129.5	425	roof level, center of SW face
104125	133.4	437.5	3.8 meters above roof height, center of SW face
104250	137.2	450	7.6 meters above roof height, center of SW face
104375	141.0	462.5	11.4 meters above roof height, center of SW face
104500	144.8	475	15.24 meters above roof height, center of SW face
105000	129.5	425	roof level, center of roof or roof penthouse
105125	133.4	437.5	3.8 meters above roof height, center of roof or roof penthouse
105250	137.2	450	7.6 meters above roof height, center of roof or roof penthouse
105375	141.0	462.5	11.4 meters above roof height, center of roof or roof penthouse
105500	144.8	475	15.24 meters above roof height, center of roof or roof penthouse

▨ = point does not exist on this building; either the point is covered up by another building, is part of the base of the building (which is ignored) or exceeds the local height of the building

Table 5. Folsom and Main West point location descriptions.

2.2 Wind Data

One of the reasons that San Francisco was chosen for this study is because of its relatively high winds. The meteorological wind data used for the analysis of San Francisco was obtained from an anemometer at the old Federal Building at 50 U.N. Plaza, positioned at a height of 40.2 meters (132 feet) above ground level. Data was taken from 1945 through 1947 and is reported in percentages of occurrence per year. Originally, the data was broken down into 3-hour increments per month (i.e. January 12am through 2am, January 3am through 5am, December 12pm through 3pm, etc.). A Microsoft Excel® spreadsheet then was used to digitize and compile this wind data into percentages of time per year, as shown in Table 6. Table 6 shows the percentage of time per year the winds between two speeds, forming a *wind bin*, blow from a certain direction. The wind direction is indicated in the left column, and the wind bins are located in the top rows of the table and are broken down into knots, miles per hour and meters per second. The table also shows the total percent time the wind blows from a certain direction, as well as the average wind speeds for each wind direction.

Certain calculations require that the wind data also be separated into a *percent exceeded wind speed* table. A percent exceeded wind speed is the wind speed that is exceeded for a specified percent of time during a typical year. For example, a ten-percent exceeded wind speed would be the wind speed that is exceeded for ten-percent of the time during a typical year, and would be written as $U_{10\%}$. These values can be separated by wind direction as well; for example, $U_{10\%SW}$ would be the wind speed that is exceeded ten-percent of the time as the wind blows from the southwest. When including a directional reference in the percent exceeded wind speed, however, the percent time exceeded is still in reference to all occurrences in one year.

The cumulative wind speeds that form the percent exceeded wind speed table are calculated by starting at the highest recorded wind speed, adding up all of the occurrences (or percentages per year), creating one data point of speed versus percent time exceeded. The next data point would be the next lowest wind speed's percent occurrence plus the higher wind speed's percent occurrence, using that wind speed and the cumulative percent exceeded. This calculation continues until the speed is zero, and the data verifies that the winds exceed zero for approximately 100-percent of the time. Figure 19 shows the percent exceeded wind speeds for the San Francisco wind data, and is also separated by wind direction.

Wind-tunnel testing did not include an analysis of 16 wind directions; rather, four wind directions were chosen for testing: northwest, west-northwest, west and southwest winds were simulated in the wind tunnel. Northwest, west-northwest and west wind directions were chosen since they had the highest number of occurrences of all wind directions: 207 hours per year, 244 hours per year and 131 hours per year, respectively. The southwest wind direction was chosen to test any buildings south of Market Street in San Francisco since the street grids align with the southwest such that wind-tunnel effects may occur, causing higher wind speeds along these streets.

Since wind conditions should not significantly change with a slight change in the wind's angle, certain winds were grouped together for the percent exceeded wind speed's percent exceeded time values. Ideally, half of each neighboring wind speed would be included with the tested wind's data. Northwest included half of the north-northwest information, though none of west-northwest's data since west-northwest is analyzed separately. Similarly, west-northwest does not include any information from other wind directions because northwest and west winds are analyzed individually. West includes half of west-southwest's information. Southwest includes half of west-southwest's information as well as half of south-southwest's information. All other winds are lumped together and referred to as the wind direction *other*, and are summed together, excluding any parts of wind bins used in the analysis for the above mentioned four wind direction. *All* refers to the cumulative effects of all wind directions, and equals the sum of the data from the four wind directions and the data from the *other* wind directions.

Data points for each wind direction were then connected with a smoothed line in Excel®. Since the wind bins given in Table 6 re rather large, covering at least 3 knots in any given wind bin, data points are relatively more sparse than the ideal, and the smoothed line gives a realistic interpolation between points. It was desired for the percentages of time exceeded to be chosen, and the corresponding velocities were catalogued by hand from the graph accordingly. Time bins of five-percent were chosen, creating twenty data points for the percent wind speed exceeded table. This gave more data points than the original data set.

First, the wind speed from all directions was found for a given percentage of time exceeded. Since this is the percent exceeded wind for the whole year, the corresponding percent exceeded wind speeds for each wind direction are the same speed. The times for which these occur, however, are different for each wind direction; i.e., the percent times that this percent exceeded wind speed occurs for each wind direction analyzed (northwest, west-northwest, west, southwest and others) must add up to the percentage of time that wind speed occurs for all wind directions. This is true simply by the definition of how the wind directions' percentages of occurrences were defined. These results are shown in Table 7, where the left column indicates wind direction, the upper rows illustrate the wind speeds, and the data is given as the percentage of time that wind speed is exceeded per year during a typical year.

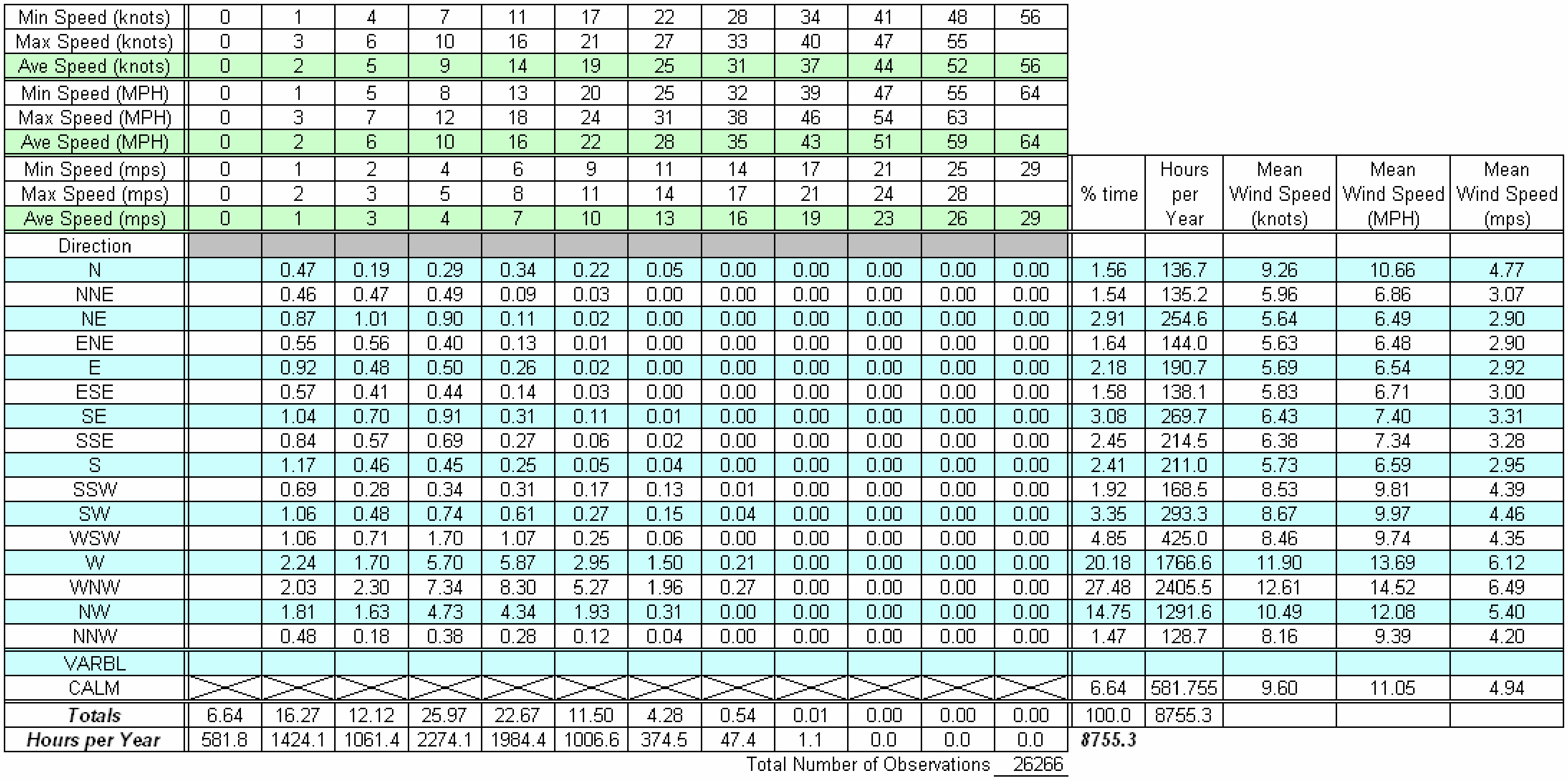

Min Speed (knots)	0	1	4	7	11	17	22	28	34	41	48	56					
Max Speed (knots)	0	3	6	10	16	21	27	33	40	47	55						
Ave Speed (knots)	0	2	5	9	14	19	25	31	37	44	52	56					
Min Speed (MPH)	0	1	5	8	13	20	25	32	39	47	55	64					
Max Speed (MPH)	0	3	7	12	18	24	31	38	46	54	63						
Ave Speed (MPH)	0	2	6	10	16	22	28	35	43	51	59	64					
Min Speed (mps)	0	1	2	4	6	9	11	14	17	21	25	29	% time	Hours per Year	Mean Wind Speed (knots)	Mean Wind Speed (MPH)	Mean Wind Speed (mps)
Max Speed (mps)	0	2	3	5	8	11	14	17	21	24	28						
Ave Speed (mps)	0	1	3	4	7	10	13	16	19	23	26	29					
Direction																	
N		0.47	0.19	0.29	0.34	0.22	0.05	0.00	0.00	0.00	0.00	0.00	1.56	136.7	9.26	10.66	4.77
NNE		0.46	0.47	0.49	0.09	0.03	0.00	0.00	0.00	0.00	0.00	0.00	1.54	135.2	5.96	6.86	3.07
NE		0.87	1.01	0.90	0.11	0.02	0.00	0.00	0.00	0.00	0.00	0.00	2.91	254.6	5.64	6.49	2.90
ENE		0.55	0.56	0.40	0.13	0.01	0.00	0.00	0.00	0.00	0.00	0.00	1.64	144.0	5.63	6.48	2.90
E		0.92	0.48	0.50	0.26	0.02	0.00	0.00	0.00	0.00	0.00	0.00	2.18	190.7	5.69	6.54	2.92
ESE		0.57	0.41	0.44	0.14	0.03	0.00	0.00	0.00	0.00	0.00	0.00	1.58	138.1	5.83	6.71	3.00
SE		1.04	0.70	0.91	0.31	0.11	0.01	0.00	0.00	0.00	0.00	0.00	3.08	269.7	6.43	7.40	3.31
SSE		0.84	0.57	0.69	0.27	0.06	0.02	0.00	0.00	0.00	0.00	0.00	2.45	214.5	6.38	7.34	3.28
S		1.17	0.46	0.45	0.25	0.05	0.04	0.00	0.00	0.00	0.00	0.00	2.41	211.0	5.73	6.59	2.95
SSW		0.69	0.28	0.34	0.31	0.17	0.13	0.01	0.00	0.00	0.00	0.00	1.92	168.5	8.53	9.81	4.39
SW		1.06	0.48	0.74	0.61	0.27	0.15	0.04	0.00	0.00	0.00	0.00	3.35	293.3	8.67	9.97	4.46
WSW		1.06	0.71	1.70	1.07	0.25	0.06	0.00	0.00	0.00	0.00	0.00	4.85	425.0	8.46	9.74	4.35
W		2.24	1.70	5.70	5.87	2.95	1.50	0.21	0.00	0.00	0.00	0.00	20.18	1766.6	11.90	13.69	6.12
WNW		2.03	2.30	7.34	8.30	5.27	1.96	0.27	0.00	0.00	0.00	0.00	27.48	2405.5	12.61	14.52	6.49
NW		1.81	1.63	4.73	4.34	1.93	0.31	0.00	0.00	0.00	0.00	0.00	14.75	1291.6	10.49	12.08	5.40
NNW		0.48	0.18	0.38	0.28	0.12	0.04	0.00	0.00	0.00	0.00	0.00	1.47	128.7	8.16	9.39	4.20
VARBL																	
CALM													6.64	581.755	9.60	11.05	4.94
Totals	6.64	16.27	12.12	25.97	22.67	11.50	4.28	0.54	0.01	0.00	0.00	0.00	100.0	8755.3			
Hours per Year	581.8	1424.1	1061.4	2274.1	1984.4	1006.6	374.5	47.4	1.1	0.0	0.0	0.0	***8755.3***				
								Total Number of Observations				26266					

Table 6. San Francisco wind data in percent occurrence per year by wind direction and speed.

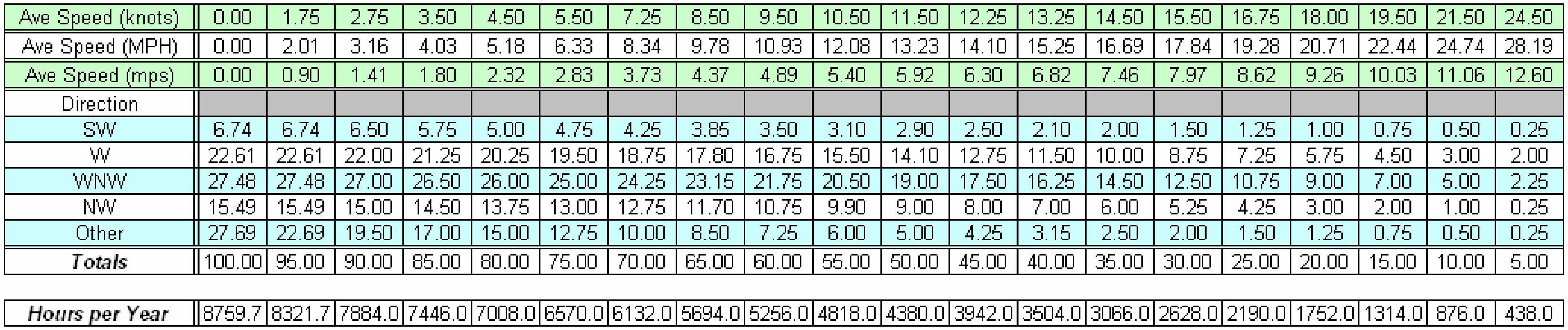

Ave Speed (knots)	0.00	1.75	2.75	3.50	4.50	5.50	7.25	8.50	9.50	10.50	11.50	12.25	13.25	14.50	15.50	16.75	18.00	19.50	21.50	24.50
Ave Speed (MPH)	0.00	2.01	3.16	4.03	5.18	6.33	8.34	9.78	10.93	12.08	13.23	14.10	15.25	16.69	17.84	19.28	20.71	22.44	24.74	28.19
Ave Speed (mps)	0.00	0.90	1.41	1.80	2.32	2.83	3.73	4.37	4.89	5.40	5.92	6.30	6.82	7.46	7.97	8.62	9.26	10.03	11.06	12.60
Direction																				
SW	6.74	6.74	6.50	5.75	5.00	4.75	4.25	3.85	3.50	3.10	2.90	2.50	2.10	2.00	1.50	1.25	1.00	0.75	0.50	0.25
W	22.61	22.61	22.00	21.25	20.25	19.50	18.75	17.80	16.75	15.50	14.10	12.75	11.50	10.00	8.75	7.25	5.75	4.50	3.00	2.00
WNW	27.48	27.48	27.00	26.50	26.00	25.00	24.25	23.15	21.75	20.50	19.00	17.50	16.25	14.50	12.50	10.75	9.00	7.00	5.00	2.25
NW	15.49	15.49	15.00	14.50	13.75	13.00	12.75	11.70	10.75	9.90	9.00	8.00	7.00	6.00	5.25	4.25	3.00	2.00	1.00	0.25
Other	27.69	22.69	19.50	17.00	15.00	12.75	10.00	8.50	7.25	6.00	5.00	4.25	3.15	2.50	2.00	1.50	1.25	0.75	0.50	0.25
Totals	100.00	95.00	90.00	85.00	80.00	75.00	70.00	65.00	60.00	55.00	50.00	45.00	40.00	35.00	30.00	25.00	20.00	15.00	10.00	5.00
Hours per Year	8759.7	8321.7	7884.0	7446.0	7008.0	6570.0	6132.0	5694.0	5256.0	4818.0	4380.0	3942.0	3504.0	3066.0	2628.0	2190.0	1752.0	1314.0	876.0	438.0

Table 7. San Francisco wind data in percent exceeded wind speeds, calculated manually.

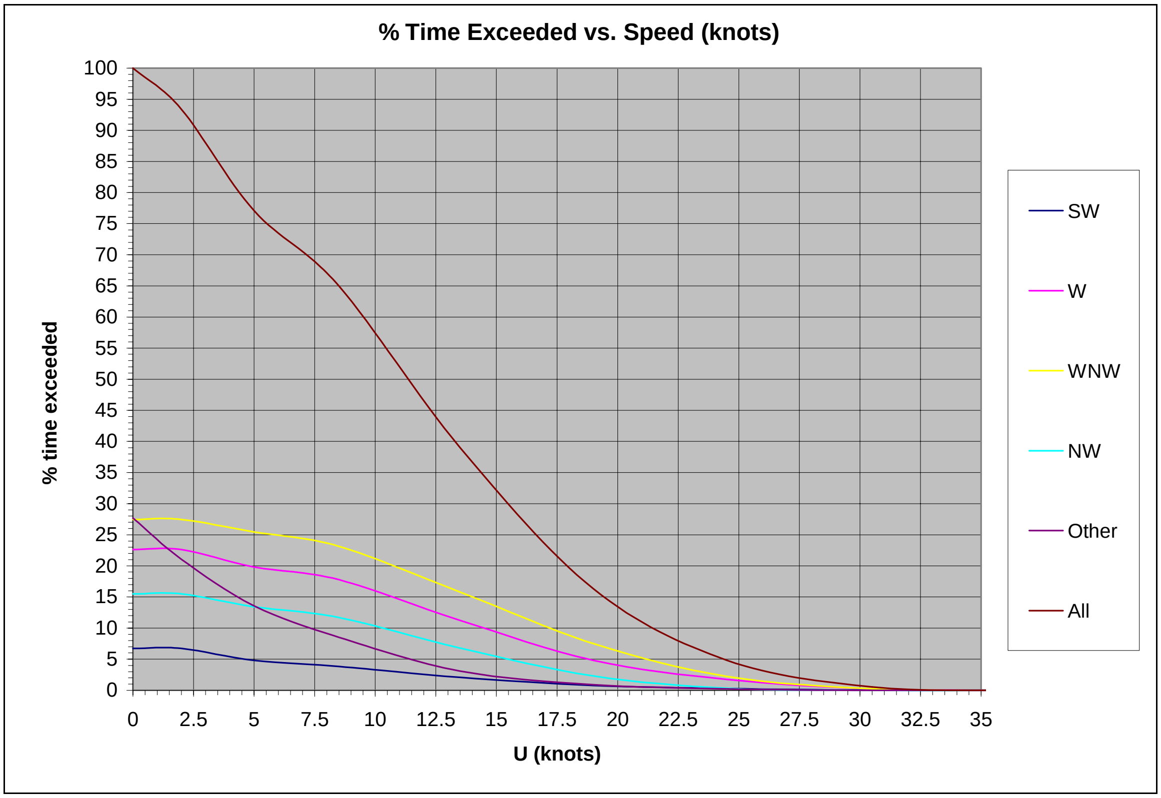

Figure 19. Percent exceeded time versus wind speed (knots as given in Table 6).

2.2.1 San Francisco Winds from 6am – 8pm

While the above analysis included San Francisco winds for all the hours in a day, there do exist hours for which energy usage is higher than average. San Francisco's municipal code (1985) has wind ordinances that limit the creation of high wind speeds due to development projects between the hours of 7am and 6pm, which means that the city considers itself active between those hours, making this a good range of times to perform wind analyses (Arens 1989) . Because the wind data for the years 1945 through 1947 was taken in three-hour averages, the following analysis will include wind data from 6am to 8pm. Methods for calculating annual wind data and percent exceedences occurring between 6am and 8pm are equivalent to the twenty-four hour per day wind data examined and illustrated by Tables 6 and 7. Table 8 shows the distributions of winds between 6am and 8pm for a typical year; Figure 20 illustrates the percent exceeded times versus wind speeds for the hours of 6am to 8pm for all wind directions and includes a breakdown by the four wind-tunnel tested wind directions; and Table 9 shows the hand tabulations of percent exceeded winds, broken into time bins of five-percent per year.

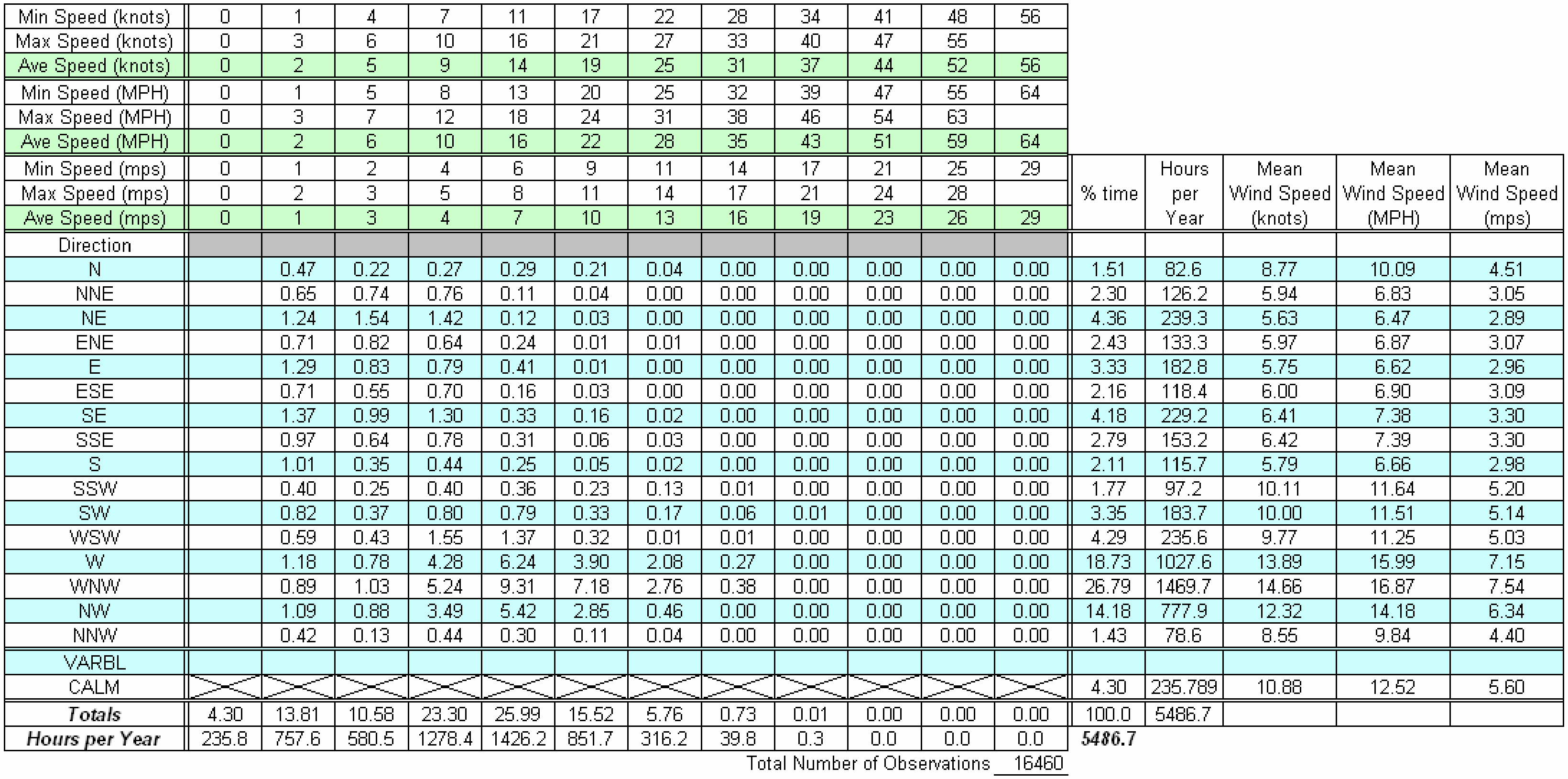

Min Speed (knots)	0	1	4	7	11	17	22	28	34	41	48	56					
Max Speed (knots)	0	3	6	10	16	21	27	33	40	47	55						
Ave Speed (knots)	0	2	5	9	14	19	25	31	37	44	52	56					
Min Speed (MPH)	0	1	5	8	13	20	25	32	39	47	55	64					
Max Speed (MPH)	0	3	7	12	18	24	31	38	46	54	63						
Ave Speed (MPH)	0	2	6	10	16	22	28	35	43	51	59	64					
Min Speed (mps)	0	1	2	4	6	9	11	14	17	21	25	29	% time	Hours per Year	Mean Wind Speed (knots)	Mean Wind Speed (MPH)	Mean Wind Speed (mps)
Max Speed (mps)	0	2	3	5	8	11	14	17	21	24	28						
Ave Speed (mps)	0	1	3	4	7	10	13	16	19	23	26	29					
Direction																	
N		0.47	0.22	0.27	0.29	0.21	0.04	0.00	0.00	0.00	0.00	0.00	1.51	82.6	8.77	10.09	4.51
NNE		0.65	0.74	0.76	0.11	0.04	0.00	0.00	0.00	0.00	0.00	0.00	2.30	126.2	5.94	6.83	3.05
NE		1.24	1.54	1.42	0.12	0.03	0.00	0.00	0.00	0.00	0.00	0.00	4.36	239.3	5.63	6.47	2.89
ENE		0.71	0.82	0.64	0.24	0.01	0.01	0.00	0.00	0.00	0.00	0.00	2.43	133.3	5.97	6.87	3.07
E		1.29	0.83	0.79	0.41	0.01	0.00	0.00	0.00	0.00	0.00	0.00	3.33	182.8	5.75	6.62	2.96
ESE		0.71	0.55	0.70	0.16	0.03	0.00	0.00	0.00	0.00	0.00	0.00	2.16	118.4	6.00	6.90	3.09
SE		1.37	0.99	1.30	0.33	0.16	0.02	0.00	0.00	0.00	0.00	0.00	4.18	229.2	6.41	7.38	3.30
SSE		0.97	0.64	0.78	0.31	0.06	0.03	0.00	0.00	0.00	0.00	0.00	2.79	153.2	6.42	7.39	3.30
S		1.01	0.35	0.44	0.25	0.05	0.02	0.00	0.00	0.00	0.00	0.00	2.11	115.7	5.79	6.66	2.98
SSW		0.40	0.25	0.40	0.36	0.23	0.13	0.01	0.00	0.00	0.00	0.00	1.77	97.2	10.11	11.64	5.20
SW		0.82	0.37	0.80	0.79	0.33	0.17	0.06	0.01	0.00	0.00	0.00	3.35	183.7	10.00	11.51	5.14
WSW		0.59	0.43	1.55	1.37	0.32	0.01	0.01	0.00	0.00	0.00	0.00	4.29	235.6	9.77	11.25	5.03
W		1.18	0.78	4.28	6.24	3.90	2.08	0.27	0.00	0.00	0.00	0.00	18.73	1027.6	13.89	15.99	7.15
WNW		0.89	1.03	5.24	9.31	7.18	2.76	0.38	0.00	0.00	0.00	0.00	26.79	1469.7	14.66	16.87	7.54
NW		1.09	0.88	3.49	5.42	2.85	0.46	0.00	0.00	0.00	0.00	0.00	14.18	777.9	12.32	14.18	6.34
NNW		0.42	0.13	0.44	0.30	0.11	0.04	0.00	0.00	0.00	0.00	0.00	1.43	78.6	8.55	9.84	4.40
VARBL																	
CALM													4.30	235.789	10.88	12.52	5.60
Totals	4.30	13.81	10.58	23.30	25.99	15.52	5.76	0.73	0.01	0.00	0.00	0.00	100.0	5486.7			
Hours per Year	235.8	757.6	580.5	1278.4	1426.2	851.7	316.2	39.8	0.3	0.0	0.0	0.0	***5486.7***				

Total Number of Observations 16460

Table 8. San Francisco wind data in percent occurrence per year by wind direction and speed from 6am – 8pm.

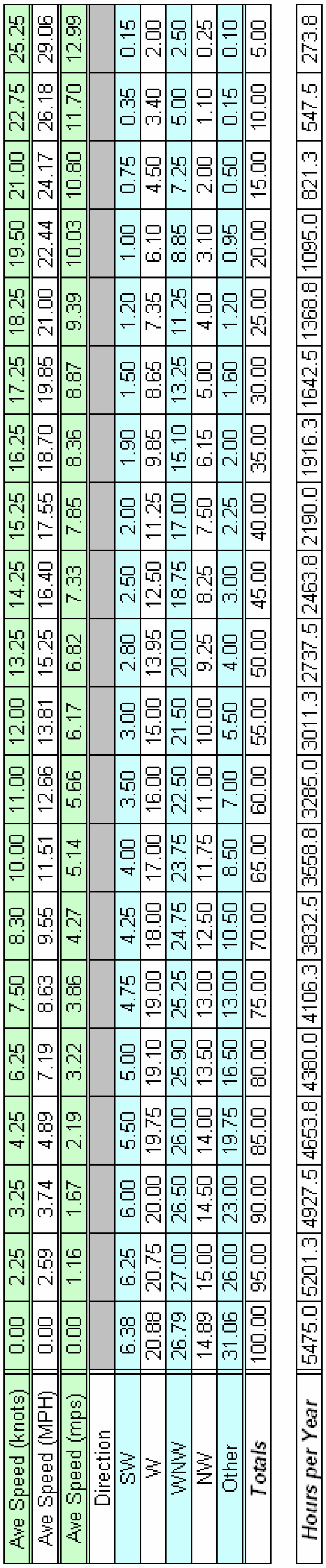

Ave Speed (knots)	0.00	2.25	3.25	4.25	6.25	7.50	8.30	10.00	11.00	12.00	13.25	14.25	15.25	16.25	17.25	18.25	19.50	21.00	22.75	25.25
Ave Speed (MPH)	0.00	2.59	3.74	4.89	7.19	8.63	9.55	11.51	12.66	13.81	15.25	16.40	17.55	18.70	19.85	21.00	22.44	24.17	26.18	29.06
Ave Speed (mps)	0.00	1.16	1.67	2.19	3.22	3.86	4.27	5.14	5.66	6.17	6.82	7.33	7.85	8.36	8.87	9.39	10.03	10.80	11.70	12.99
Direction																				
SW	6.38	6.25	6.00	5.50	5.00	4.75	4.25	4.00	3.50	3.00	2.80	2.50	2.00	1.90	1.50	1.20	1.00	0.75	0.35	0.15
W	20.88	20.75	20.00	19.75	19.10	19.00	18.00	17.00	16.00	15.00	13.95	12.50	11.25	9.85	8.65	7.35	6.10	4.50	3.40	2.00
WNW	26.79	27.00	26.50	26.00	25.90	25.25	24.75	23.75	22.50	21.50	20.00	18.75	17.00	15.10	13.25	11.25	8.85	7.25	5.00	2.50
NW	14.89	15.00	14.50	14.00	13.50	13.00	12.50	11.75	11.00	10.00	9.25	8.25	7.50	6.15	5.00	4.00	3.10	2.00	1.10	0.25
Other	31.06	26.00	23.00	19.75	16.50	13.00	10.50	8.50	7.00	5.50	4.00	3.00	2.25	2.00	1.60	1.20	0.95	0.50	0.15	0.10
Totals	100.00	95.00	90.00	85.00	80.00	75.00	70.00	65.00	60.00	55.00	50.00	45.00	40.00	35.00	30.00	25.00	20.00	15.00	10.00	5.00
Hours per Year	5475.0	5201.3	4927.5	4653.8	4380.0	4106.3	3832.5	3558.8	3285.0	3011.3	2737.5	2463.8	2190.0	1916.3	1642.5	1368.8	1095.0	821.3	547.5	273.8

Table 9. San Francisco wind data in percent exceeded wind speeds from 6am – 8pm, calculated manually.

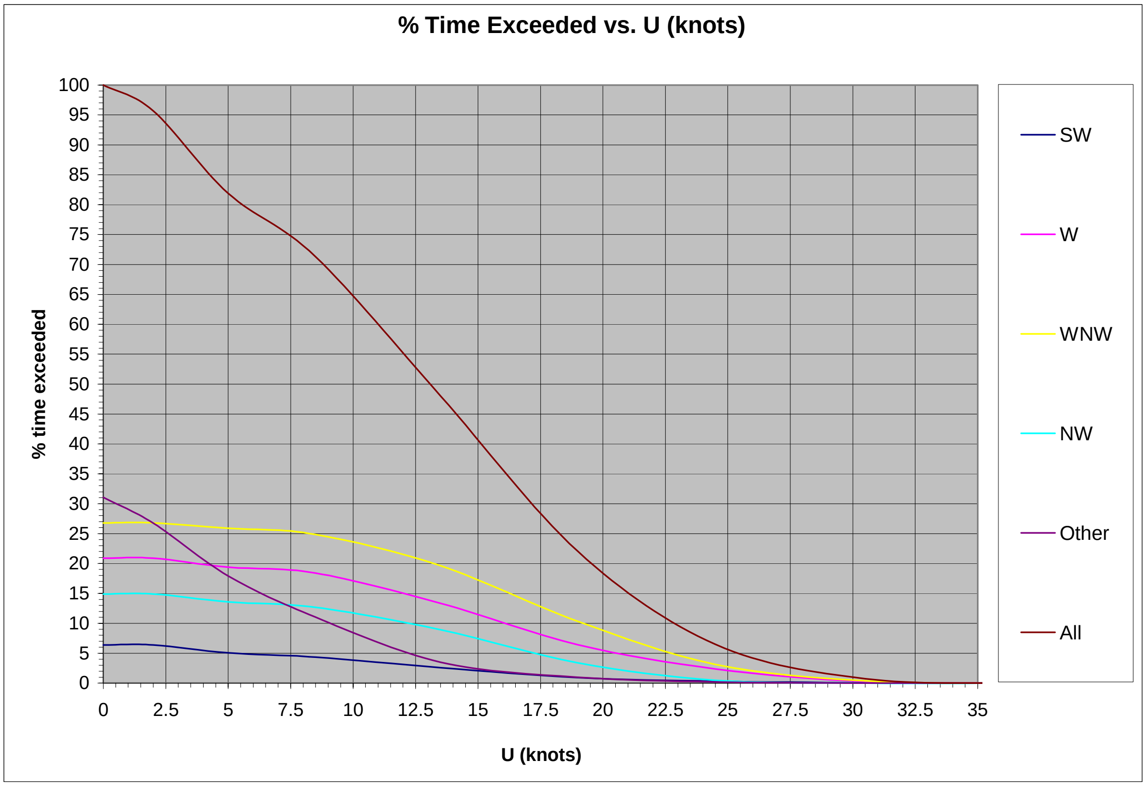

Figure 20. Percent exceeded time versus wind speed (knots as given in original wind charts) from 6am – 8pm.

2.2.2 Atmospheric Stability Conditions

There are various stability conditions that occur within the atmospheric boundary layer. Those stability conditions are illustrated in Table 10. Since no heating or cooling elements are employed in this study, and due to the scale of the boundary layer simulated in the wind tunnel, the wind tunnel simulated only neutrally stable flow conditions. Fortunately, Pasquill (1971) suggests that in strong winds, thermal stratification effects in the lower portion of the boundary layer are negligible as shown in the table. In addition, the tall building structures in the urban areas of San Francisco further add to the mixing within the boundary layer due to the turbulent wakes shedding from the upwind structures. Taking this into consideration, the neutrally stable flow conditions in the wind-tunnel study are realistic.

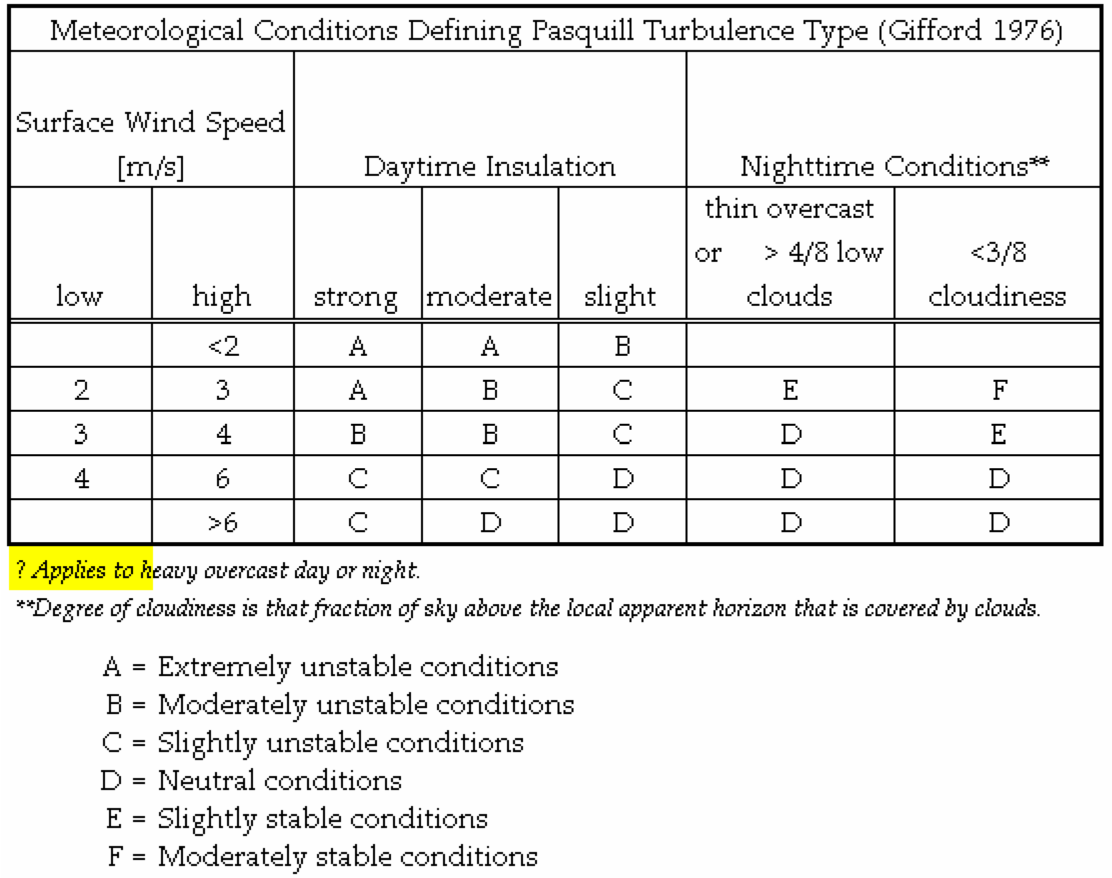

Meteorological Conditions Defining Pasquill Turbulence Type (Gifford 1976)						
Surface Wind Speed [m/s]		Daytime Insulation			Nighttime Conditions**	
low	high	strong	moderate	slight	thin overcast or > 4/8 low clouds	<3/8 cloudiness
	<2	A	A	B		
2	3	A	B	C	E	F
3	4	B	B	C	D	E
4	6	C	C	D	D	D
	>6	C	D	D	D	D

? Applies to heavy overcast day or night.

***Degree of cloudiness is that fraction of sky above the local apparent horizon that is covered by clouds.*

A = Extremely unstable conditions
B = Moderately unstable conditions
C = Slightly unstable conditions
D = Neutral conditions
E = Slightly stable conditions
F = Moderately stable conditions

Table 10. Stability criteria: meteorological conditions defining Pasquill Turbulence Type (Gifford 1976).

2.3 Data Collection

Wind-tunnel measurements of the mean velocity, R-values and turbulence intensity were performed using hotwire anemometry. The hotwire used in this study was a standard Thermo Systems Inc. (TSI) single hotwire sensor, model 1210-60. The sensor was placed at the end of a 50 centimeter TSI probe support, model 1150. The probe support was attached to a platform of a three-dimensional positioning system above the test section of the ABLWT. The probe was connected to a 10 meter long shielded tri-axial cable which ran from the end of the probe support to a TSI model IFA (Intelligent Flow Analyzer) 100, which is a constant temperature thermal-anemometry flow analyzer with included signal conditioner. Each hotwire probe used in this study was calibrated using the ABLWT facility and equipment before testing.

The IFA 100 was run by a LabVIEW software virtual instrument (VI), which initialized and configured the analog-to-digital data acquisition board by United Electronics Inc., linked to a multi-channel daughter board connected to the output of the IFA 100. The multi-channel daughter board was installed in an ISA slot of a PC which digitally stored the raw voltage data from each measurement by saving it under a specified filename.

Each measurement was made by collecting the raw voltages at a sampling rate of 1000 Hz with a total of 30,000 samples in order to satisfy the Nyquist sampling theorem for which the average wind tunnel turbulence signal was 300 Hz. Further information and specifications are located in Appendix B.

2.4 Data Reduction and Analysis

Data reduction and analysis were done in several steps, explained in detail in this section and summarized as follows: first, the raw data was reduced; second, the estimated full-scale speeds were calculated for each measurement location, also referred to as *receptor location* or *point*; next, wind speed information for each point was used to estimate power densities as well as predict annual energy outputs for multiple WECs.

2.4.1 Reducing the Raw Data

Since the raw data acquired by LabVIEW was collected in the form of one file with 30,000 voltage readings for each measurement taken, a Quick Basic code was used to run each reading of the raw data through the calibration of the hotwire to obtain a wind speed for each measurement point. The code then calculates the *wind speed ratio* and *turbulence intensity values* for each measurement. The wind speed ratio (R- value), is defined as the ratio of the wind tunnel velocity at the measurement location over the wind tunnel velocity at the reference height, which in this case is 0.70 meters (2.3 feet), and the turbulence intensity is defined as the "root mean square of the instantaneous deviations from the mean velocity, divided by the mean velocity" (Arens 1989).

2.4.2 Estimated Full-scale Speed Calculations

After the raw data is reduced into R-values and the percent exceeded wind speeds are determined for each wind direction for the full-scale, the estimated full-scale speeds are calculated. All calculations were done using an Excel® spreadsheet. The definitions below are used to describe the variables used in the following equations:

- $U_{\%}$ = the percent exceeded wind speed; for example, $U_{10\%}$ is the wind speed exceeded 10% of the time in a typical year.
- $t_{\%direction}$ = the percentage of time $U_{\%}$ is exceeded for the specified wind direction; for example, $t_{75\%SW}$ is the percentage of time winds from the southwest exceed $U_{75\%}$.

- $R_{direction}$ = the R-value of one point for the specified wind direction; for example, R_{WNW} is the R-value of a single point for the west-northwest wind direction.
- $CF_{direction}$ = the correction factor for a specified wind direction; for example, CF_{W} is the correction factor to be applied west winds.
- U_{point} = the wind speed at the point.
- U_{ref} = the reference wind speed.
- U_{∞} = free stream wind speed.
- $U_{geostropic}$ = the geostropic wind speed.
- z_{ref} = the height corresponding to Uref, which for full-scale is 40.2 meters (132 feet), or the height of the anemometer on the Old Federal Building (White 1992).
- z_{point} = the height corresponding to U_{point}.
- δ = the boundary layer height, which is 402.3 meters (1320 feet) for San Francisco (White 1992).
- α = the power-law exponent, which is 0.3 for San Francisco (White 1992).
- The subscript “direction” shall denote that the value is for one wind direction. The actual wind direction in consideration may also be used instead of the word “direction”.
- The subscript “wind tunnel” refers to wind tunnel data.
- The subscript “full-scale” refers to full-scale values.

The power-law is used to show the relationship of full-scale wind speeds to measured wind speeds in the wind tunnel:

$$\left(\frac{U_{\text{point}}}{U_{\text{ref}}}\right)_{\text{Full Scale}} = \left(\frac{U_{\text{point}}}{U_{\text{ref}}}\right)_{\text{Wind Tunnel}} = \left(\frac{z_{\text{point}}}{z_{\text{ref}}}\right)^{\alpha} \tag{1}$$

Rearranging the variables and incorporating U_∞ yields (White, 1992):

$$\begin{gathered}\left(U_{\text{point}}\right)_{\text{Full Scale}} = \left(U_{\text{point}}\right)_{\text{Wind Tunnel}} \cdot \frac{\left(U_{\text{ref}}\right)_{\text{Full Scale}}}{\left(U_{\text{ref}}\right)_{\text{Wind Tunnel}}} \rightarrow \\ \left(U_{\text{point}}\right)_{\text{Full Scale}} = \left(\frac{U_{\text{point}}}{U_\infty}\right)_{\text{Wind Tunnel}} \cdot \left(U_{\text{ref}}\right)_{\text{Wind Tunnel}} \cdot \left(\frac{U_\infty}{\text{Uref}}\right)_{\text{Wind Tunnel}}\end{gathered} \tag{2}$$

By definition, $(U_{\text{point}}/U_{\text{ref}})$ is the R-value. However, wind tunnel data is not accurate at the level of U_∞ due to the Coriolis effect in full-scale (White 1992). Therefore, it is desired to have another relationship between all of these variables. Wind tunnel data collected by testing a model of the old Federal Building shows that $(U_\infty/U_{\text{ref}})$ is equal to 2. Using the information for the boundary layer height, the height of the reference velocity and power-law exponent for San Francisco, the power-law yields the following (White 1992):

$$\left(\frac{U_{\text{ref}}}{U_{\text{geostropic}}}\right)_{\text{Full Scale}} = \left(\frac{z_{\text{ref}}}{\delta}\right)^{\alpha} = 0.5 \quad \text{or} \quad \left(\frac{U_{\text{geostropic}}}{U_{\text{ref}}}\right)_{\text{Full Scale}} = 2 \tag{3}$$

which correlates quite well with the wind tunnel results described above. Substituting this finding into the above equations gives the relationship between the reference wind speed, R-value and full-scale speed at a specific point with wind from one wind direction (White, 1992):

$$\left(U_{\text{point}}\right)_{\text{Full Scale}} = 2 \cdot R \cdot \left(U_{\text{ref}}\right)_{\text{Full Scale}} \tag{4}$$

Since the only R-values obtained were for the four wind directions tested, the R-value for the others was calculated as the weighted average of the R-values from the tested wind directions:

$$R_{\text{others}} = \frac{R_{NW} \cdot t_{\%NW} + R_{WNW} \cdot t_{\%WNW} + R_{W} \cdot t_{\%W} + R_{SW} \cdot t_{\%SW} + R_{\text{others}} \cdot t_{\%\text{others}}}{t_{\%NW} + t_{\%WNW} + t_{\%W} + t_{\%SW} + t_{\%\text{others}}} \tag{5}$$

While the wind data for San Francisco between 1945 and 1947 was taken by an anemometer on top of the Federal Building, the surrounding buildings were close enough to the Federal Building to influence the anemometer readings. In order to find a correction for the changes in wind speeds due to the influence of these buildings, the model of the old Federal Building area was tested in the wind tunnel. It was found that the speeds at the points in questions should be multiplied by a *correction factor*, or CF, for each of the various wind directions tested to account for these influences (White 1992). These correction factors are 1.02 for northwest, 1.00 for west-northwest, 0.96 for west, 0.85 for southwest and 0.96 for all other wind directions. Since Tables 6 through 9 illustrate the wind conditions at the height of the anemometer on top of the Federal Building as the area existed from 1945 to 1947, these correction factors were applied to the reduced data, and the new equation to determine the full-scale speed at a specific point becomes (White 1992):

$$\left(U_{\text{point}_{\text{direction}}}\right)_{\text{Full Scale}} = 2 \cdot R_{\text{direction}} \cdot CF_{\text{direction}} \cdot \left(U_{\text{ref}}\right)_{\text{Full Scale}} \tag{6}$$

The U_{point} input into the equation can either be a regular speed from the San Francisco wind data, or can be in the form of $U_{\%}$ to obtain the exceeded wind speed at the point. This was done for this study's analysis, and the percent exceeded wind speed was found for each direction, northwest, west-northwest, west, southwest and others, and each point, in increments of five-percent time exceeded (i.e. percent exceedences ranged from 5- to 100-percent in increments of 5-percent). Once these values were obtained, the weighted average was calculated to find the average *estimated full-scale* (or EFS) percent exceeded wind speed for all wind directions. This calculation was performed for each point. The weighted average calculation was conducted as follows:

$$U_{\%\text{EFS}} = \frac{U_{\%\text{NW}} \cdot t_{\%\text{NW}} + U_{\%\text{WNW}} \cdot t_{\%\text{WNW}} + U_{\%\text{W}} \cdot t_{\%\text{W}} + U_{\%\text{SW}} \cdot t_{\%\text{SW}} + U_{\%\text{others}} \cdot t_{\%\text{others}}}{t_{\%\text{NW}} + t_{\%\text{WNW}} + t_{\%\text{W}} + t_{\%\text{SW}} + t_{\%\text{others}}} \tag{7}$$

At this point, only the percent exceeded wind speeds are known. In order to calculate the wind speeds at each point through a power curve of a specific WEC or to obtain power densities, the wind speed histogram needs to be constructed for each point. It is reasonable to say that if a wind speed of 5 meters per second is exceeded 80-percent of the time, and a wind speed of 6 meters per second is exceeded 75-percent of the time, then there is a wind speed between 5 and 6 meters per second that occurs for 5-percent of the time in one year.

It was most reasonable for the scope of this study to take the average of the two exceeded speeds rather than fit a curve through each data point and get a more precise analytical solution. Therefore, the percent exceeded wind speed data was transformed into a histogram by inputting values into the following equation, where the subscript "%" is the still the percent exceeded (there are a total of 20 *bins*, as noted before, ranging from zero-percent exceeded to one-hundred-percent exceeded), starting from $U_{100\%}$:

$$U = \frac{U_{\%} + U_{\%\text{-}5\%}}{2} \tag{8}$$

for the time duration, in percent time per year, of $t = t_{\%+5\%} - t_{\%}$, which is always five-percent due to the even spacing of the percent exceeded time bins. Also, since there is no calculation past the five-percent exceeded wind speed, a value for zero-percent exceeded wind speed was chosen by adding two meters per second to the speed in the five-percent exceeded case. When reviewing the wind data, it appeared that no speeds were recorded for more than two meters per second past the value in the five-percent exceeded bin. The result of these calculations is a histogram with the average wind speed for every five-percent of time in one year, or twenty wind speeds that each occur for five-percent of the time in one year, for each point measured in the wind tunnel.

2.4.3 Error Estimates

Since the meteorological wind data for San Francisco used in this study had large wind bins, as illustrated in Tables 6 and 8, it was necessary to manually convert the wind data to fit into smaller wind bins. In doing so, one value must be chosen to represent the wind speed for any given wind bin to perform further analysis. A typical way to do this is to select the average value in the bin, or the midpoint between the lowest and highest wind speeds in the bin. Such was the case in this study. The total variation in the possible selection of the wind speed's value is then equal to the maximum wind speed, U_{i+1}, in that bin minus the minimum wind speed, U_i, in that bin. Therefore, the error in any wind power calculated by converting percent exceeded wind speed to the wind speed used to run through the power curves can be estimated by taking the cube of the differences of the exceeded wind speeds, divided by the cube of the average and summing all twenty occurrences:

$$\text{estimated error in power} = \sum_{i=1}^{20} \frac{\left(U_{i+1} - U_i\right)^3}{\left(\frac{U_{i+1} + U_i}{2}\right)^3} \tag{9}$$

It is generally accepted that hotwire measurements made close to a surface are within ±5% of the true values, the calibration of the hotwire is within ±2% accuracy and the data acquisition process is 99.95% efficient (White 1989).

2.4.4 Wind Power Density Calculations

It is important to utilize quantifiable standards wherever possible. In the case of wind energy generation, the *wind power density* and *average wind power density* calculations give a good understanding of resource at a specific location. The wind power density is the available power in the wind per unit area perpendicular to the wind; if a WEC has an efficiency of 100%, this is the amount of power it would produce for each unit area perpendicular to the flow (Manwell 2003):

$$\frac{P}{A} = \frac{1}{2}\rho U^3 \tag{10}$$

where P is power, A is the unit cross-sectional area, ρ is the density of air, and U is the speed of air perpendicular to the area. The total annual energy density can be calculated by taking the histogram of speed versus hours of occurrence per year for each point measured in the wind tunnel and inputting each speed into the above equation, then multiplying it by the number of hours each speed occurs and summing the values (the resulting number is in kilowatt-hours per meter squared, per year):

$$\frac{E_{\text{annual}}}{A} = \sum_{i=1}^{8760} \frac{1}{2} \rho U_i^3 \tag{11}$$

The average wind power density is used to classify the "quality" of a wind site. It takes into account the wind data at the site and performs a weighted averaging scheme to come up with a qualitative value for the site's resource (Manwell 2003):

$$\frac{\overline{P}}{A} = \frac{1}{2} \rho \overline{U}^3 \cdot K_e \quad \text{where} \quad K_e = \frac{1}{8760 \cdot \overline{U}^3} \sum_{i=1}^{8760} U_i^3 \Delta t \tag{12}$$

i is each hour in a year, Δt is the time elapsed for each i term (one hour, in this case), $\overline{U}$ is the annual average wind speed and K_e is called the *energy pattern factor*. Manwell (2003) classifies the wind resource quality from average wind power density into the following categories:

- $\frac{\overline{P}}{A} < 100 \frac{W}{m^2} \rightarrow$ poor
- $\frac{\overline{P}}{A} \approx 400 \frac{W}{m^2} \rightarrow$ good
- $\frac{\overline{P}}{A} > 700 \frac{W}{m^2} \rightarrow$ great

This value then can be calculated for each measurement location on each building so show where the "great" wind sites are. These are the most likely places to place an anemometer for future studies since they may be of interest to potential urban wind farm developers.

2.4.5 Average 1kW Turbine Power Production

Although it is uncertain whether horizontal axis wind turbines (versus vertical axis turbines or other forms of urban WECs) will be permitted for use in urban areas, since horizontal axis wind turbines are a prevailing WEC, it is useful to see what power could be produced by one at in an urban environment for comparison purposes. A reasonable size horizontal axis wind turbine to be placed in an urban environment is a 1kW wind turbine. Since there are many 1kW turbine models available and it is not desired to advertise any specific brand in this study whenever possible, an average 1kW wind turbine power curve was created by averaging the power curves of several 1kW wind turbines, resulting in the power curve shown in Figure 21, which also includes the power curve for an Aeroturbine WEC as depicted on the Aerotecture International, Inc. website found in the References of this report.

A *cut-in* speed of 2.5 meters per second was chosen for this simulation wind turbine, meaning that even if the power curve shows power production available before 2.5 meters per second, the actual power produced will be zero until a wind speed of 2.5 meters per second is reached at the site. The *cut-out* speed for each of the turbines used for the average either did not exist or was around 30 meters per second, so the cut-out speed for the average 1kW wind turbine was chosen to have no cut-out speed since few points exceeded a speed of 30 meters per second or above. Maximum power production of 1080 Watts occurs at 12.5 meters per second.

By considering each measurement location in the wind tunnel to be an individual wind site, as was done in previous sections of this report, the annual energy production of this turbine can be calculated at each measurement location on each building. This is done by finding the corresponding power production for a given wind speed from Figure 21 and multiplying it by the number of hours that speed occurs at the site. For this study, each average wind speed occurred for five-percent of the time over a typical year in the city of San Francisco; therefore, there were twenty discrete velocities used to calculate the annual energy production at a measurement location (or point on a building) all occurring for equal percentages of time during the year:

$$\text{Annual Energy Production in kW - hours per year} = \left(\frac{1}{20}\right) \cdot 8760 \cdot \sum_{i=1}^{20} P\left(U_i\right) \tag{13}$$

where P(U) is the power production at the speed, U_i.

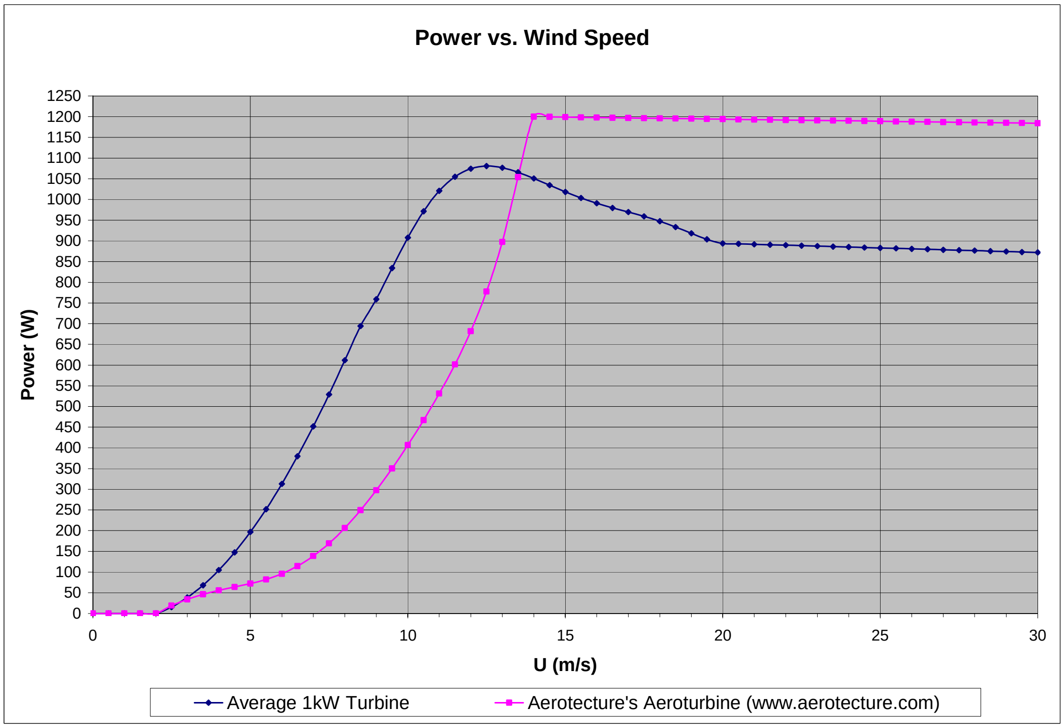

Figure 21. Power curves for an average 1kW horizontal axis wind turbine and an Aerotecture WEC.

2.4.6 Urban Wind Energy Converter Power Production

Since the Aerotecture's Aeroturbine WEC was one of the only WECs designed specifically for an urban environment that had a published power curve, illustrated in Figure 21, and specifications available, it was chosen for comparison against the average 1kW wind turbine. The purpose of this analysis is not to promote the Aeroturbine, but to have a relative comparison of power production between a well-known type of wind turbine, which is not typically designed to be used in an urban environment, with a WEC that is designed for that purpose. The Aeroturbine has a cut-in speed of 2.5 meters per second, and a maximum power production of 1200 Watts at 14 meters per second The calculations for annual power production were calculated in the same manner as they were for the average 1kW wind turbine, only using the power curve for the Aeroturbine instead of the curve for the average 1kW wind turbine.

3.0 Results

All of the following results presented in were calculated using the equations 1 through 13. Results are presented by area: Fox Plaza, the Bank of America and CSAA Buildings' results are grouped together as the "10th and Market Street Buildings". The Folsom and Main East and West buildings are grouped together as the "Folsom and Main Street Buildings".

3.1 10th and Market Street Buildings' Results

Results for each of the buildings in the area of 10th Street and Market Street are presented in two tables. The first table shows all points with "good" average wind power densities. The table identifies, in the following order, the point, height above ground level, then for the existing setting, the average wind power density, annual power produced by the average 1kW wind turbine, annual energy produced by Aerotecture's Aeroturbine, the maximum turbulence intensity for all wind directions, the average turbulence intensity and the estimated error in calculating power production. The cumulative setting results for the same point are displayed in the next few columns of data. Any turbulence intensities above 50 percent are marked with red, bold faced text. The final column of data shows the ratio of the cumulative setting's average wind power density to the existing setting's average wind power density. This ratio will show how building developments could change the power production of a WEC located at that point. Values under 0.95 are marked with red, bold faced text, and values above 1.05 are marked with bold faced text.

Results for the Folsom and Main Street Buildings are the same as for the 10th and Market Street Buildings' results, except that there are no values for the cumulative setting since that setting was not wind-tunnel tested for those buildings.

3.1.1 Fox Plaza Results

The “good” wind resource points’ results of the wind-tunnel testing for Fox Plaza are shown in Table 11, and the “great” wind resource points’ results are in Table 12.

Average wind power densities were highest near or above the roof level. The highest average wind power density was 1629.1 Watts per square meter at point 105125 for the existing setting, and 1488.3 for the cumulative setting. The northern face of the building is a “great” wind resource due to its high average wind power density from point 3 to point 8. The point that showed the most increase in average wind power density due to local development was point 7 which had an increase of 36-percent, and the point that showed the most decrease was point 102375 which had a decrease of 26-percent.

The highest turbulence intensity for the existing setting of a point with “good” or “great” wind resource was point 101000 with 67.4 percent; this point also held the highest value for cumulative setting, at 70.5 percent. The average average wind power density for Fox Plaza was 466.61 Watts per square meter for the existing setting and 448.81 Watts per square meter for the cumulative setting, meaning that there could be an overall decrease in power production at this building if the city chooses to develop in this area.

"Good" Wind Resource Locations - Fox Plaza

	Existing Setting						Cumulative Setting						
Point #	Height Above Ground [m]	Average Wind Power Density [W/m^2]	Average 1kW Wind Turbine Annual Power Production [kW-hr/year]	Aerotecture WEC Annual Power Production [kW-hr/year]	Maximum Turbulence Intensity [%]	Turbulence Intensity [%]	Estimated Error in Power Calculations [%]	Average Wind Power Density [W/m^2]	Average 1kW Wind Turbine Annual Power Production [kW-hr/year]	Aerotecture WEC Annual Power Production [kW-hr/year]	Maximum Turbulence Intensity [%]	Turbulence Intensity [%]	Estimated Error in Power Calculations [%]	Ratio of Cumulative Setting to Existing Setting Average Wind Power Density
1	0.00	415.8	4045.8	2252.0	**66.6**	27.0	5.05	373.4	3847.4	2144.3	**54.2**	27.5	5.01	**0.90**
2	15.24	636.7	4732.2	3076.3	49.6	22.7	6.55	578.8	4565.6	2962.7	**52.4**	24.9	4.95	**0.91**
37	91.44	465.6	4390.4	2547.4	45.6	25.0	4.63	625.8	4800.9	3226.0	41.9	24.1	6.21	**1.34**
64	45.72	403.9	4210.7	2293.2	37.8	24.3	4.59	421.1	4207.4	2415.6	34.5	22.8	4.72	1.04
65	60.96	564.9	4723.7	2970.2	37.0	22.6	6.21	554.0	4652.0	2984.8	36.7	23.0	6.25	0.98
66	76.20	493.5	4512.4	2729.1	37.4	22.0	4.65	490.8	4476.5	2758.4	35.0	22.6	4.68	0.99
67	91.44	638.9	4838.9	3188.9	48.9	26.2	6.21	644.8	4847.2	3276.3	40.2	24.4	6.21	1.01
77	91.44	419.0	4078.3	2264.5	35.5	22.7	4.92	430.8	4138.0	2405.3	36.8	24.1	4.91	1.03
102375	102.87	902.5	5382.2	3953.3	**54.0**	47.9	6.01	669.9	5045.5	3447.4	**58.8**	48.0	5.94	**0.74**
104125	95.25	712.0	5023.5	3389.2	45.1	26.5	6.07	598.0	4817.4	3160.0	42.7	27.6	6.02	**0.84**

"Great" Wind Resource Locations - Fox Plaza

	Existing Setting						Cumulative Setting						
Point #	Height Above Ground [m]	Average Wind Power Density [W/m^2]	Average 1kW Wind Turbine Annual Power Production [kW-hr/year]	Aerotecture WEC Annual Power Production [kW-hr/year]	Maximum Turbulence Intensity [%]	Turbulence Intensity [%]	Estimated Error in Power Calculations [%]	Average Wind Power Density [W/m^2]	Average 1kW Wind Turbine Annual Power Production [kW-hr/year]	Aerotecture WEC Annual Power Production [kW-hr/year]	Maximum Turbulence Intensity [%]	Turbulence Intensity [%]	Estimated Error in Power Calculations [%]	Ratio of Cumulative Setting to Existing Setting Average Wind Power Density
3	30.48	710.2	4901.7	3264.4	49.8	21.6	6.51	702.7	4832.2	3314.0	45.3	23.6	6.59	0.99
4	45.72	800.6	5020.4	3452.6	45.6	22.3	6.59	771.5	4968.1	3497.9	40.0	25.2	6.56	0.96
5	60.96	870.6	5106.3	3619.9	49.5	23.8	6.62	817.5	5024.8	3603.2	39.2	24.6	6.60	**0.94**
6	76.20	743.6	4899.4	3285.7	**54.7**	25.4	6.62	730.6	4882.2	3379.0	47.6	26.8	6.59	0.98
7	91.44	756.4	4914.5	3314.6	49.1	27.0	6.62	1030.4	5255.5	4027.8	**52.1**	29.6	6.70	**1.36**
8	102.87	1149.2	5442.5	4238.3	**51.9**	23.2	6.56	1067.8	5371.4	4196.2	**56.0**	26.0	6.52	**0.93**
875	91.44	734.6	4998.7	3364.1	47.2	33.2	6.32	701.5	4956.9	3411.5	**56.6**	37.0	6.23	0.96
101000	102.87	1542.3	5796.4	4948.0	**67.4**	47.5	9.83	1287.8	5637.4	4765.3	**70.5**	42.1	6.19	**0.83**
101125	106.68	1418.0	5740.0	4756.4	35.1	19.9	6.19	1372.5	5711.3	4833.6	32.0	19.6	6.17	0.97
101250	110.49	1334.4	5682.6	4670.2	30.1	17.8	6.19	1312.1	5653.3	4741.1	31.0	19.0	6.21	0.98
101375	114.30	1329.5	5668.5	4645.2	29.3	17.9	6.22	1241.2	5600.2	4603.0	30.8	18.7	6.22	**0.93**
101500	118.11	1385.1	5708.5	4703.6	28.0	17.5	6.21	1320.4	5666.0	4768.4	27.9	17.9	6.20	0.95
102375	102.87	902.5	5382.2	3953.3	**54.0**	47.9	6.01	669.9	5045.5	3447.4	**58.8**	48.0	5.94	**0.74**
102500	106.68	1552.9	5833.5	4996.3	43.4	28.5	9.56	1412.2	5741.4	4917.1	40.3	29.5	6.08	**0.91**
103125	106.68	1566.3	5828.6	4998.5	42.4	27.5	9.62	1488.3	5784.2	5010.6	32.3	25.7	9.62	0.95
103250	110.49	1333.8	5679.6	4664.7	39.8	21.7	6.15	1269.0	5630.3	4700.3	30.4	19.0	6.15	0.95
103375	114.30	1289.7	5648.0	4607.9	38.6	20.1	6.16	1237.8	5603.3	4628.4	30.5	18.3	6.17	0.96
103500	118.11	1326.9	5675.5	4650.1	37.5	19.6	6.16	1248.5	5614.3	4646.1	31.4	17.7	6.18	**0.94**
104125	95.25	712.0	5023.5	3389.2	45.1	26.5	6.07	598.0	4817.4	3160.0	42.7	27.6	6.02	**0.84**
104250	99.06	834.7	5224.6	3744.6	42.6	22.4	6.06	903.0	5299.7	3993.8	37.2	21.6	6.09	**1.08**
104375	102.87	916.6	5321.1	3898.6	39.1	20.9	6.09	896.9	5288.8	3973.6	32.6	18.6	6.09	0.98
104500	106.68	936.9	5335.6	3931.2	37.3	19.7	6.09	928.5	5324.4	4038.4	34.7	18.7	6.10	0.99
105125	106.68	1629.1	5879.6	5085.3	44.8	27.2	9.55	1402.9	5752.6	4929.0	41.7	28.4	6.03	**0.86**
105250	110.49	1296.7	5669.2	4653.0	40.4	21.4	6.11	1296.8	5660.7	4770.7	37.2	21.3	6.12	1.00
105375	114.30	1258.0	5629.9	4547.5	38.8	19.8	6.15	1145.1	5541.3	4487.1	32.8	18.6	6.13	**0.91**
105500	118.11	1281.1	5651.1	4602.1	35.9	19.4	6.14	1153.4	5543.5	4490.0	34.0	18.8	6.14	**0.90**

Table 11. Results for "good" points at Fox Plaza (shown left).
Table 12. Results for "great" points at Fox Plaza (shown right).

Fox Plaza Results with Winds from 6am – 8pm

The reduced, full-scale data for Fox Plaza for winds from 6am to 8pm are displayed in the same manner as in the previous section. The "good" wind resource points' results of the wind-tunnel testing for the Fox Plaza are shown in Table 13, and the "great" wind resource points' results are in Table 14. Tables 15a and 15b show the ratio of the average wind speed densities of 6am to 8pm case to the all hours' case for each point tested.

The point with the highest average wind power density during the hours of 6am to 8pm (the 15-hour day case) for the existing setting was point 105125 which had a value of 2067.29 Watts per square meter, and the same point held the highest value, 1777.63 Watts per square meter, for the cumulative setting, All points showed an increase in average wind power density from the 24-hour day case, demonstrating that the winds are higher during business hours.

"Good" Wind Resource Locations - Fox Plaza - 6am - 8pm													
	Existing Setting						Cumulative Setting						
Point #	Height Above Ground [m]	Average Wind Power Density [W/m²]	Average 1kW Wind Turbine Annual Energy Production [kW-hr/year]	Aerotecture WEC Annual Energy Production [kW-hr/year]	Maximum Turbulence Intensity [%]	Turbulence Intensity [%]	Estimated Error in Ave. Wind Power Density [%]	Average Wind Power Density [W/m²]	Average 1kW Wind Turbine Annual Energy Production [kW-hr/year]	Aerotecture WEC Annual Energy Production [kW-hr/year]	Maximum Turbulence Intensity [%]	Turbulence Intensity [%]	Estimated Error in Ave. Wind Power Density [%]	Ratio of Cumulative Setting to Existing Setting Average Wind Power Density
1	0.00	528.2	2956.0	1749.5	**66.6**	27.0	7.57	470.8	2828.4	1666.6	**54.2**	27.4	7.51	**0.89**
25	60.96	452.4	2790.3	1543.6	43.4	36.0	7.34	362.7	2494.3	1324.2	46.2	34.5	3.89	**0.80**
37	91.44	589.6	3187.8	1972.0	45.6	24.7	7.13	796.7	3424.2	2463.4	41.9	23.8	7.23	**1.35**
61	0.00	449.8	2875.9	1590.8	39.1	24.1	7.43	508.4	2967.1	1811.7	37.5	23.8	7.46	**1.13**
62	15.24	480.3	2968.0	1685.6	37.9	24.3	7.32	481.8	2951.1	1731.1	38.5	26.9	7.36	1.00
63	30.48	498.7	3038.7	1750.6	38.8	25.6	7.23	471.6	2934.3	1696.9	38.9	25.7	7.33	**0.95**
64	45.72	521.9	3083.5	1823.2	37.8	24.1	7.23	540.2	3072.3	1898.9	34.5	22.6	7.32	1.04
66	76.20	638.4	3257.9	2105.3	37.4	21.8	7.29	634.4	3238.9	2143.9	35.0	22.4	7.33	0.99
77	91.44	521.8	2980.2	1753.8	35.5	22.5	7.29	535.4	3017.4	1843.8	36.8	23.9	7.25	1.03

"Great" Wind Resource Locations - Fox Plaza - 6am - 8pm													
	Existing Setting						Cumulative Setting						
Point #	Height Above Ground [m]	Average Wind Power Density [W/m²]	Average 1kW Wind Turbine Annual Energy Production [kW-hr/year]	Aerotecture WEC Annual Energy Production [kW-hr/year]	Maximum Turbulence Intensity [%]	Turbulence Intensity [%]	Estimated Error in Ave. Wind Power Density [%]	Average Wind Power Density [W/m²]	Average 1kW Wind Turbine Annual Energy Production [kW-hr/year]	Aerotecture WEC Annual Energy Production [kW-hr/year]	Maximum Turbulence Intensity [%]	Turbulence Intensity [%]	Estimated Error in Ave. Wind Power Density [%]	Ratio of Cumulative Setting to Existing Setting Average Wind Power Density
2	15.24	817.5	3366.4	2345.3	49.6	22.6	7.57	741.3	3272.7	2266.9	**52.4**	24.8	7.57	**0.91**
3	30.48	910.8	3463.1	2509.9	49.8	21.5	7.52	897.9	3421.9	2537.0	45.3	23.4	7.59	0.99
4	45.72	1024.4	3523.5	2648.3	45.6	22.1	7.58	985.6	3495.7	2672.4	40.0	25.0	7.56	0.96
5	60.96	1111.9	3572.7	2753.7	49.5	23.6	7.61	1043.0	3527.0	2748.9	39.2	24.4	7.59	**0.94**
6	76.20	949.6	3455.9	2521.0	**54.7**	25.2	7.62	932.3	3448.1	2583.7	47.6	26.5	7.59	0.98
7	91.44	966.2	3464.8	2542.4	49.1	26.7	7.62	1313.7	3643.7	3037.6	**52.1**	29.3	10.70	**1.36**
8	102.87	1461.5	3746.6	3140.5	**51.9**	22.9	10.51	1357.3	3709.8	3134.5	**56.0**	25.7	10.48	**0.93**
37	91.44	589.6	3187.8	1972.0	45.6	24.7	7.13	796.7	3424.2	2463.4	41.9	23.8	7.23	**1.35**
65	60.96	731.7	3381.8	2300.1	37.0	22.4	7.27	713.9	3336.9	2303.6	36.7	22.8	7.31	0.98
67	91.44	815.7	3445.8	2440.7	48.9	25.8	7.24	821.7	3449.4	2518.1	40.2	24.2	7.24	1.01
875	91.44	934.4	3522.5	2586.6	47.2	33.0	7.32	891.4	3505.5	2616.0	**56.6**	36.7	7.24	0.95
101000	102.87	1986.8	3921.0	3610.2	**67.4**	47.4	10.31	1653.3	3850.2	3493.3	**70.5**	41.7	10.21	**0.83**
101125	106.68	1784.4	3896.5	3504.7	35.1	19.7	10.09	1725.0	3884.1	3540.1	32.0	19.4	10.06	0.97
101250	110.49	1678.1	3869.9	3412.9	30.1	17.6	10.09	1650.9	3855.4	3463.7	31.0	18.9	10.11	0.98
101375	114.30	1674.1	3862.3	3399.2	29.3	17.7	10.12	1560.0	3827.9	3389.9	30.8	18.5	10.12	**0.93**
101500	118.11	1744.9	3881.3	3460.6	28.0	17.4	10.12	1661.5	3861.8	3478.4	27.9	17.8	10.10	0.95
102375	102.87	1148.3	3737.3	3005.4	**54.0**	47.9	9.94	841.5	3564.6	2629.7	**58.8**	48.1	6.90	**0.73**
102500	106.68	1971.9	3949.0	3644.1	43.4	28.3	10.04	1790.3	3902.2	3605.7	40.3	29.4	10.04	**0.91**
103125	106.68	1993.9	3945.3	3644.1	42.4	27.3	10.10	1888.6	3919.2	3653.8	32.3	25.6	10.09	**0.95**
103250	110.49	1692.9	3870.8	3441.0	39.8	21.4	10.11	1608.4	3846.6	3451.3	30.4	18.9	10.10	0.95
103375	114.30	1634.4	3854.8	3388.2	38.6	19.8	10.11	1566.4	3831.9	3410.9	30.5	18.1	10.11	0.96
103500	118.11	1679.4	3867.9	3423.9	37.5	19.3	10.10	1577.7	3836.6	3418.7	31.4	17.5	10.11	**0.94**
104125	95.25	906.3	3552.1	2612.9	45.1	26.2	7.12	757.4	3440.6	2434.1	42.7	27.4	7.04	**0.84**
104250	99.06	1060.7	3656.5	2843.6	42.6	22.2	10.01	1147.5	3691.5	3026.1	37.2	21.4	10.05	**1.08**
104375	102.87	1162.9	3702.9	2965.9	39.1	20.6	10.03	1137.5	3685.7	3008.5	32.6	18.4	10.04	0.98
104500	106.68	1187.3	3711.1	2993.3	37.3	19.4	10.03	1175.9	3704.7	3058.4	34.7	18.5	10.03	0.99
105125	106.68	2067.3	3968.8	3710.5	44.8	26.9	10.03	1777.5	3909.3	3614.0	41.7	28.2	9.98	**0.86**
105250	110.49	1643.5	3866.9	3415.5	40.4	21.1	10.05	1642.0	3862.6	3489.8	37.2	21.1	10.06	1.00
105375	114.30	1590.9	3845.5	3355.1	38.8	19.5	10.09	1449.9	3804.7	3342.3	32.8	18.4	10.07	**0.91**
105500	118.11	1621.4	3856.6	3385.1	35.9	19.2	10.08	1457.3	3804.8	3341.7	34.0	18.6	10.07	**0.90**

Table 13. Results for "good" points at Fox Plaza from 6am – 8pm (shown left).
Table 14. Results for "great" points at Fox Plaza from 6am – 8pm (shown right).

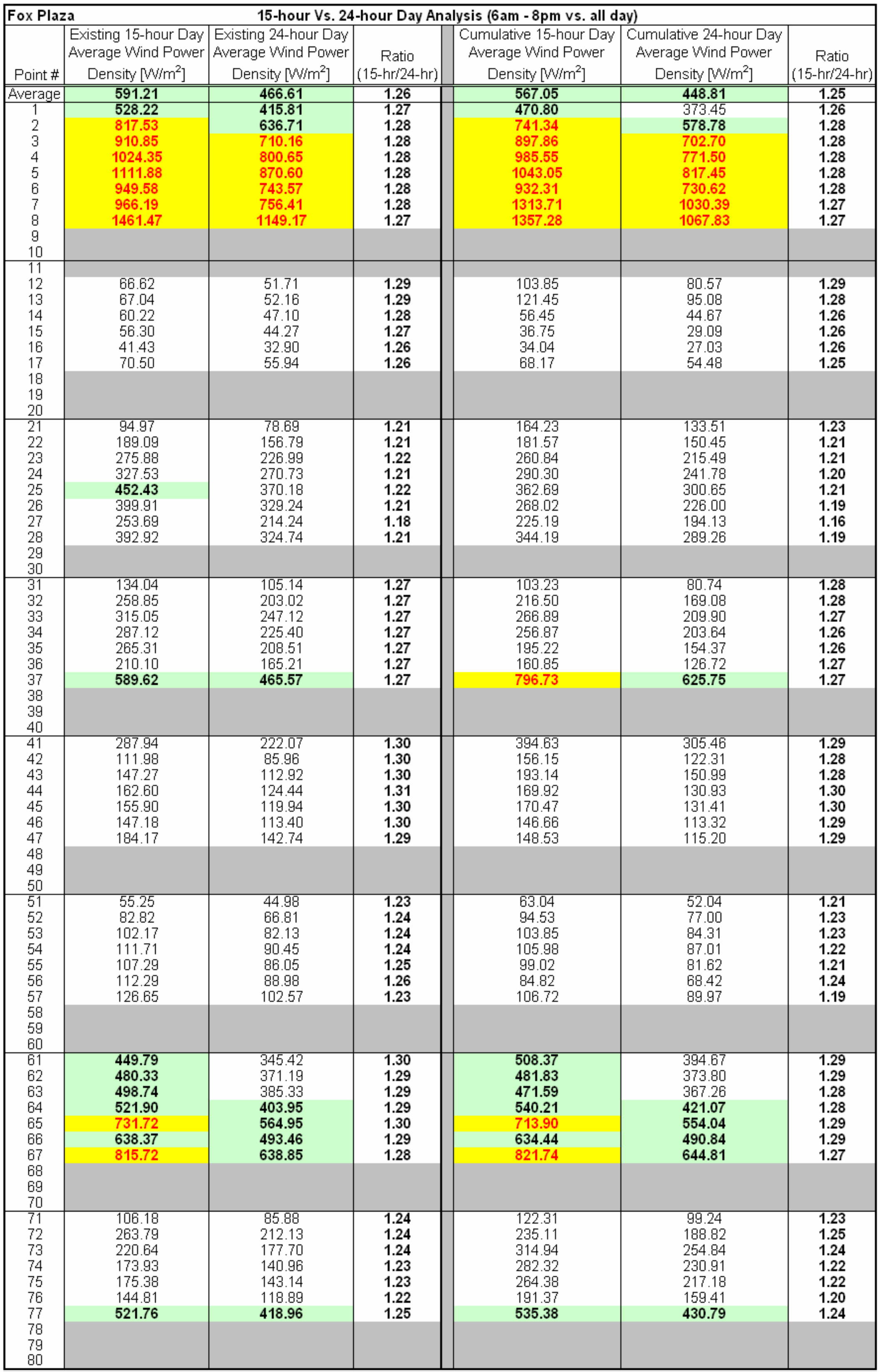

Fox Plaza	15-hour Vs. 24-hour Day Analysis (6am - 8pm vs. all day)					
Point #	Existing 15-hour Day Average Wind Power Density [W/m^2]	Existing 24-hour Day Average Wind Power Density [W/m^2]	Ratio (15-hr/24-hr)	Cumulative 15-hour Day Average Wind Power Density [W/m^2]	Cumulative 24-hour Day Average Wind Power Density [W/m^2]	Ratio (15-hr/24-hr)
Average	591.21	466.61	1.26	567.05	448.81	1.25
1	528.22	415.81	1.27	470.80	373.45	1.26
2	817.53	636.71	1.28	741.34	578.78	1.28
3	910.85	710.16	1.28	897.86	702.70	1.28
4	1024.35	800.65	1.28	985.55	771.50	1.28
5	1111.88	870.60	1.28	1043.05	817.45	1.28
6	949.58	743.57	1.28	932.31	730.62	1.28
7	966.19	756.41	1.28	1313.71	1030.39	1.27
8	1461.47	1149.17	1.27	1357.28	1067.83	1.27
9						
10						
11						
12	66.62	51.71	1.29	103.85	80.57	1.29
13	67.04	52.16	1.29	121.45	95.08	1.28
14	60.22	47.10	1.28	56.45	44.67	1.26
15	56.30	44.27	1.27	36.75	29.09	1.26
16	41.43	32.90	1.26	34.04	27.03	1.26
17	70.50	55.94	1.26	68.17	54.48	1.25
18						
19						
20						
21	94.97	78.69	1.21	164.23	133.51	1.23
22	189.09	156.79	1.21	181.57	150.45	1.21
23	275.88	226.99	1.22	260.84	215.49	1.21
24	327.53	270.73	1.21	290.30	241.78	1.20
25	452.43	370.18	1.22	362.69	300.65	1.21
26	399.91	329.24	1.21	268.02	226.00	1.19
27	253.69	214.24	1.18	225.19	194.13	1.16
28	392.92	324.74	1.21	344.19	289.26	1.19
29						
30						
31	134.04	105.14	1.27	103.23	80.74	1.28
32	258.85	203.02	1.27	216.50	169.08	1.28
33	315.05	247.12	1.27	266.89	209.90	1.27
34	287.12	225.40	1.27	256.87	203.64	1.26
35	265.31	208.51	1.27	195.22	154.37	1.26
36	210.10	165.21	1.27	160.85	126.72	1.27
37	589.62	465.57	1.27	796.73	625.75	1.27
38						
39						
40						
41	287.94	222.07	1.30	394.63	305.46	1.29
42	111.98	85.96	1.30	156.15	122.31	1.28
43	147.27	112.92	1.30	193.14	150.99	1.28
44	162.60	124.44	1.31	169.92	130.93	1.30
45	155.90	119.94	1.30	170.47	131.41	1.30
46	147.18	113.40	1.30	146.66	113.32	1.29
47	184.17	142.74	1.29	148.53	115.20	1.29
48						
49						
50						
51	55.25	44.98	1.23	63.04	52.04	1.21
52	82.82	66.81	1.24	94.53	77.00	1.23
53	102.17	82.13	1.24	103.85	84.31	1.23
54	111.71	90.45	1.24	105.98	87.01	1.22
55	107.29	86.05	1.25	99.02	81.62	1.21
56	112.29	88.98	1.26	84.82	68.42	1.24
57	126.65	102.57	1.23	106.72	89.97	1.19
58						
59						
60						
61	449.79	345.42	1.30	508.37	394.67	1.29
62	480.33	371.19	1.29	481.83	373.80	1.29
63	498.74	385.33	1.29	471.59	367.26	1.28
64	521.90	403.95	1.29	540.21	421.07	1.28
65	731.72	564.95	1.30	713.90	554.04	1.29
66	638.37	493.46	1.29	634.44	490.84	1.29
67	815.72	638.85	1.28	821.74	644.81	1.27
68						
69						
70						
71	106.18	85.88	1.24	122.31	99.24	1.23
72	263.79	212.13	1.24	235.11	188.82	1.25
73	220.64	177.70	1.24	314.94	254.84	1.24
74	173.93	140.96	1.23	282.32	230.91	1.22
75	175.38	143.14	1.23	264.38	217.18	1.22
76	144.81	118.89	1.22	191.37	159.41	1.20
77	521.76	418.96	1.25	535.38	430.79	1.24
78						
79						
80						

Table 15a. Ratio of average wind power densities of the 6am – 8pm case to the 24-hours per day case for Fox Plaza.

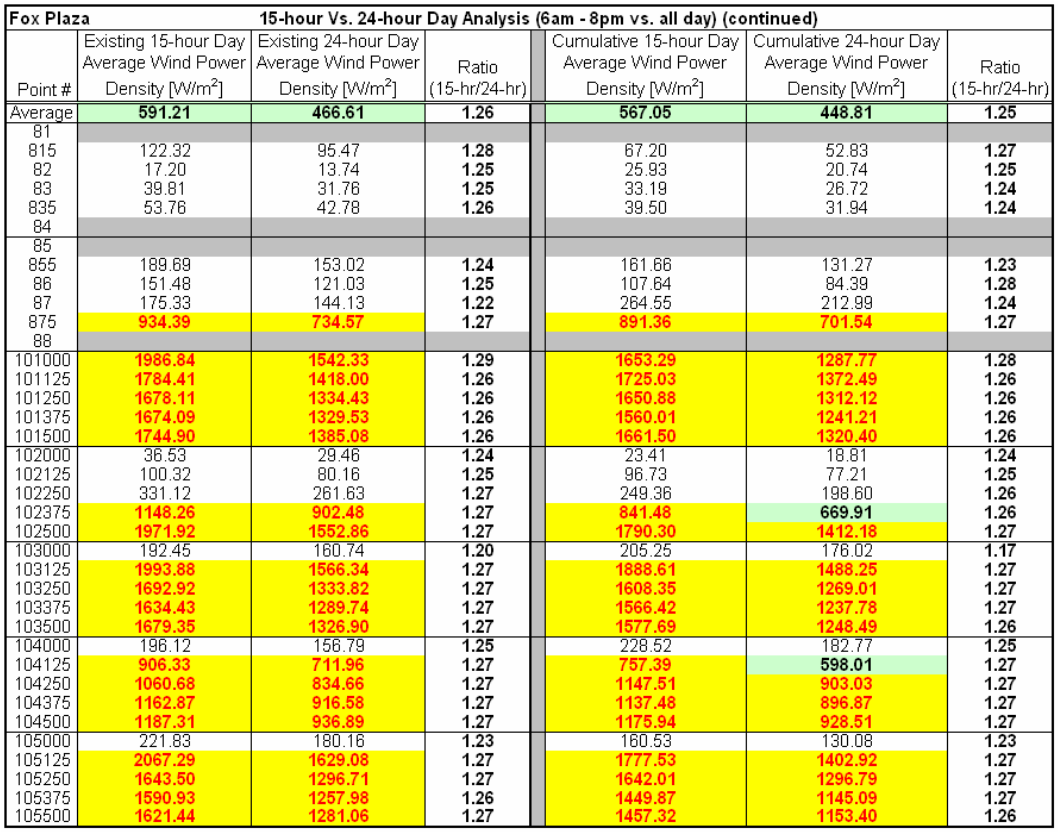

Fox Plaza	**15-hour Vs. 24-hour Day Analysis (6am - 8pm vs. all day) (continued)**					
Point #	Existing 15-hour Day Average Wind Power Density [W/m^2]	Existing 24-hour Day Average Wind Power Density [W/m^2]	Ratio (15-hr/24-hr)	Cumulative 15-hour Day Average Wind Power Density [W/m^2]	Cumulative 24-hour Day Average Wind Power Density [W/m^2]	Ratio (15-hr/24-hr)
Average	**591.21**	**466.61**	**1.26**	**567.05**	**448.81**	**1.25**
81						
815	122.32	95.47	**1.28**	67.20	52.83	**1.27**
82	17.20	13.74	**1.25**	25.93	20.74	**1.25**
83	39.81	31.76	**1.25**	33.19	26.72	**1.24**
835	53.76	42.78	**1.26**	39.50	31.94	**1.24**
84						
85						
855	189.69	153.02	**1.24**	161.66	131.27	**1.23**
86	151.48	121.03	**1.25**	107.64	84.39	**1.28**
87	175.33	144.13	**1.22**	264.55	212.99	**1.24**
875	**934.39**	**734.57**	**1.27**	**891.36**	**701.54**	**1.27**
88						
101000	**1986.84**	**1542.33**	**1.29**	**1653.29**	**1287.77**	**1.28**
101125	**1784.41**	**1418.00**	**1.26**	**1725.03**	**1372.49**	**1.26**
101250	**1678.11**	**1334.43**	**1.26**	**1650.88**	**1312.12**	**1.26**
101375	**1674.09**	**1329.53**	**1.26**	**1560.01**	**1241.21**	**1.26**
101500	**1744.90**	**1385.08**	**1.26**	**1661.50**	**1320.40**	**1.26**
102000	36.53	29.46	**1.24**	23.41	18.81	**1.24**
102125	100.32	80.16	**1.25**	96.73	77.21	**1.25**
102250	331.12	261.63	**1.27**	249.36	198.60	**1.26**
102375	**1148.26**	**902.48**	**1.27**	**841.48**	**669.91**	**1.26**
102500	**1971.92**	**1552.86**	**1.27**	**1790.30**	**1412.18**	**1.27**
103000	192.45	160.74	**1.20**	205.25	176.02	**1.17**
103125	**1993.88**	**1566.34**	**1.27**	**1888.61**	**1488.25**	**1.27**
103250	**1692.92**	**1333.82**	**1.27**	**1608.35**	**1269.01**	**1.27**
103375	**1634.43**	**1289.74**	**1.27**	**1566.42**	**1237.78**	**1.27**
103500	**1679.35**	**1326.90**	**1.27**	**1577.69**	**1248.49**	**1.26**
104000	196.12	156.79	**1.25**	228.52	182.77	**1.25**
104125	**906.33**	**711.96**	**1.27**	**757.39**	**598.01**	**1.27**
104250	**1060.68**	**834.66**	**1.27**	**1147.51**	**903.03**	**1.27**
104375	**1162.87**	**916.58**	**1.27**	**1137.48**	**896.87**	**1.27**
104500	**1187.31**	**936.89**	**1.27**	**1175.94**	**928.51**	**1.27**
105000	221.83	180.16	**1.23**	160.53	130.08	**1.23**
105125	**2067.29**	**1629.08**	**1.27**	**1777.53**	**1402.92**	**1.27**
105250	**1643.50**	**1296.71**	**1.27**	**1642.01**	**1296.79**	**1.27**
105375	**1590.93**	**1257.98**	**1.26**	**1449.87**	**1145.09**	**1.27**
105500	**1621.44**	**1281.06**	**1.27**	**1457.32**	**1153.40**	**1.26**

Table 15b. Ratio of average wind power densities of the 6am – 8pm case to the 24-hours per day case for Fox Plaza (continued from Table 15a).

3.1.2 CSAA Building Results

The “good” wind resource points’ results of the wind-tunnel testing for the CSAA Building are shown in Table 16, and the “great” wind resource points’ results are in Table 17.

Average wind power densities were highest near or above the roof level. The highest average wind power density was 2476.3 Watts per square meter at point 105125 for the existing setting, and 2181.0 Watts per square meter for the cumulative setting for the same point. The northeastern and southwestern corner of the building are a “good” wind resource due to its high average wind power densities from point 44 to point 49 and point 63 to point 69, respectively, for the existing setting. The southeastern corner of the building is a “great” wind resource due to its high average wind power densities from point 63 to point 69 for the cumulative setting. The point that showed the most increase due to local development was point 65 which had an increase of 103 percent, and the point that showed the most decrease was point 102125 which had a decrease of 27 percent.

The highest turbulence intensity for the existing setting of a point with “good” or “great” wind resource was point 815 with 60.04 percent; and point 88 held the highest value for cumulative setting at 77.0 percent. The average of the measurement locations’ average wind power density for the CSAA building was 544.13 Watts per square meter for the existing setting and 578.91 Watts per square meter for the cumulative setting, meaning that there could be an overall increase in power production at this building if the city chooses to develop in this area.

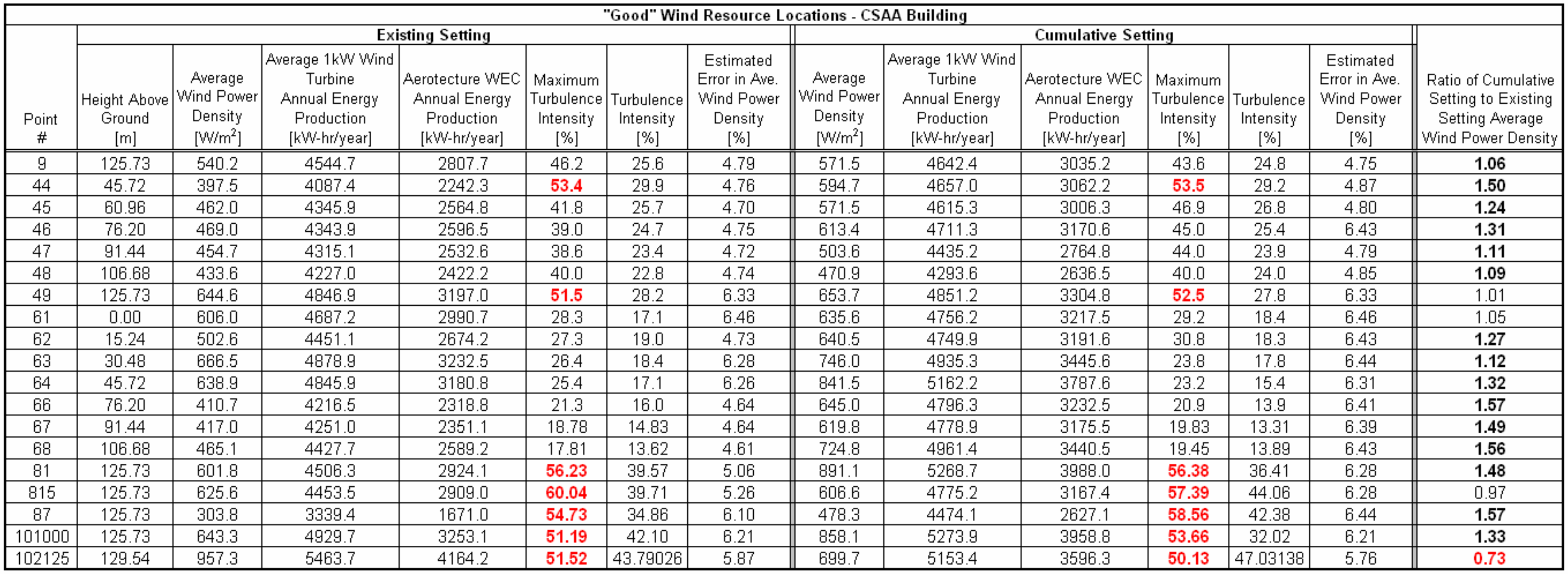

	"Good" Wind Resource Locations - CSAA Building														
	Existing Setting							Cumulative Setting							
Point #	Height Above Ground [m]	Average Wind Power Density [W/m^2]	Average 1kW Wind Turbine Annual Energy Production [kW-hr/year]	Aerotecture WEC Annual Energy Production [kW-hr/year]	Maximum Turbulence Intensity [%]	Turbulence Intensity [%]	Estimated Error in Ave. Wind Power Density [%]	Average Wind Power Density [W/m^2]	Average 1kW Wind Turbine Annual Energy Production [kW-hr/year]	Aerotecture WEC Annual Energy Production [kW-hr/year]	Maximum Turbulence Intensity [%]	Turbulence Intensity [%]	Estimated Error in Ave. Wind Power Density [%]	Ratio of Cumulative Setting to Existing Setting Average Wind Power Density
9	125.73	540.2	4544.7	2807.7	46.2	25.6	4.79	571.5	4642.4	3035.2	43.6	24.8	4.75	**1.06**
44	45.72	397.5	4087.4	2242.3	**53.4**	29.9	4.76	594.7	4657.0	3062.2	**53.5**	29.2	4.87	**1.50**
45	60.96	462.0	4345.9	2564.8	41.8	25.7	4.70	571.5	4615.3	3006.3	46.9	26.8	4.80	**1.24**
46	76.20	469.0	4343.9	2596.5	39.0	24.7	4.75	613.4	4711.3	3170.6	45.0	25.4	6.43	**1.31**
47	91.44	454.7	4315.1	2532.6	38.6	23.4	4.72	503.6	4435.2	2764.8	44.0	23.9	4.79	**1.11**
48	106.68	433.6	4227.0	2422.2	40.0	22.8	4.74	470.9	4293.6	2636.5	40.0	24.0	4.85	**1.09**
49	125.73	644.6	4846.9	3197.0	**51.5**	28.2	6.33	653.7	4851.2	3304.8	**52.5**	27.8	6.33	1.01
61	0.00	606.0	4687.2	2990.7	28.3	17.1	6.46	635.6	4756.2	3217.5	29.2	18.4	6.46	1.05
62	15.24	502.6	4451.1	2674.2	27.3	19.0	4.73	640.5	4749.9	3191.6	30.8	18.3	6.43	**1.27**
63	30.48	666.5	4878.9	3232.5	26.4	18.4	6.28	746.0	4935.3	3445.6	23.8	17.8	6.44	**1.12**
64	45.72	638.9	4845.9	3180.8	25.4	17.1	6.26	841.5	5162.2	3787.6	23.2	15.4	6.31	**1.32**
66	76.20	410.7	4216.5	2318.8	21.3	16.0	4.64	645.0	4796.3	3232.5	20.9	13.9	6.41	**1.57**
67	91.44	417.0	4251.0	2351.1	18.78	14.83	4.64	619.8	4778.9	3175.5	19.83	13.31	6.39	**1.49**
68	106.68	465.1	4427.7	2589.2	17.81	13.62	4.61	724.8	4961.4	3440.5	19.45	13.89	6.43	**1.56**
81	125.73	601.8	4506.3	2924.1	**56.23**	39.57	5.06	891.1	5268.7	3988.0	**56.38**	36.41	6.28	**1.48**
815	125.73	625.6	4453.5	2909.0	**60.04**	39.71	5.26	606.6	4775.2	3167.4	**57.39**	44.06	6.28	0.97
87	125.73	303.8	3339.4	1671.0	**54.73**	34.86	6.10	478.3	4474.1	2627.1	**58.56**	42.38	6.44	**1.57**
101000	125.73	643.3	4929.7	3253.1	**51.19**	42.10	6.21	858.1	5273.9	3958.8	**53.66**	32.02	6.21	**1.33**
102125	129.54	957.3	5463.7	4164.2	**51.52**	43.79026	5.87	699.7	5153.4	3596.3	**50.13**	47.03138	5.76	**0.73**

Table 16. Results for "good" points at the CSAA Building.

"Great" Wind Resource Locations - CSAA Building														
	Existing Setting							Cumulative Setting						
Point #	Height Above Ground [m]	Average Wind Power Density [W/m^2]	Average 1kW Wind Turbine Annual Energy Production [kW-hr/year]	Aerotecture WEC Annual Energy Production [kW-hr/year]	Maximum Turbulence Intensity [%]	Turbulence Intensity [%]	Estimated Error in Ave. Wind Power Density [%]	Average Wind Power Density [W/m^2]	Average 1kW Wind Turbine Annual Energy Production [kW-hr/year]	Aerotecture WEC Annual Energy Production [kW-hr/year]	Maximum Turbulence Intensity [%]	Turbulence Intensity [%]	Estimated Error in Ave. Wind Power Density [%]	Ratio of Cumulative Setting to Existing Setting Average Wind Power Density
39	125.73	808.2	5108.1	3535.2	13.8	12.7	6.27	830.5	5157.9	3753.5	13.9	13.1	6.25	1.03
63	30.48	666.5	4878.9	3232.5	26.4	18.4	6.28	746.0	4935.3	3445.6	23.8	17.8	6.44	**1.12**
64	45.72	638.9	4845.9	3180.8	25.4	17.1	6.26	841.5	5162.2	3787.6	23.2	15.4	6.31	**1.32**
65	60.96	380.8	3749.4	2087.5	24.0	19.7	5.23	771.2	5052.9	3579.2	26.6	14.9	6.36	**2.03**
68	106.68	465.1	4427.7	2589.2	17.8	13.6	4.61	724.8	4961.4	3440.5	19.5	13.9	6.43	**1.56**
69	125.73	976.0	5343.9	3956.8	15.7	13.1	6.22	1022.9	5310.7	4075.9	33.2	17.1	6.38	1.05
79	125.73	1076.5	5430.8	4167.5	14.5	13.1	6.24	858.9	5221.2	3853.0	14.1	13.3	6.18	**0.80**
81	125.73	601.8	4506.3	2924.1	**56.2**	39.6	5.06	891.1	5268.7	3988.0	**56.4**	36.4	6.28	**1.48**
875	125.73	1810.2	5893.8	5159.5	**61.7**	20.7	9.95	1402.9	5710.6	4877.4	**82.7**	39.7	6.32	**0.78**
88	125.73	858.9	5153.3	3742.6	**77.0**	42.5	6.40	961.8	5409.6	4232.9	**55.3**	34.0	6.17	**1.12**
101000	125.73	643.3	4929.7	3253.1	**51.2**	42.1	6.21	858.1	5273.9	3958.8	**53.7**	32.0	6.21	**1.33**
101125	129.54	1337.8	5648.2	4641.7	47.4	26.0	6.41	1287.2	5607.3	4664.0	46.7	25.0	6.43	0.96
101250	133.35	1445.9	5731.1	4750.6	46.0	18.0	6.29	1435.0	5719.7	4863.5	**53.0**	17.5	6.30	0.99
101375	137.16	1287.8	5645.2	4572.8	17.6	12.1	6.17	1258.1	5621.2	4642.9	25.6	12.2	6.17	0.98
101500	140.97	1240.1	5599.2	4473.7	12.6	11.3	6.21	1269.5	5622.7	4656.7	13.4	11.3	6.21	1.02
102125	129.54	957.3	5463.7	4164.2	**51.5**	43.8	5.87	699.7	5153.4	3596.3	**50.1**	47.0	5.76	**0.73**
102250	133.35	1819.2	5961.3	5282.6	**50.4**	34.8	9.57	1949.5	6005.5	5539.1	48.0	35.4	9.59	**1.07**
102375	137.16	1934.2	5979.9	5325.1	30.6	21.0	9.72	1881.0	5962.1	5413.0	33.1	22.4	9.69	0.97
102500	140.97	1592.6	5831.8	4983.4	16.3	14.2	9.69	1581.8	5824.4	5093.6	17.6	13.8	9.69	0.99
103125	129.54	730.2	5183.8	3460.6	41.9	37.3	6.11	763.5	5272.6	3681.7	45.2	40.0	6.03	1.05
103250	133.35	1299.6	5729.1	4702.5	**53.1**	33.3	6.13	1348.3	5760.9	4872.9	**52.0**	33.4	9.57	1.04
103375	137.16	1701.3	5874.2	5093.0	36.5	21.7	9.73	1707.9	5867.7	5219.4	29.0	18.2	9.75	1.00
103500	140.97	1563.6	5795.3	4918.7	19.2	14.0	9.73	1439.6	5729.3	4895.9	15.6	12.7	6.22	**0.92**
104125	129.54	2129.0	6025.4	5505.1	37.5	22.2	9.75	1914.8	5957.9	5421.5	40.4	23.4	9.71	**0.90**
104250	133.35	1439.3	5730.4	4758.0	11.7	10.9	6.23	1455.8	5742.7	4914.8	12.5	11.5	6.23	1.01
104375	137.16	1307.6	5653.9	4614.4	11.6	11.2	6.20	1304.7	5645.5	4731.4	11.7	11.0	6.21	1.00
104500	140.97	1253.4	5615.9	4508.6	12.0	10.9	6.21	1249.6	5604.5	4628.1	12.0	10.9	6.21	1.00
105000	129.54	1491.9	5786.2	4909.2	**55.1**	40.8	9.51	1489.4	5793.4	5026.1	**54.5**	42.0	9.52	1.00
105125	133.35	2476.3	6135.5	5742.7	33.3	25.6	9.71	2181.0	6054.1	5662.9	39.5	29.4	9.68	**0.88**
105250	137.16	1747.9	5900.1	5133.4	16.1	14.6	9.71	1773.7	5907.8	5282.3	21.2	15.6	9.72	1.01
105375	140.97	1393.8	5712.8	4715.3	13.2	11.4	6.21	1414.1	5721.8	4870.8	12.9	11.5	6.21	1.01
105500	144.78	1350.2	5684.7	4665.7	11.5	10.7	6.20	1317.7	5659.7	4760.2	12.2	10.7	6.20	0.98

Table 17. Results for “great” points at the CSAA Building.

CSAA Building Results with Winds from 6am to 8pm

The reduced, full-scale data for Fox Plaza for winds from 6am to 8pm are displayed in the same manner as in the previous section. The "good" wind resource points' results of the wind-tunnel testing for the CSAA Building are shown in Table 18, and the "great" wind resource points' results are in Table 19. Tables 20a and 20b show the ratio of the average wind speed densities of 6am to 8pm case to the all hours' case for each point tested.

The point with the highest average wind power density during the hours of 6am to 8pm (the 15-hour day case) for the existing setting was point 104125 which had a value of 2699.04 Watts per square meter, and point 105125 held the highest value, 2748.45 Watts per square meter, for the cumulative setting, All points showed an increase in average wind power density from the 24-hour day case, demonstrating that the winds are higher during business hours.

"Good" Wind Resource Locations - CSAA Building - 6am - 8pm														
	Existing Setting							Cumulative Setting						
Point #	Height Above Ground [m]	Average Wind Power Density [W/m^2]	Average 1kW Wind Turbine Annual Energy Production [kW-hr/year]	Aerotecture WEC Annual Energy Production [kW-hr/year]	Maximum Turbulence Intensity [%]	Turbulence Intensity [%]	Estimated Error in Ave. Wind Power Density [%]	Average Wind Power Density [W/m^2]	Average 1kW Wind Turbine Annual Energy Production [kW-hr/year]	Aerotecture WEC Annual Energy Production [kW-hr/year]	Maximum Turbulence Intensity [%]	Turbulence Intensity [%]	Estimated Error in Ave. Wind Power Density [%]	Ratio of Cumulative Setting to Existing Setting Average Wind Power Density
4	45.72	421.0	2701.9	1466.9	**63.6**	36.6	3.81	509.6	2870.4	1748.6	**62.7**	37.7	7.75	**1.21**
5	60.96	467.3	2817.7	1609.0	49.8	33.3	7.64	428.5	2725.7	1544.0	49.5	32.6	3.79	**0.92**
6	76.20	444.7	2757.7	1540.3	44.9	30.5	3.80	464.2	2787.8	1650.1	46.7	30.2	3.84	1.04
7	91.44	417.4	2674.2	1455.0	47.6	31.2	3.85	455.1	2754.1	1618.6	48.0	29.8	3.88	**1.09**
8	106.68	357.1	2489.3	1286.2	46.9	28.2	3.92	413.0	2640.2	1486.1	45.4	29.2	3.91	**1.16**
9	125.73	698.6	3271.1	2174.3	46.2	25.2	7.47	739.9	3329.8	2326.9	43.6	24.5	7.44	**1.06**
44	45.72	515.9	2998.8	1789.1	**53.4**	29.5	7.47	765.6	3329.0	2340.1	**53.5**	28.8	7.51	**1.48**
45	60.96	599.5	3163.9	1992.8	41.8	25.4	7.40	737.3	3310.7	2304.2	46.9	26.5	7.47	**1.23**
46	76.20	609.4	3160.5	2004.5	39.0	24.5	7.47	793.3	3364.7	2409.3	45.0	25.2	7.50	**1.30**
47	91.44	592.2	3143.8	1973.4	38.6	23.1	7.45	650.8	3210.4	2155.1	44.0	23.7	7.46	**1.10**
48	106.68	564.3	3088.3	1899.9	40.0	22.6	7.47	608.4	3121.9	2030.7	40.0	23.7	7.54	**1.08**
62	15.24	644.8	3221.8	2088.3	27.3	18.9	7.35	812.8	3379.8	2422.5	30.8	18.3	7.42	**1.26**
65	60.96	485.4	2760.6	1616.9	23.97	19.64	3.99	985.3	3551.7	2739.9	26.60	14.87	7.37	**2.03**
66	76.20	532.2	3084.7	1854.1	21.31	15.89	7.30	821.8	3410.0	2464.0	20.93	13.84	7.40	**1.54**
67	91.44	541.7	3106.3	1888.1	18.78	14.78	7.31	796.1	3399.3	2429.5	19.83	13.28	7.40	**1.47**
68	106.68	603.5	3215.8	2030.9	17.81	13.60	7.28	928.5	3498.2	2635.7	19.45	13.86	7.44	**1.54**
87	125.73	367.8	2458.8	1268.7	**54.73**	35.03	4.18	593.9	3214.4	2005.3	**58.56**	42.24	7.11	**1.62**

Table 18. Results for "good" points at the CSAA Building from 6am – 8pm.

"Great" Wind Resource Locations - CSAA Building - 6am - 8pm														
	Existing Setting							Cumulative Setting						
Point #	Height Above Ground [m]	Average Wind Power Density [W/m²]	Average 1kW Wind Turbine Annual Energy Production [kW-hr/year]	Aerotecture WEC Annual Energy Production [kW-hr/year]	Maximum Turbulence Intensity [%]	Turbulence Intensity [%]	Estimated Error in Ave. Wind Power Density [%]	Average Wind Power Density [W/m²]	Average 1kW Wind Turbine Annual Energy Production [kW-hr/year]	Aerotecture WEC Annual Energy Production [kW-hr/year]	Maximum Turbulence Intensity [%]	Turbulence Intensity [%]	Estimated Error in Ave. Wind Power Density [%]	Ratio of Cumulative Setting to Existing Setting Average Wind Power Density
39	125.73	1017.2	3584.4	2713.1	13.8	12.7	10.16	1051.6	3611.7	2870.5	13.9	13.1	10.18	1.03
49	125.73	837.5	3449.8	2483.8	**51.5**	27.8	7.41	844.8	3450.4	2558.0	**52.5**	27.4	7.39	1.01
61	0.00	777.4	3344.7	2292.4	28.3	17.0	7.49	817.5	3386.1	2443.3	29.2	18.4	7.50	**1.05**
62	15.24	644.8	3221.8	2088.3	27.3	18.9	7.35	812.8	3379.8	2422.5	30.8	18.3	7.42	**1.26**
63	30.48	857.8	3466.7	2494.3	26.4	18.3	7.34	948.2	3484.1	2634.4	23.8	17.8	7.45	**1.11**
64	45.72	823.8	3450.0	2461.7	25.4	17.1	7.32	1072.8	3611.9	2871.7	23.2	15.4	10.28	**1.30**
65	60.96	485.4	2760.6	1616.9	24.0	19.6	3.99	985.3	3551.7	2739.9	26.6	14.9	7.37	**2.03**
66	76.20	532.2	3084.7	1854.1	21.3	15.9	7.30	821.8	3410.0	2464.0	20.9	13.8	7.40	**1.54**
67	91.44	541.7	3106.3	1888.1	18.8	14.8	7.31	796.1	3399.3	2429.5	19.8	13.3	7.40	**1.47**
68	106.68	603.5	3215.8	2030.9	17.8	13.6	7.28	928.5	3498.2	2635.7	19.5	13.9	7.44	**1.54**
69	125.73	1232.9	3709.9	3009.1	15.7	13.2	10.14	1283.8	3684.8	3076.5	33.2	17.2	10.28	1.04
79	125.73	1361.1	3752.9	3118.9	14.5	13.1	10.18	1082.1	3646.1	2908.8	14.1	13.3	10.07	**0.79**
81	125.73	778.0	3242.8	2215.9	**56.2**	39.2	7.82	1160.6	3671.2	3034.1	**56.4**	36.1	10.35	**1.49**
815	125.73	799.2	3201.7	2185.8	**60.0**	39.4	7.95	780.3	3404.2	2425.9	**57.4**	43.8	7.32	0.98
875	125.73	2315.6	3964.9	3743.0	**61.7**	20.7	10.40	1803.8	3878.7	3593.4	**82.7**	39.1	10.34	**0.78**
88	125.73	1112.6	3608.3	2825.9	**77.0**	42.2	7.48	1254.1	3748.8	3187.9	**55.3**	33.6	10.23	**1.13**
101000	125.73	835.8	3499.0	2516.7	**51.2**	41.9	7.28	1117.0	3677.1	3009.2	**53.7**	31.7	10.26	**1.34**
101125	129.54	1709.7	3845.9	3393.5	47.4	25.6	10.39	1642.2	3824.8	3417.8	46.7	24.6	10.40	0.96
101250	133.35	1819.7	3888.3	3494.5	46.0	17.9	10.19	1804.3	3882.7	3559.5	**53.0**	17.4	10.20	0.99
101375	137.16	1617.1	3852.4	3363.0	17.6	12.1	10.06	1577.3	3839.8	3412.9	25.6	12.1	10.05	0.98
101500	140.97	1561.3	3828.3	3310.8	12.6	11.4	10.11	1596.1	3839.1	3419.3	13.4	11.2	10.11	1.02
102125	129.54	1227.4	3787.9	3141.5	**51.5**	43.8	9.84	888.2	3641.8	2771.1	**50.1**	47.0	9.67	**0.72**
102250	133.35	2314.3	4006.6	3822.0	**50.4**	34.6	10.04	2476.0	4025.7	3970.2	48.0	35.3	10.07	**1.07**
102375	137.16	2441.5	4009.7	3833.1	30.6	20.8	10.16	2375.1	4002.7	3893.9	33.1	22.3	10.14	0.97
102500	140.97	2010.9	3942.7	3624.9	16.3	14.2	10.14	1993.1	3938.6	3694.4	17.6	13.8	10.13	0.99
103125	129.54	900.4	3629.7	2643.5	41.9	37.3	9.73	945.9	3677.9	2819.3	45.2	40.0	9.69	**1.05**
103250	133.35	1630.7	3892.2	3428.7	**53.1**	33.5	9.97	1690.6	3907.8	3563.1	**52.0**	33.6	9.97	1.04
103375	137.16	2157.3	3962.0	3709.0	36.5	21.9	10.19	2164.0	3958.8	3785.1	29.0	18.4	10.21	1.00
103500	140.97	1979.8	3920.9	3586.1	19.2	14.1	10.19	1819.9	3890.5	3599.7	15.6	12.7	10.16	**0.92**
104125	129.54	2699.0	4032.2	3932.6	37.5	22.4	10.22	2419.1	4000.8	3899.2	40.4	23.6	10.17	**0.90**
104250	133.35	1815.9	3890.6	3509.2	11.7	10.9	10.15	1835.7	3896.4	3594.2	12.5	11.5	10.15	1.01
104375	137.16	1650.6	3855.9	3386.0	11.6	11.2	10.12	1646.2	3851.6	3460.3	11.7	11.0	10.13	1.00
104500	140.97	1580.7	3835.9	3329.7	12.0	10.9	10.12	1577.7	3830.7	3406.5	12.0	10.9	10.14	1.00
105000	129.54	1899.7	3926.3	3598.8	**55.1**	40.6	10.01	1883.7	3926.7	3665.1	**54.5**	41.9	10.00	0.99
105125	133.35	3125.0	4086.3	4068.4	33.3	25.6	10.16	2748.4	4047.1	4053.7	39.5	29.3	10.13	**0.88**
105250	137.16	2206.6	3973.1	3740.3	16.1	14.6	10.16	2233.2	3976.5	3832.6	21.2	15.5	10.16	1.01
105375	140.97	1757.9	3883.5	3472.4	13.2	11.4	10.12	1784.1	3887.5	3575.5	12.9	11.5	10.13	1.01
105500	144.78	1705.4	3871.0	3432.6	11.5	10.7	10.13	1660.1	3858.7	3474.8	12.2	10.7	10.11	0.97

Table 19. Results for "great" points at the CSAA Building from 6am – 8pm.

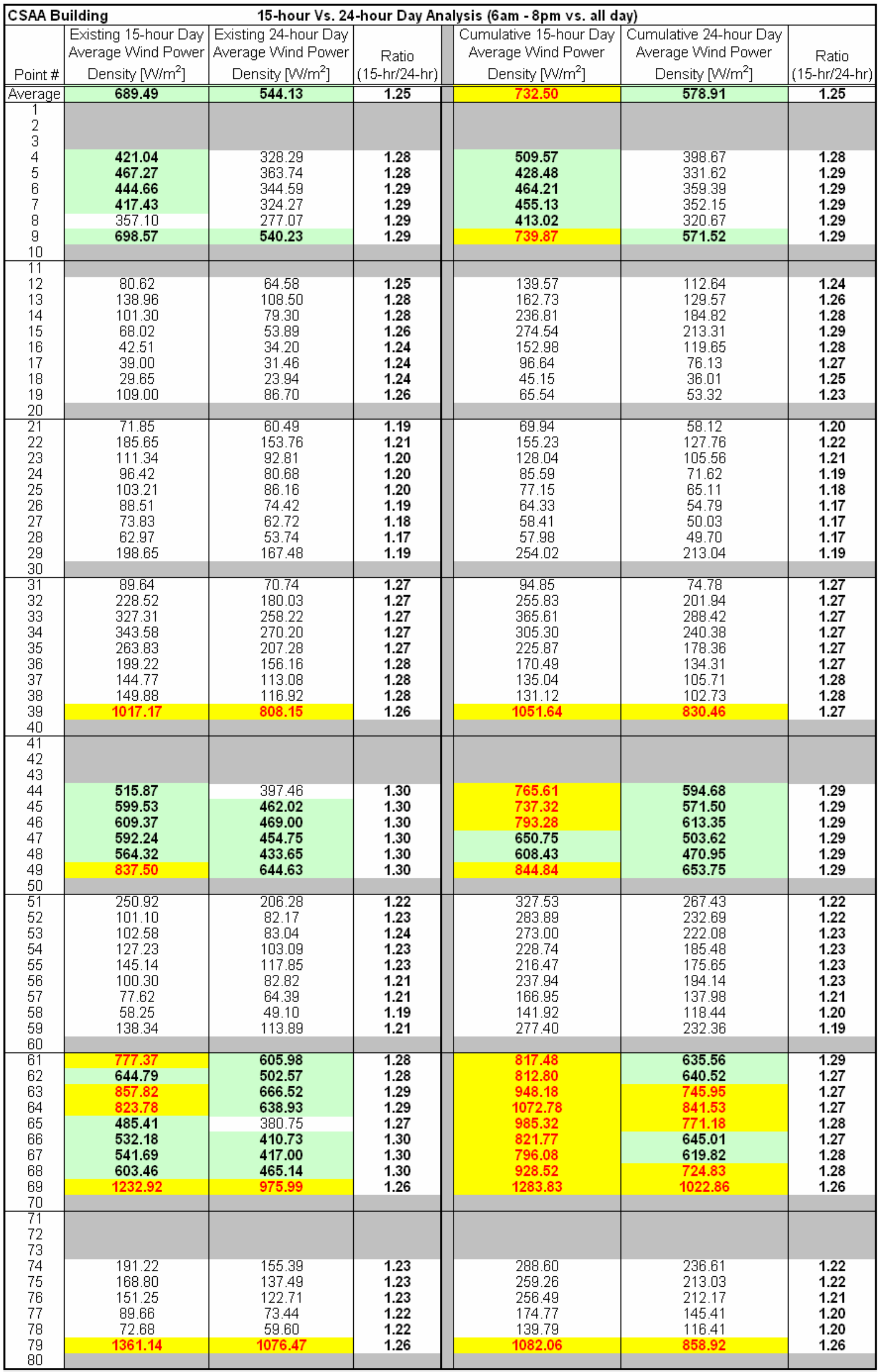

CSAA Building	15-hour Vs. 24-hour Day Analysis (6am - 8pm vs. all day)					
Point #	Existing 15-hour Day Average Wind Power Density [W/m^2]	Existing 24-hour Day Average Wind Power Density [W/m^2]	Ratio (15-hr/24-hr)	Cumulative 15-hour Day Average Wind Power Density [W/m^2]	Cumulative 24-hour Day Average Wind Power Density [W/m^2]	Ratio (15-hr/24-hr)
Average	689.49	544.13	1.25	732.50	578.91	1.25
1						
2						
3						
4	421.04	328.29	1.28	509.57	398.67	1.28
5	467.27	363.74	1.28	428.48	331.62	1.29
6	444.66	344.59	1.29	464.21	359.39	1.29
7	417.43	324.27	1.29	455.13	352.15	1.29
8	357.10	277.07	1.29	413.02	320.67	1.29
9	698.57	540.23	1.29	739.87	571.52	1.29
10						
11						
12	80.62	64.58	1.25	139.57	112.64	1.24
13	138.96	108.50	1.28	162.73	129.57	1.26
14	101.30	79.30	1.28	236.81	184.82	1.28
15	68.02	53.89	1.26	274.54	213.31	1.29
16	42.51	34.20	1.24	152.98	119.65	1.28
17	39.00	31.46	1.24	96.64	76.13	1.27
18	29.65	23.94	1.24	45.15	36.01	1.25
19	109.00	86.70	1.26	65.54	53.32	1.23
20						
21	71.85	60.49	1.19	69.94	58.12	1.20
22	185.65	153.76	1.21	155.23	127.76	1.22
23	111.34	92.81	1.20	128.04	105.56	1.21
24	96.42	80.68	1.20	85.59	71.62	1.19
25	103.21	86.16	1.20	77.15	65.11	1.18
26	88.51	74.42	1.19	64.33	54.79	1.17
27	73.83	62.72	1.18	58.41	50.03	1.17
28	62.97	53.74	1.17	57.98	49.70	1.17
29	198.65	167.48	1.19	254.02	213.04	1.19
30						
31	89.64	70.74	1.27	94.85	74.78	1.27
32	228.52	180.03	1.27	255.83	201.94	1.27
33	327.31	258.22	1.27	365.61	288.42	1.27
34	343.58	270.20	1.27	305.30	240.38	1.27
35	263.83	207.28	1.27	225.87	178.36	1.27
36	199.22	156.16	1.28	170.49	134.31	1.27
37	144.77	113.08	1.28	135.04	105.71	1.28
38	149.88	116.92	1.28	131.12	102.73	1.28
39	1017.17	808.15	1.26	1051.64	830.46	1.27
40						
41						
42						
43						
44	515.87	397.46	1.30	765.61	594.68	1.29
45	599.53	462.02	1.30	737.32	571.50	1.29
46	609.37	469.00	1.30	793.28	613.35	1.29
47	592.24	454.75	1.30	650.75	503.62	1.29
48	564.32	433.65	1.30	608.43	470.95	1.29
49	837.50	644.63	1.30	844.84	653.75	1.29
50						
51	250.92	206.28	1.22	327.53	267.43	1.22
52	101.10	82.17	1.23	283.89	232.69	1.22
53	102.58	83.04	1.24	273.00	222.08	1.23
54	127.23	103.09	1.23	228.74	185.48	1.23
55	145.14	117.85	1.23	216.47	175.65	1.23
56	100.30	82.82	1.21	237.94	194.14	1.23
57	77.62	64.39	1.21	166.95	137.98	1.21
58	58.25	49.10	1.19	141.92	118.44	1.20
59	138.34	113.89	1.21	277.40	232.36	1.19
60						
61	777.37	605.98	1.28	817.48	635.56	1.29
62	644.79	502.57	1.28	812.80	640.52	1.27
63	857.82	666.52	1.29	948.18	745.95	1.27
64	823.78	638.93	1.29	1072.78	841.53	1.27
65	485.41	380.75	1.27	985.32	771.18	1.28
66	532.18	410.73	1.30	821.77	645.01	1.27
67	541.69	417.00	1.30	796.08	619.82	1.28
68	603.46	465.14	1.30	928.52	724.83	1.28
69	1232.92	975.99	1.26	1283.83	1022.86	1.26
70						
71						
72						
73						
74	191.22	155.39	1.23	288.60	236.61	1.22
75	168.80	137.49	1.23	259.26	213.03	1.22
76	151.25	122.71	1.23	256.49	212.17	1.21
77	89.66	73.44	1.22	174.77	145.41	1.20
78	72.68	59.60	1.22	139.79	116.41	1.20
79	1361.14	1076.47	1.26	1082.06	858.92	1.26
80						

Table 20a. Ratio of average wind power densities of the 6am – 8pm case to the 24-hours per day case for the CSAA Building.

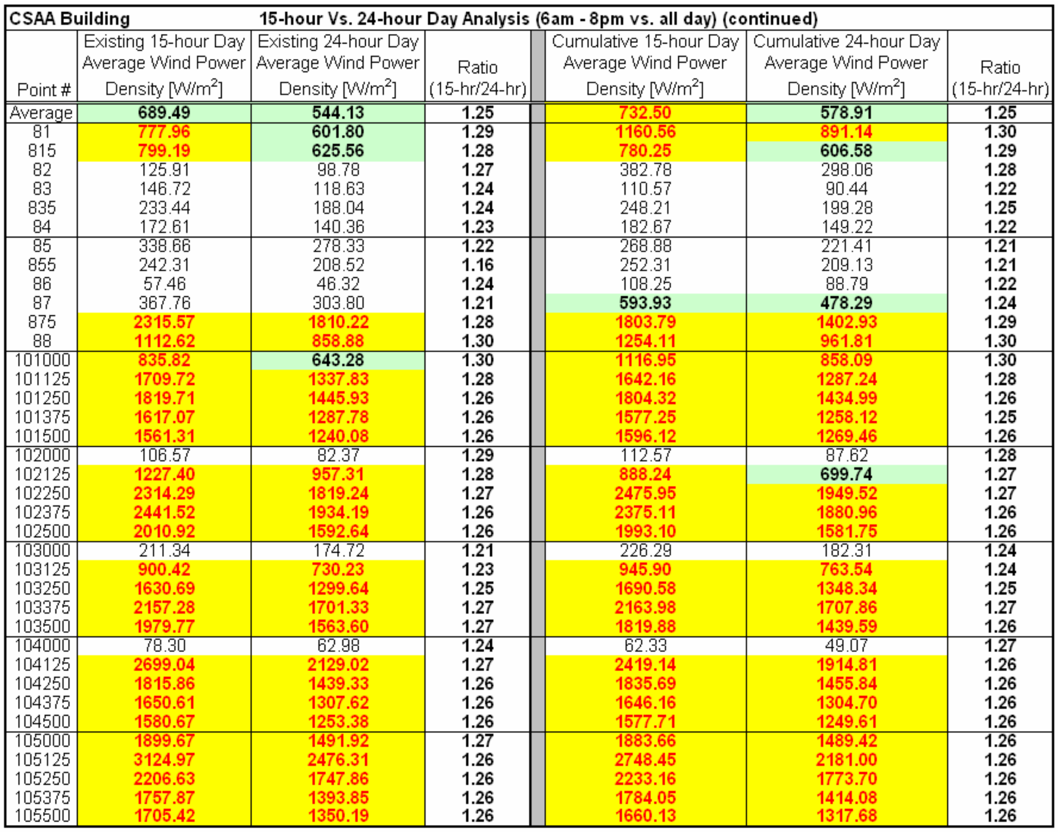

CSAA Building	15-hour Vs. 24-hour Day Analysis (6am - 8pm vs. all day) (continued)					
Point #	Existing 15-hour Day Average Wind Power Density [W/m^2]	Existing 24-hour Day Average Wind Power Density [W/m^2]	Ratio (15-hr/24-hr)	Cumulative 15-hour Day Average Wind Power Density [W/m^2]	Cumulative 24-hour Day Average Wind Power Density [W/m^2]	Ratio (15-hr/24-hr)
Average	**689.49**	**544.13**	**1.25**	**732.50**	**578.91**	**1.25**
81	**777.96**	**601.80**	**1.29**	**1160.56**	**891.14**	**1.30**
815	**799.19**	**625.56**	**1.28**	**780.25**	**606.58**	**1.29**
82	125.91	98.78	**1.27**	382.78	298.06	**1.28**
83	146.72	118.63	**1.24**	110.57	90.44	**1.22**
835	233.44	188.04	**1.24**	248.21	199.28	**1.25**
84	172.61	140.36	**1.23**	182.67	149.22	**1.22**
85	338.66	278.33	**1.22**	268.88	221.41	**1.21**
855	242.31	208.52	**1.16**	252.31	209.13	**1.21**
86	57.46	46.32	**1.24**	108.25	88.79	**1.22**
87	367.76	303.80	**1.21**	**593.93**	**478.29**	**1.24**
875	**2315.57**	**1810.22**	**1.28**	**1803.79**	**1402.93**	**1.29**
88	**1112.62**	**858.88**	**1.30**	**1254.11**	**961.81**	**1.30**
101000	**835.82**	**643.28**	**1.30**	**1116.95**	**858.09**	**1.30**
101125	**1709.72**	**1337.83**	**1.28**	**1642.16**	**1287.24**	**1.28**
101250	**1819.71**	**1445.93**	**1.26**	**1804.32**	**1434.99**	**1.26**
101375	**1617.07**	**1287.78**	**1.26**	**1577.25**	**1258.12**	**1.25**
101500	**1561.31**	**1240.08**	**1.26**	**1596.12**	**1269.46**	**1.26**
102000	106.57	82.37	**1.29**	112.57	87.62	**1.28**
102125	**1227.40**	**957.31**	**1.28**	**888.24**	**699.74**	**1.27**
102250	**2314.29**	**1819.24**	**1.27**	**2475.95**	**1949.52**	**1.27**
102375	**2441.52**	**1934.19**	**1.26**	**2375.11**	**1880.96**	**1.26**
102500	**2010.92**	**1592.64**	**1.26**	**1993.10**	**1581.75**	**1.26**
103000	211.34	174.72	**1.21**	226.29	182.31	**1.24**
103125	**900.42**	**730.23**	**1.23**	**945.90**	**763.54**	**1.24**
103250	**1630.69**	**1299.64**	**1.25**	**1690.58**	**1348.34**	**1.25**
103375	**2157.28**	**1701.33**	**1.27**	**2163.98**	**1707.86**	**1.27**
103500	**1979.77**	**1563.60**	**1.27**	**1819.88**	**1439.59**	**1.26**
104000	78.30	62.98	**1.24**	62.33	49.07	**1.27**
104125	**2699.04**	**2129.02**	**1.27**	**2419.14**	**1914.81**	**1.26**
104250	**1815.86**	**1439.33**	**1.26**	**1835.69**	**1455.84**	**1.26**
104375	**1650.61**	**1307.62**	**1.26**	**1646.16**	**1304.70**	**1.26**
104500	**1580.67**	**1253.38**	**1.26**	**1577.71**	**1249.61**	**1.26**
105000	**1899.67**	**1491.92**	**1.27**	**1883.66**	**1489.42**	**1.26**
105125	**3124.97**	**2476.31**	**1.26**	**2748.45**	**2181.00**	**1.26**
105250	**2206.63**	**1747.86**	**1.26**	**2233.16**	**1773.70**	**1.26**
105375	**1757.87**	**1393.85**	**1.26**	**1784.05**	**1414.08**	**1.26**
105500	**1705.42**	**1350.19**	**1.26**	**1660.13**	**1317.68**	**1.26**

Table 20b. Ratio of average wind power densities of the 6am – 8pm case to the 24-hours per day case for the CSAA Building (continued from Table 20a).

3.1.3 Bank of America Building Results

The "good" wind resource points' results of the wind-tunnel testing for the Bank of America Building are shown in Table 21, and the "great" wind resource points' results are in Table 22.

Average wind power densities were highest near or above the roof level. The highest average wind power density was 2084.5 Watts per square meter at point 81 for the existing setting, and 1910.8 Watts per square meter for the cumulative setting for point 101000. The southwestern face and northern corner of the building are "good" wind resources due to their high average wind power densities from point 33 to point 36 and point 43 to point 46, respectively, for the existing setting. The southwestern face of the building is a “great” wind resource due to its high average wind power densities from point 37 to point 37 for the cumulative setting. The point that showed the most increase due to local development was point 47 which had an increase of 105 percent, and the point that showed the most decrease was point 63 which had a decrease of 59 percent.

The highest turbulence intensity for the existing setting of a point with “good” or “great” wind resource was point 86 with 63.7 percent; and point 88 held the highest value for cumulative setting at 69.6 percent. The average of the measurement locations’ average wind power density for the Bank of America Building was 776.21 Watts per square meter for the existing setting and 793.95 Watts per square meter for the cumulative setting, meaning that there could be an overall increase in power production at this building if the city chooses to develop in this area.

"Good" Wind Resource Locations - Bank of America Building														
	Existing Setting							Cumulative Setting						
Point #	Height Above Ground [m]	Average Wind Power Density [W/m^2]	Average 1kW Wind Turbine Annual Energy Production [kW-hr/year]	Aerotecture WEC Annual Energy Production [kW-hr/year]	Maximum Turbulence Intensity [%]	Turbulence Intensity [%]	Estimated Error in Ave. Wind Power Density [%]	Average Wind Power Density [W/m^2]	Average 1kW Wind Turbine Annual Energy Production [kW-hr/year]	Aerotecture WEC Annual Energy Production [kW-hr/year]	Maximum Turbulence Intensity [%]	Turbulence Intensity [%]	Estimated Error in Ave. Wind Power Density [%]	Ratio of Cumulative Setting to Existing Setting Average Wind Power Density
33	30.48	501.6	4467.9	2691.6	42.2	32.9	4.69	552.6	4552.5	2946.9	47.5	33.0	4.77	**1.10**
34	45.72	712.1	4952.0	3327.4	49.3	30.1	6.30	650.1	4707.4	3194.4	**55.3**	33.3	6.49	**0.91**
35	60.96	763.2	5041.3	3484.7	46.2	27.9	6.33	608.3	4620.0	3106.5	**53.4**	29.7	4.90	**0.80**
36	76.20	671.9	4851.7	3226.2	45.3	28.5	6.42	598.5	4592.6	3072.0	48.6	28.8	4.93	**0.89**
43	30.48	399.9	3816.8	2127.2	45.3	35.4	5.44	410.4	3889.1	2315.6	44.1	39.6	5.24	1.03
45	60.96	248.4	3321.9	1624.0	46.3	43.1	3.60	413.2	4039.4	2387.6	46.7	42.3	4.91	**1.66**
46	76.20	341.3	3854.3	2026.0	**50.2**	41.8	4.76	560.2	4471.1	2945.3	**56.0**	35.9	4.93	**1.64**
63	30.48	548.8	4277.4	2575.0	47.0	28.1	5.38	225.2	2830.6	1392.0	45.0	31.4	4.72	**0.41**
85	91.44	856.4	5084.8	3577.9	**54.5**	36.2	6.43	655.9	4842.8	3287.1	**52.9**	34.6	6.17	**0.77**
855	91.44	803.4	5011.6	3427.2	**55.9**	48.1	6.27	633.2	4786.2	3231.8	**53.5**	41.4	6.02	**0.79**
86	91.44	586.7	4606.8	2834.0	**63.7**	**51.6**	6.21	1029.0	5298.0	4046.5	**65.1**	41.7	6.31	**1.75**
87	91.44	770.8	4846.8	3177.1	**52.3**	39.6	6.81	448.6	4147.0	2424.6	48.2	32.6	5.27	**0.58**

Table 21. Results for “good” points at the Bank of America Building.

"Great" Wind Resource Locations - Bank of America Building														
	Existing Setting							Cumulative Setting						
Point #	Height Above Ground [m]	Average Wind Power Density [W/m^2]	Average 1kW Wind Turbine Annual Energy Production [kW-hr/year]	Aerotecture WEC Annual Energy Production [kW-hr/year]	Maximum Turbulence Intensity [%]	Turbulence Intensity [%]	Estimated Error in Ave. Wind Power Density [%]	Average Wind Power Density [W/m^2]	Average 1kW Wind Turbine Annual Energy Production [kW-hr/year]	Aerotecture WEC Annual Energy Production [kW-hr/year]	Maximum Turbulence Intensity [%]	Turbulence Intensity [%]	Estimated Error in Ave. Wind Power Density [%]	Ratio of Cumulative Setting to Existing Setting Average Wind Power Density
7	91.44	907.0	5250.9	3785.4	33.0	18.3	6.20	801.5	5069.1	3615.1	28.4	18.6	6.22	**0.88**
34	45.72	712.1	4952.0	3327.4	49.3	30.1	6.30	650.1	4707.4	3194.4	**55.3**	33.3	6.49	**0.91**
35	60.96	763.2	5041.3	3484.7	46.2	27.9	6.33	608.3	4620.0	3106.5	**53.4**	29.7	4.90	**0.80**
36	76.20	671.9	4851.7	3226.2	45.3	28.5	6.42	598.5	4592.6	3072.0	48.6	28.8	4.93	**0.89**
37	91.44	1172.1	5517.8	4338.5	40.8	19.4	6.29	1092.6	5418.1	4301.8	35.3	17.1	6.26	**0.93**
47	91.44	748.8	5028.6	3473.4	**53.9**	35.2	6.34	1537.6	5701.1	4890.2	43.9	29.6	6.50	**2.05**
77	91.44	872.8	5214.6	3728.0	34.6	17.5	6.22	935.3	5253.6	3961.0	29.2	16.8	6.23	**1.07**
81	91.44	2084.5	5978.9	5378.5	41.5	33.6	9.84	1896.6	5927.2	5358.1	32.6	23.1	9.82	**0.91**
815	91.44	1164.7	5445.1	4275.7	**59.3**	44.9	6.25	1835.7	5909.0	5322.6	38.5	32.6	9.78	**1.58**
82	91.44	1091.6	5397.4	4184.2	**53.2**	43.7	6.27	1703.7	5846.5	5196.9	37.6	30.2	9.84	**1.56**
83	91.44	1072.8	5407.5	4127.8	38.6	30.0	6.30	1097.0	5475.7	4387.5	34.7	28.1	6.24	1.02
835	91.44	1033.9	5368.2	4030.6	**50.7**	30.4	6.29	1042.4	5421.0	4245.3	40.8	26.7	6.23	1.01
84	91.44	1087.0	5420.2	4128.0	41.3	26.9	6.28	1161.6	5516.6	4449.9	39.1	26.1	6.27	**1.07**
85	91.44	856.4	5084.8	3577.9	**54.5**	36.2	6.43	655.9	4842.8	3287.1	**52.9**	34.6	6.17	**0.77**
855	91.44	803.4	5011.6	3427.2	**55.9**	48.1	6.27	633.2	4786.2	3231.8	**53.5**	41.4	6.02	**0.79**
87	91.44	770.8	4846.8	3177.1	**52.3**	39.6	6.81	448.6	4147.0	2424.6	48.2	32.6	5.27	**0.58**
88	91.44	1837.1	5752.1	4969.6	**69.6**	32.2	6.73	1829.8	5877.6	5261.9	**51.6**	24.3	9.80	1.00
101000	91.44	1882.6	5814.5	5057.6	**65.8**	36.3	10.08	1910.8	5912.9	5348.9	48.8	32.9	9.86	1.01
101125	95.25	1495.7	5723.3	4774.9	34.2	16.7	6.29	1552.2	5755.0	4983.9	22.5	15.8	6.28	1.04
101250	99.06	1348.7	5617.8	4580.9	26.8	15.2	6.32	1410.6	5654.4	4787.2	20.6	15.5	6.31	1.05
101375	102.87	1247.8	5535.7	4394.7	26.0	15.0	6.33	1365.9	5625.9	4748.8	23.1	16.8	6.31	**1.09**
101500	106.68	1259.1	5543.2	4411.0	25.6	15.8	6.33	1283.5	5568.1	4604.8	23.4	16.3	6.30	1.02
102000	91.44	1231.2	5534.1	4386.6	**51.9**	37.6	6.38	1481.1	5735.3	4921.2	36.5	29.5	6.36	**1.20**
102125	95.25	1568.5	5772.3	4866.2	37.3	29.7	9.81	1522.0	5760.3	4966.9	26.2	22.6	6.30	0.97
102250	99.06	1589.2	5787.5	4899.6	31.3	23.9	9.77	1444.3	5719.7	4881.9	23.0	19.8	6.24	**0.91**
102375	102.87	1415.6	5696.6	4702.6	29.5	20.1	6.25	1268.2	5620.9	4671.3	23.9	19.3	6.18	**0.90**
102500	106.68	1323.2	5647.0	4614.2	28.8	19.1	6.22	1225.7	5590.7	4594.8	24.1	18.7	6.19	**0.93**
103000	91.44	1105.1	5416.8	4148.8	37.3	28.8	6.29	1011.1	5352.6	4132.7	45.5	29.7	6.24	**0.91**
103125	95.25	1304.0	5597.7	4500.4	33.4	22.7	6.29	1291.3	5612.6	4665.3	31.2	23.5	6.21	0.99
103250	99.06	1321.0	5602.3	4521.3	31.3	19.1	6.33	1380.7	5658.1	4797.2	22.4	18.6	6.29	1.05
103375	102.87	1267.4	5585.7	4469.5	30.6	17.3	6.27	1309.0	5623.1	4700.5	22.1	16.9	6.25	1.03
103500	106.68	1271.1	5587.9	4477.5	30.6	16.4	6.27	1357.6	5655.5	4796.7	21.7	15.7	6.25	**1.07**
104000	91.44	926.5	5058.1	3667.3	**69.5**	**53.9**	6.74	785.4	4963.6	3563.2	**59.6**	43.9	6.53	**0.85**
104125	95.25	1433.6	5677.2	4673.8	43.8	19.4	6.33	1448.5	5664.3	4803.1	31.1	17.8	6.39	1.01
104250	99.06	1277.6	5595.3	4487.6	38.9	16.9	6.26	1252.4	5542.4	4540.1	27.1	15.2	6.33	0.98
104375	102.87	1221.2	5558.7	4405.7	32.4	15.9	6.25	1200.2	5507.4	4465.9	24.2	14.4	6.31	0.98
104500	106.68	1220.4	5552.5	4396.4	29.6	15.2	6.26	1157.9	5469.6	4396.0	23.7	14.4	6.31	**0.95**
105000	91.44	1030.2	5237.3	3882.5	**51.4**	33.9	6.56	951.2	5238.2	3968.8	49.8	32.7	6.40	**0.92**
105125	95.25	1262.4	5516.9	4379.4	39.2	24.9	6.38	1339.4	5623.8	4734.5	39.1	23.3	6.28	**1.06**
105250	99.06	1267.4	5557.9	4433.6	37.3	19.9	6.29	1250.1	5573.2	4589.6	22.8	18.4	6.22	0.99
105375	102.87	1209.8	5517.0	4345.5	31.8	16.8	6.30	1244.8	5569.7	4580.4	21.8	16.4	6.23	1.03
105500	106.68	1282.2	5583.2	4476.9	28.4	15.8	6.30	1283.8	5601.3	4650.3	22.4	16.0	6.24	1.00

Table 22. Results for “great” points at the Bank of America Buiding.

Bank of America Building Results with Winds from 6am to 8pm

The reduced, full-scale data for Fox Plaza for winds from 6am to 8pm are displayed in the same manner as in the previous section. The “good” wind resource points’ results of the wind-tunnel testing for the Bank of America Building are shown in Table 23, and the “great” wind resource points’ results are in Table 24. Tables 25a and 25b show the ratio of the average wind speed densities of 6am to 8pm case to the all hours’ case for each point tested.

The point with the highest average wind power density during the hours of 6am to 8pm (the 15-hour day case) for the existing setting was point 875 which had a value of 2781.34 Watts per square meter, and the same point held the highest value, 2649.70 Watts per square meter, for the cumulative setting, All points showed an increase in average wind power density from the 24-hour day case, demonstrating that the winds are higher during business hours.

"Good" Wind Resource Locations - Bank of America Building - 6am - 8pm														
	Existing Setting							Cumulative Setting						
Point #	Height Above Ground [m]	Average Wind Power Density [W/m^2]	Average 1kW Wind Turbine Annual Energy Production [kW-hr/year]	Aerotecture WEC Annual Energy Production [kW-hr/year]	Maximum Turbulence Intensity [%]	Turbulence Intensity [%]	Estimated Error in Ave. Wind Power Density [%]	Average Wind Power Density [W/m^2]	Average 1kW Wind Turbine Annual Energy Production [kW-hr/year]	Aerotecture WEC Annual Energy Production [kW-hr/year]	Maximum Turbulence Intensity [%]	Turbulence Intensity [%]	Estimated Error in Ave. Wind Power Density [%]	Ratio of Cumulative Setting to Existing Setting Average Wind Power Density
33	30.48	645.9	3234.5	2105.0	42.2	33.0	7.33	712.3	3278.5	2260.5	47.5	33.1	7.45	**1.10**
43	30.48	503.1	2793.6	1630.5	45.3	35.7	7.90	528.1	2850.8	1764.6	44.1	39.6	7.97	1.05
45	60.96	324.6	2507.6	1245.3	46.3	43.1	3.61	538.4	2965.8	1856.6	46.7	42.2	7.70	**1.66**
46	76.20	448.9	2855.5	1587.8	**50.2**	41.7	7.57	729.5	3232.2	2246.1	**56.0**	35.6	7.71	**1.63**
63	30.48	679.4	3085.3	2000.1	47.0	28.3	7.74	271.4	2101.4	1039.3	45.0	31.6	4.17	**0.40**

Table 23. Results for “good” points at the Bank of America Building from 6am – 8pm.

"Great" Wind Resource Locations - Bank of America Building - 6am - 8pm														
	Existing Setting							Cumulative Setting						
Point #	Height Above Ground [m]	Average Wind Power Density [W/m²]	Average 1kW Wind Turbine Annual Energy Production [kW-hr/year]	Aerotecture WEC Annual Energy Production [kW-hr/year]	Maximum Turbulence Intensity [%]	Turbulence Intensity [%]	Estimated Error in Ave. Wind Power Density [%]	Average Wind Power Density [W/m²]	Average 1kW Wind Turbine Annual Energy Production [kW-hr/year]	Aerotecture WEC Annual Energy Production [kW-hr/year]	Maximum Turbulence Intensity [%]	Turbulence Intensity [%]	Estimated Error in Ave. Wind Power Density [%]	Ratio of Cumulative Setting to Existing Setting Average Wind Power Density
7	91.44	1134.5	3661.1	2867.8	33.0	18.3	10.06	1002.4	3565.5	2759.0	28.4	18.6	7.19	**0.88**
17	91.44	347.9	2652.8	1328.4	47.1	42.2	3.47	1124.1	3625.1	2923.0	44.7	37.2	10.44	**3.23**
34	45.72	912.9	3502.4	2561.6	49.3	30.2	7.35	832.8	3359.3	2444.1	**55.3**	33.5	7.55	**0.91**
35	60.96	986.5	3551.6	2680.7	46.2	27.9	7.40	783.4	3310.0	2350.2	**53.4**	29.8	7.59	**0.79**
36	76.20	872.0	3447.9	2488.1	45.3	28.5	7.50	775.0	3293.4	2328.7	48.6	28.9	7.66	**0.89**
37	91.44	1487.8	3787.9	3241.2	40.8	19.4	10.25	1378.6	3746.5	3201.2	35.3	17.1	10.19	**0.93**
47	91.44	974.2	3546.9	2674.9	**53.9**	34.8	7.43	1946.8	3868.1	3586.2	43.9	29.4	10.47	**2.00**
77	91.44	1095.2	3641.0	2822.2	34.6	17.6	10.09	1178.9	3663.5	2993.5	29.2	16.8	10.16	**1.08**
81	91.44	2631.7	4008.3	3859.5	41.5	33.5	10.30	2394.5	3984.1	3860.9	32.6	23.0	10.26	**0.91**
815	91.44	1484.6	3763.5	3223.4	**59.3**	44.7	10.26	2328.7	3977.1	3845.7	38.5	32.5	10.25	**1.57**
82	91.44	1392.3	3738.6	3131.5	**53.2**	43.5	10.28	2168.6	3948.8	3767.2	37.6	30.1	10.30	**1.56**
83	91.44	1356.2	3738.6	3094.8	38.6	30.1	10.23	1390.4	3770.3	3244.8	34.7	28.2	10.18	1.03
835	91.44	1302.2	3718.7	3042.5	**50.7**	30.5	10.20	1317.1	3748.0	3173.3	40.8	26.7	10.14	1.01
84	91.44	1358.5	3744.8	3091.4	41.3	27.0	10.14	1463.8	3787.0	3299.1	39.1	26.1	10.18	**1.08**
85	91.44	1078.0	3568.1	2741.0	**54.5**	36.0	7.40	831.1	3449.4	2533.1	**52.9**	34.3	7.20	**0.77**
855	91.44	994.5	3531.1	2623.9	**55.9**	48.1	7.21	795.6	3427.3	2478.8	**53.5**	41.2	7.06	**0.80**
87	91.44	931.1	3414.7	2428.8	**52.3**	39.9	7.46	537.3	3009.5	1815.2	48.2	33.0	7.16	**0.58**
88	91.44	2330.7	3891.9	3594.5	**69.6**	32.3	10.76	2304.0	3962.6	3820.0	**51.6**	24.3	10.26	0.99
101000	91.44	2374.4	3925.4	3665.7	**65.8**	36.6	10.54	2421.2	3977.2	3857.5	48.8	33.2	10.32	1.02
101125	95.25	1886.2	3885.8	3506.3	34.2	16.8	10.23	1959.9	3901.6	3631.4	22.5	15.8	10.23	1.04
101250	99.06	1699.5	3835.4	3363.7	26.8	15.3	10.25	1780.3	3852.8	3507.8	20.6	15.5	10.27	1.05
101375	102.87	1569.9	3796.8	3265.2	26.0	15.1	10.25	1725.0	3839.6	3467.2	23.1	16.8	10.27	**1.10**
101500	106.68	1584.1	3800.1	3273.6	25.6	15.8	10.26	1620.5	3812.8	3392.0	23.4	16.4	10.26	1.02
102000	91.44	1558.0	3793.6	3275.3	**51.9**	37.7	10.32	1881.9	3888.1	3595.2	36.5	29.6	10.32	**1.21**
102125	95.25	1974.4	3906.8	3550.9	37.3	29.8	10.25	1920.6	3901.8	3619.2	26.2	22.6	10.23	0.97
102250	99.06	1998.0	3915.5	3569.7	31.3	23.9	10.21	1822.0	3885.6	3586.2	23.0	19.8	10.17	**0.91**
102375	102.87	1783.4	3874.2	3461.7	29.5	20.1	10.18	1601.0	3840.7	3431.6	23.9	19.3	10.11	**0.90**
102500	106.68	1668.1	3852.6	3385.4	28.8	19.2	10.14	1548.0	3824.9	3390.2	24.1	18.8	10.12	**0.93**
103000	91.44	1381.9	3743.5	3102.1	37.3	28.7	10.17	1274.5	3713.6	3127.9	45.5	29.6	10.16	**0.92**
103125	95.25	1631.5	3826.1	3319.0	33.4	22.7	10.18	1624.1	3835.5	3425.6	31.2	23.4	10.13	1.00
103250	99.06	1657.1	3826.8	3329.1	31.3	19.1	10.23	1736.7	3854.9	3489.5	22.4	18.5	10.21	1.05
103375	102.87	1592.6	3821.0	3305.5	30.6	17.3	10.18	1651.8	3840.0	3443.0	22.1	16.9	10.19	1.04
103500	106.68	1598.8	3822.0	3310.2	30.6	16.4	10.18	1716.4	3855.8	3495.1	21.7	15.7	10.19	**1.07**
104000	91.44	1197.9	3551.7	2796.3	**69.5**	**53.6**	7.83	1015.6	3501.4	2724.4	**59.6**	43.6	7.62	**0.85**
104125	95.25	1796.0	3862.2	3430.6	43.8	19.4	10.23	1821.6	3854.4	3513.3	31.1	17.8	10.32	1.01
104250	99.06	1604.2	3825.5	3314.7	38.9	17.0	10.17	1576.5	3799.6	3354.7	27.1	15.2	10.26	0.98
104375	102.87	1535.8	3808.7	3273.3	32.4	15.9	10.16	1511.7	3783.4	3317.1	24.2	14.4	10.24	0.98
104500	106.68	1534.8	3805.3	3283.0	29.6	15.2	10.17	1457.6	3765.3	3260.6	23.7	14.4	10.23	**0.95**
105000	91.44	1304.4	3641.7	2952.0	**51.4**	34.0	10.55	1212.1	3649.9	3001.3	49.8	32.8	10.39	**0.93**
105125	95.25	1587.8	3787.1	3255.6	39.2	25.0	10.32	1694.9	3840.1	3462.5	39.1	23.3	10.23	**1.07**
105250	99.06	1590.8	3808.4	3286.6	37.3	20.0	10.20	1576.2	3817.4	3387.1	22.8	18.4	10.16	0.99
105375	102.87	1520.2	3788.3	3243.0	31.8	16.8	10.21	1570.3	3815.1	3381.5	21.8	16.4	10.17	1.03
105500	106.68	1612.1	3819.2	3308.6	28.4	15.8	10.21	1620.3	3829.3	3417.7	22.4	16.0	10.18	1.01

Table 24. Results for “great” points at the Bank of America Building from 6am – 8pm.

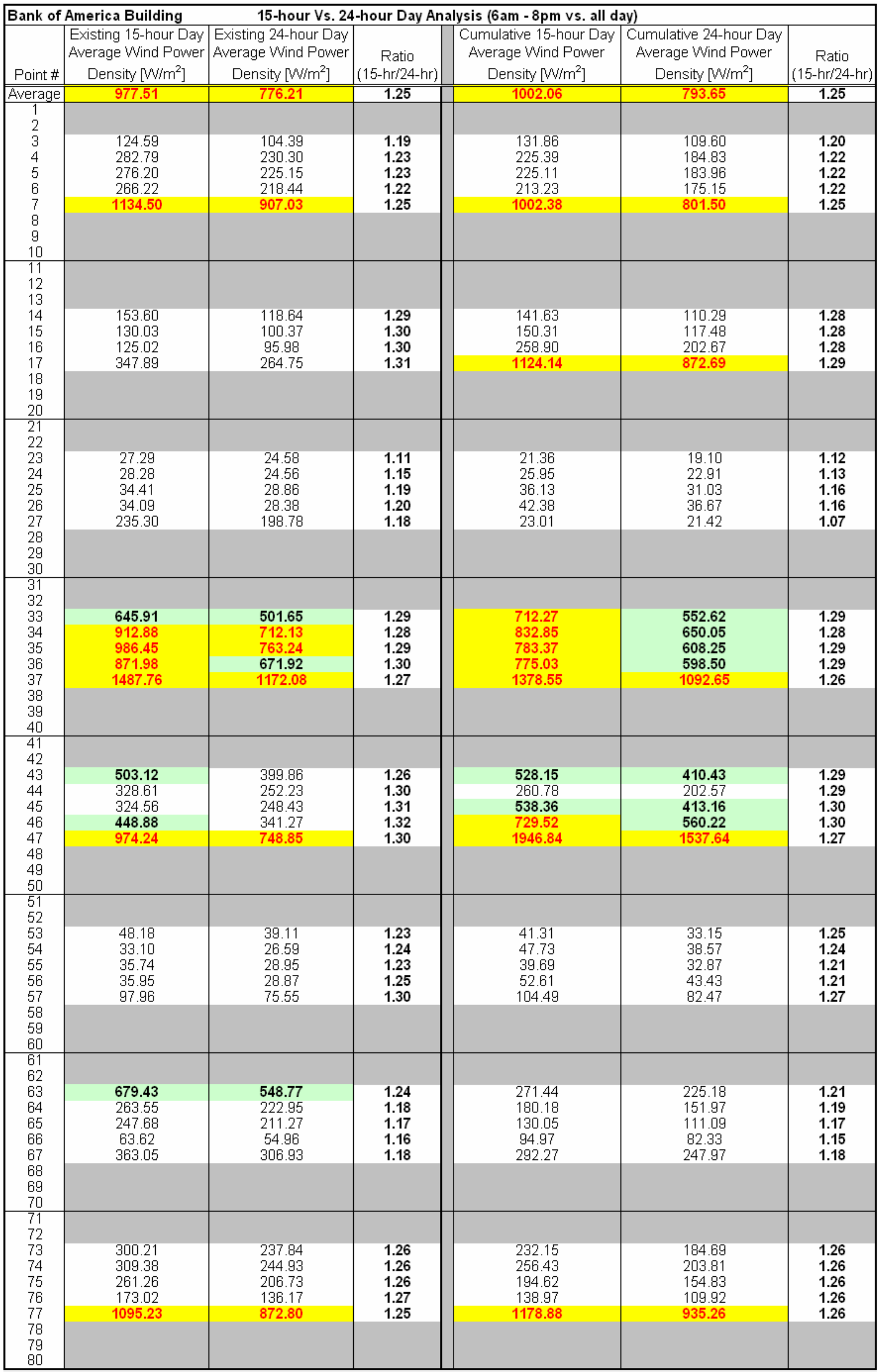

Bank of America Building **15-hour Vs. 24-hour Day Analysis (6am - 8pm vs. all day)**

Point #	Existing 15-hour Day Average Wind Power Density [W/m^2]	Existing 24-hour Day Average Wind Power Density [W/m^2]	Ratio (15-hr/24-hr)	Cumulative 15-hour Day Average Wind Power Density [W/m^2]	Cumulative 24-hour Day Average Wind Power Density [W/m^2]	Ratio (15-hr/24-hr)
Average	977.51	776.21	1.25	1002.06	793.65	1.25
1						
2						
3	124.59	104.39	1.19	131.86	109.60	1.20
4	282.79	230.30	1.23	225.39	184.83	1.22
5	276.20	225.15	1.23	225.11	183.96	1.22
6	266.22	218.44	1.22	213.23	175.15	1.22
7	1134.50	907.03	1.25	1002.38	801.50	1.25
8						
9						
10						
11						
12						
13						
14	153.60	118.64	1.29	141.63	110.29	1.28
15	130.03	100.37	1.30	150.31	117.48	1.28
16	125.02	95.98	1.30	258.90	202.67	1.28
17	347.89	264.75	1.31	1124.14	872.69	1.29
18						
19						
20						
21						
22						
23	27.29	24.58	1.11	21.36	19.10	1.12
24	28.28	24.56	1.15	25.95	22.91	1.13
25	34.41	28.86	1.19	36.13	31.03	1.16
26	34.09	28.38	1.20	42.38	36.67	1.16
27	235.30	198.78	1.18	23.01	21.42	1.07
28						
29						
30						
31						
32						
33	645.91	501.65	1.29	712.27	552.62	1.29
34	912.88	712.13	1.28	832.85	650.05	1.28
35	986.45	763.24	1.29	783.37	608.25	1.29
36	871.98	671.92	1.30	775.03	598.50	1.29
37	1487.76	1172.08	1.27	1378.55	1092.65	1.26
38						
39						
40						
41						
42						
43	503.12	399.86	1.26	528.15	410.43	1.29
44	328.61	252.23	1.30	260.78	202.57	1.29
45	324.56	248.43	1.31	538.36	413.16	1.30
46	448.88	341.27	1.32	729.52	560.22	1.30
47	974.24	748.85	1.30	1946.84	1537.64	1.27
48						
49						
50						
51						
52						
53	48.18	39.11	1.23	41.31	33.15	1.25
54	33.10	26.59	1.24	47.73	38.57	1.24
55	35.74	28.95	1.23	39.69	32.87	1.21
56	35.95	28.87	1.25	52.61	43.43	1.21
57	97.96	75.55	1.30	104.49	82.47	1.27
58						
59						
60						
61						
62						
63	679.43	548.77	1.24	271.44	225.18	1.21
64	263.55	222.95	1.18	180.18	151.97	1.19
65	247.68	211.27	1.17	130.05	111.09	1.17
66	63.62	54.96	1.16	94.97	82.33	1.15
67	363.05	306.93	1.18	292.27	247.97	1.18
68						
69						
70						
71						
72						
73	300.21	237.84	1.26	232.15	184.69	1.26
74	309.38	244.93	1.26	256.43	203.81	1.26
75	261.26	206.73	1.26	194.62	154.83	1.26
76	173.02	136.17	1.27	138.97	109.92	1.26
77	1095.23	872.80	1.25	1178.88	935.26	1.26
78						
79						
80						

Table 25a. Ratio of average wind power densities of the 6am – 8pm case to the 24-hours per day case for the Bank of America Building.

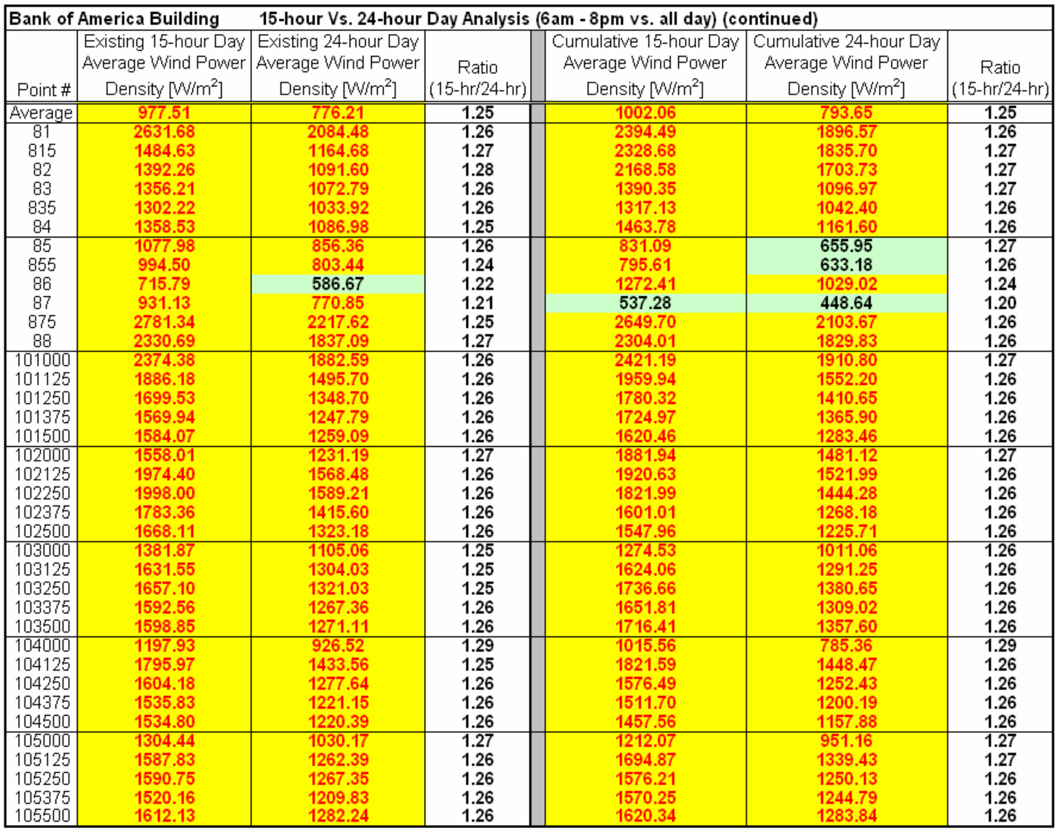

Bank of America Building **15-hour Vs. 24-hour Day Analysis (6am - 8pm vs. all day) (continued)**

Point #	Existing 15-hour Day Average Wind Power Density [W/m²]	Existing 24-hour Day Average Wind Power Density [W/m²]	Ratio (15-hr/24-hr)	Cumulative 15-hour Day Average Wind Power Density [W/m²]	Cumulative 24-hour Day Average Wind Power Density [W/m²]	Ratio (15-hr/24-hr)
Average	977.51	776.21	1.25	1002.06	793.65	1.25
81	2631.68	2084.48	1.26	2394.49	1896.57	1.26
815	1484.63	1164.68	1.27	2328.68	1835.70	1.27
82	1392.26	1091.60	1.28	2168.58	1703.73	1.27
83	1356.21	1072.79	1.26	1390.35	1096.97	1.27
835	1302.22	1033.92	1.26	1317.13	1042.40	1.26
84	1358.53	1086.98	1.25	1463.78	1161.60	1.26
85	1077.98	856.36	1.26	831.09	655.95	1.27
855	994.50	803.44	1.24	795.61	633.18	1.26
86	715.79	586.67	1.22	1272.41	1029.02	1.24
87	931.13	770.85	1.21	537.28	448.64	1.20
875	2781.34	2217.62	1.25	2649.70	2103.67	1.26
88	2330.69	1837.09	1.27	2304.01	1829.83	1.26
101000	2374.38	1882.59	1.26	2421.19	1910.80	1.27
101125	1886.18	1495.70	1.26	1959.94	1552.20	1.26
101250	1699.53	1348.70	1.26	1780.32	1410.65	1.26
101375	1569.94	1247.79	1.26	1724.97	1365.90	1.26
101500	1584.07	1259.09	1.26	1620.46	1283.46	1.26
102000	1558.01	1231.19	1.27	1881.94	1481.12	1.27
102125	1974.40	1568.48	1.26	1920.63	1521.99	1.26
102250	1998.00	1589.21	1.26	1821.99	1444.28	1.26
102375	1783.36	1415.60	1.26	1601.01	1268.18	1.26
102500	1668.11	1323.18	1.26	1547.96	1225.71	1.26
103000	1381.87	1105.06	1.25	1274.53	1011.06	1.26
103125	1631.55	1304.03	1.25	1624.06	1291.25	1.26
103250	1657.10	1321.03	1.25	1736.66	1380.65	1.26
103375	1592.56	1267.36	1.26	1651.81	1309.02	1.26
103500	1598.85	1271.11	1.26	1716.41	1357.60	1.26
104000	1197.93	926.52	1.29	1015.56	785.36	1.29
104125	1795.97	1433.56	1.25	1821.59	1448.47	1.26
104250	1604.18	1277.64	1.26	1576.49	1252.43	1.26
104375	1535.83	1221.15	1.26	1511.70	1200.19	1.26
104500	1534.80	1220.39	1.26	1457.56	1157.88	1.26
105000	1304.44	1030.17	1.27	1212.07	951.16	1.27
105125	1587.83	1262.39	1.26	1694.87	1339.43	1.27
105250	1590.75	1267.35	1.26	1576.21	1250.13	1.26
105375	1520.16	1209.83	1.26	1570.25	1244.79	1.26
105500	1612.13	1282.24	1.26	1620.34	1283.84	1.26

Table 25b. Ratio of average wind power densities of the 6am – 8pm case to the 24-hours per day case for the Bank of America Building (continued from Table 25a).

3.2 Folsom and Main Street Buildings' Results

3.2.1 Folsom and Main East Results

The "good" wind resource points' results of the wind-tunnel testing for the Folsom and Main East building are shown in Table 26, and the "great" wind resource points' results are in Table 27.

Average wind power densities were highest near or above the roof level. The highest average wind power density was 749.7 Watts per square meter at point 105500. The only "great" wind resource sites are located at or above the rooftop level of the building, and the only "good" wind resource site not on or above roof level is point 48 with an average wind power density of 408.9 Watts per square meter.

The highest turbulence intensity for a point with "good" or "great" wind resource was point 86 with 59.5 percent. The average of the measurement locations' average wind power density for Folsom and Main East was 235.07 Watts per square meter.

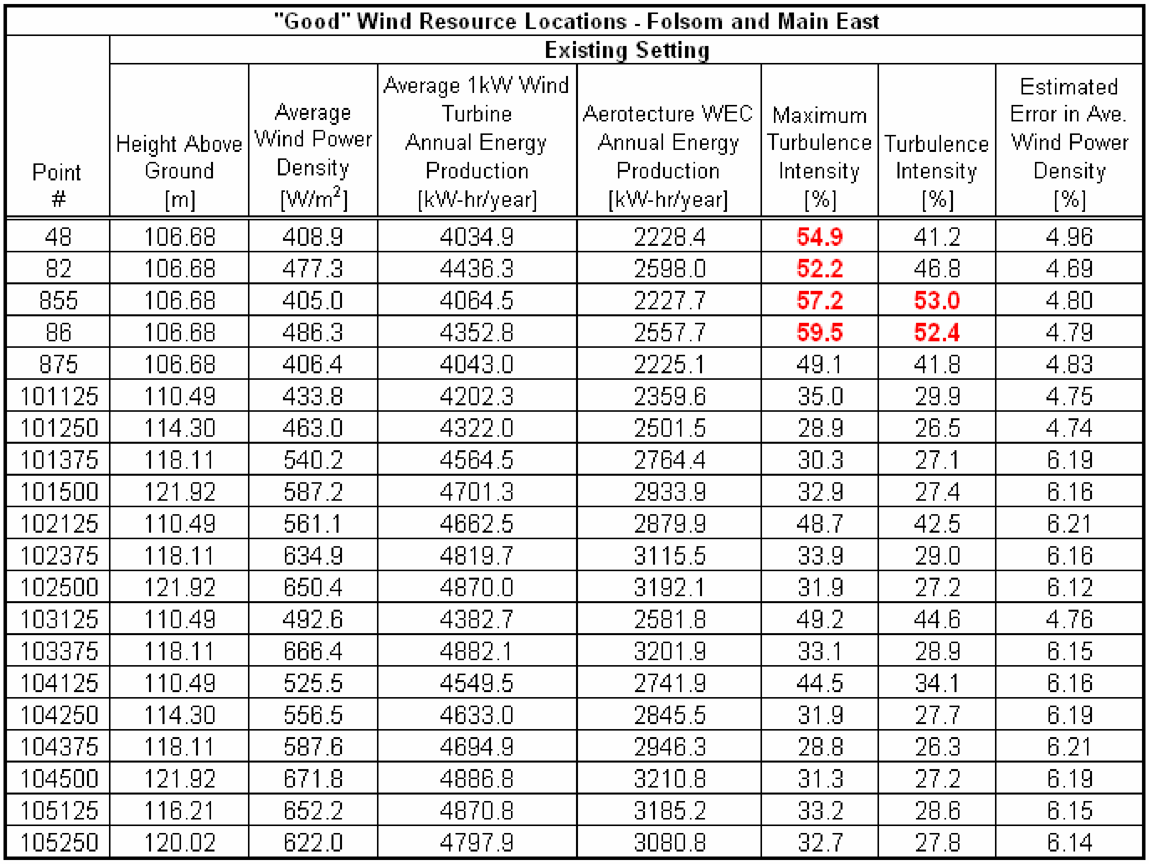

"Good" Wind Resource Locations - Folsom and Main East							
	Existing Setting						
Point #	Height Above Ground [m]	Average Wind Power Density [W/m^2]	Average 1kW Wind Turbine Annual Energy Production [kW-hr/year]	Aerotecture WEC Annual Energy Production [kW-hr/year]	Maximum Turbulence Intensity [%]	Turbulence Intensity [%]	Estimated Error in Ave. Wind Power Density [%]
48	106.68	408.9	4034.9	2228.4	**54.9**	41.2	4.96
82	106.68	477.3	4436.3	2598.0	**52.2**	46.8	4.69
855	106.68	405.0	4064.5	2227.7	**57.2**	**53.0**	4.80
86	106.68	486.3	4352.8	2557.7	**59.5**	**52.4**	4.79
875	106.68	406.4	4043.0	2225.1	49.1	41.8	4.83
101125	110.49	433.8	4202.3	2359.6	35.0	29.9	4.75
101250	114.30	463.0	4322.0	2501.5	28.9	26.5	4.74
101375	118.11	540.2	4564.5	2764.4	30.3	27.1	6.19
101500	121.92	587.2	4701.3	2933.9	32.9	27.4	6.16
102125	110.49	561.1	4662.5	2879.9	48.7	42.5	6.21
102375	118.11	634.9	4819.7	3115.5	33.9	29.0	6.16
102500	121.92	650.4	4870.0	3192.1	31.9	27.2	6.12
103125	110.49	492.6	4382.7	2581.8	49.2	44.6	4.76
103375	118.11	666.4	4882.1	3201.9	33.1	28.9	6.15
104125	110.49	525.5	4549.5	2741.9	44.5	34.1	6.16
104250	114.30	556.5	4633.0	2845.5	31.9	27.7	6.19
104375	118.11	587.6	4694.9	2946.3	28.8	26.3	6.21
104500	121.92	671.8	4886.8	3210.8	31.3	27.2	6.19
105125	116.21	652.2	4870.8	3185.2	33.2	28.6	6.15
105250	120.02	622.0	4797.9	3080.8	32.7	27.8	6.14

Table 26. Results for "good" points at Folsom and Main East.

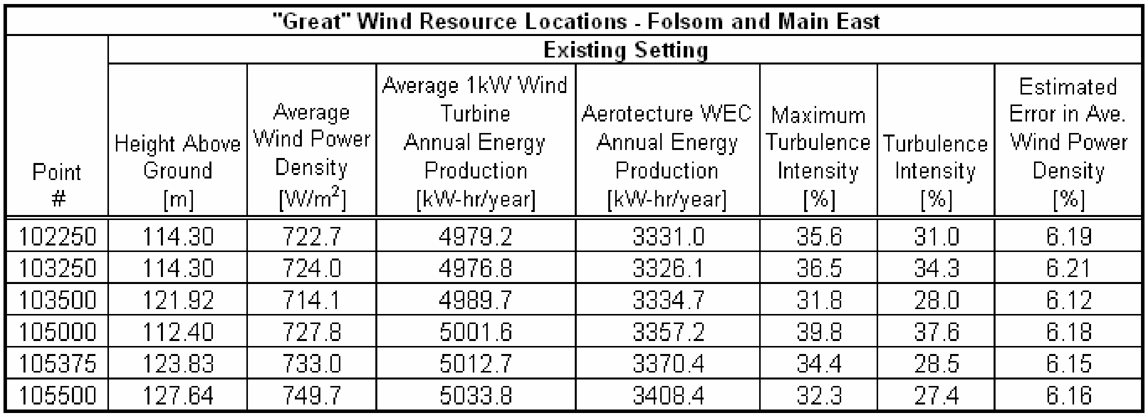

"Great" Wind Resource Locations - Folsom and Main East							
	Existing Setting						
Point #	Height Above Ground [m]	Average Wind Power Density [W/m^2]	Average 1kW Wind Turbine Annual Energy Production [kW-hr/year]	Aerotecture WEC Annual Energy Production [kW-hr/year]	Maximum Turbulence Intensity [%]	Turbulence Intensity [%]	Estimated Error in Ave. Wind Power Density [%]
102250	114.30	722.7	4979.2	3331.0	35.6	31.0	6.19
103250	114.30	724.0	4976.8	3326.1	36.5	34.3	6.21
103500	121.92	714.1	4989.7	3334.7	31.8	28.0	6.12
105000	112.40	727.8	5001.6	3357.2	39.8	37.6	6.18
105375	123.83	733.0	5012.7	3370.4	34.4	28.5	6.15
105500	127.64	749.7	5033.8	3408.4	32.3	27.4	6.16

Table 27. Results for "great" points at Folsom and Main East.

Folsom and Main East Results with Winds from 6am – 8pm

The reduced, full-scale data for Fox Plaza for winds from 6am to 8pm are displayed in the same manner as in the previous section. The "good" wind resource points' results of the wind-tunnel testing for the CSAA Building are shown in Table 28, and the "great" wind resource points' results are in Table 29. Tables 30a and 30b show the ratio of the average wind speed densities of 6am to 8pm case to the all hours' case for each point tested.

The point with the highest average wind power density during the hours of 6am to 8pm (the 15-hour day case) was point 105500 which had a value of 942.41 Watts per square meter. All points showed an increase in average wind power density from the 24-hour day case, demonstrating that the winds are higher during business hours.

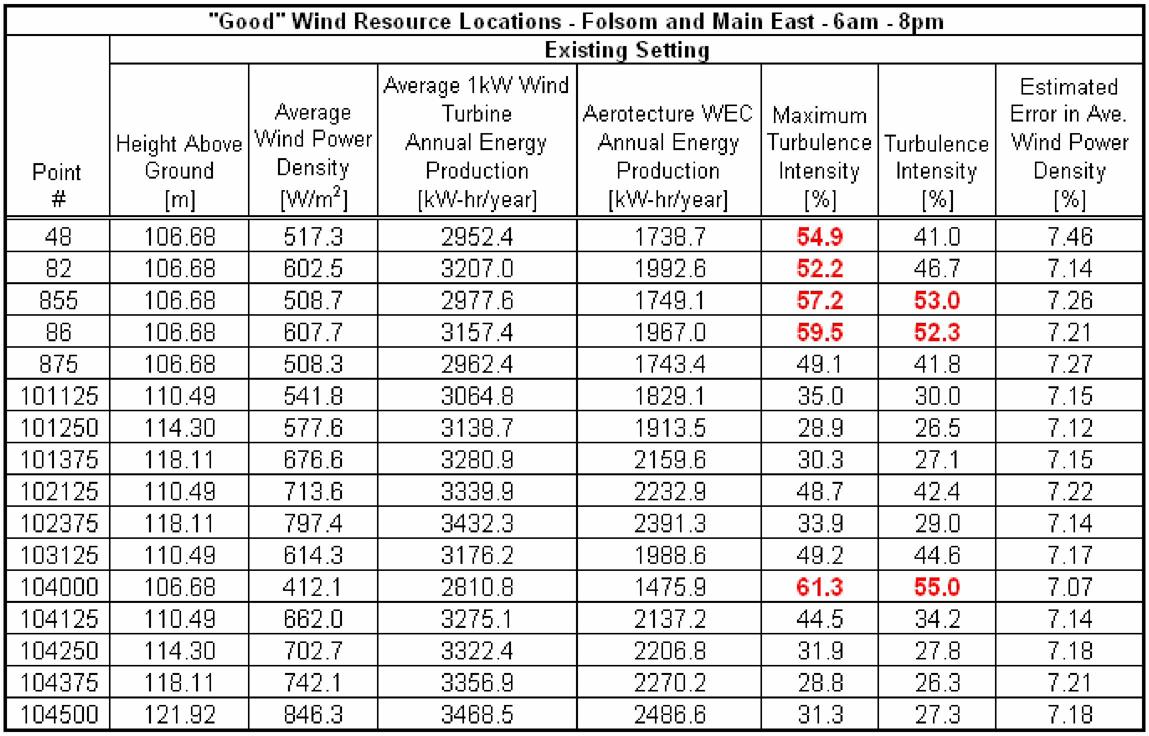

"Good" Wind Resource Locations - Folsom and Main East - 6am - 8pm							
	Existing Setting						
Point #	Height Above Ground [m]	Average Wind Power Density [W/m^2]	Average 1kW Wind Turbine Annual Energy Production [kW-hr/year]	Aerotecture WEC Annual Energy Production [kW-hr/year]	Maximum Turbulence Intensity [%]	Turbulence Intensity [%]	Estimated Error in Ave. Wind Power Density [%]
48	106.68	517.3	2952.4	1738.7	**54.9**	41.0	7.46
82	106.68	602.5	3207.0	1992.6	**52.2**	46.7	7.14
855	106.68	508.7	2977.6	1749.1	**57.2**	**53.0**	7.26
86	106.68	607.7	3157.4	1967.0	**59.5**	**52.3**	7.21
875	106.68	508.3	2962.4	1743.4	49.1	41.8	7.27
101125	110.49	541.8	3064.8	1829.1	35.0	30.0	7.15
101250	114.30	577.6	3138.7	1913.5	28.9	26.5	7.12
101375	118.11	676.6	3280.9	2159.6	30.3	27.1	7.15
102125	110.49	713.6	3339.9	2232.9	48.7	42.4	7.22
102375	118.11	797.4	3432.3	2391.3	33.9	29.0	7.14
103125	110.49	614.3	3176.2	1988.6	49.2	44.6	7.17
104000	106.68	412.1	2810.8	1475.9	**61.3**	**55.0**	7.07
104125	110.49	662.0	3275.1	2137.2	44.5	34.2	7.14
104250	114.30	702.7	3322.4	2206.8	31.9	27.8	7.18
104375	118.11	742.1	3356.9	2270.2	28.8	26.3	7.21
104500	121.92	846.3	3468.5	2486.6	31.3	27.3	7.18

Table 28. Results for "good" points at the Folsom and Main East building from 6am – 8pm.

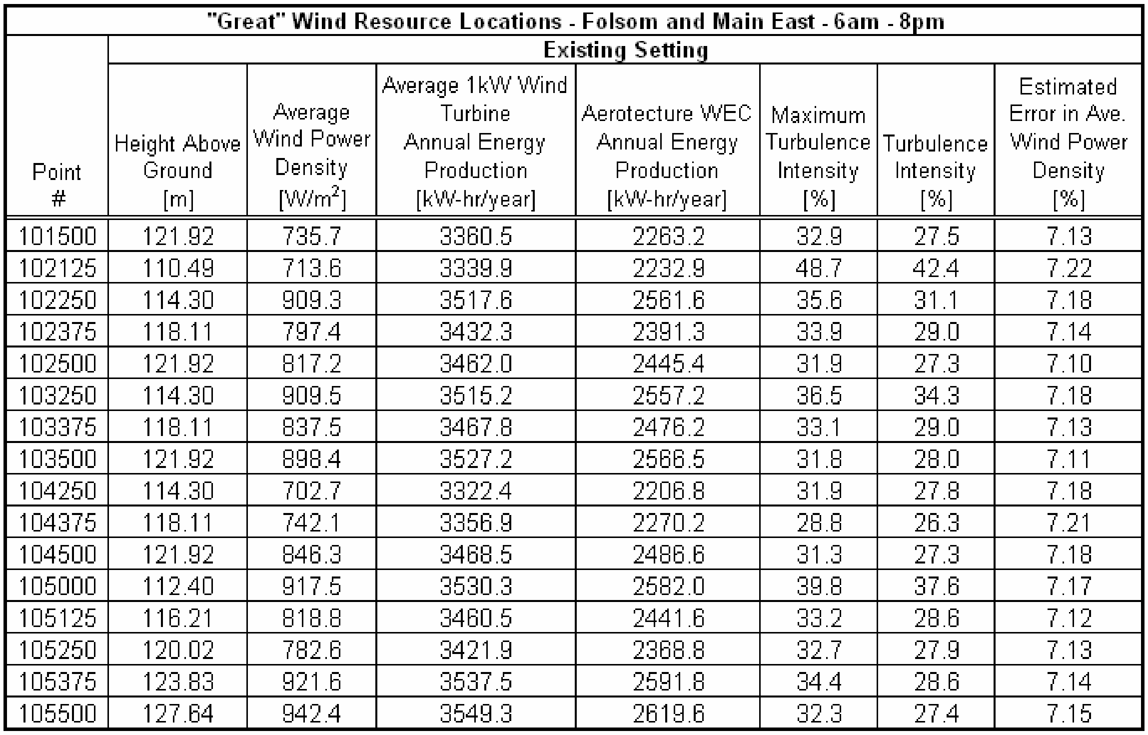

"Great" Wind Resource Locations - Folsom and Main East - 6am - 8pm							
	Existing Setting						
Point #	Height Above Ground [m]	Average Wind Power Density [W/m^2]	Average 1kW Wind Turbine Annual Energy Production [kW-hr/year]	Aerotecture WEC Annual Energy Production [kW-hr/year]	Maximum Turbulence Intensity [%]	Turbulence Intensity [%]	Estimated Error in Ave. Wind Power Density [%]
101500	121.92	735.7	3360.5	2263.2	32.9	27.5	7.13
102125	110.49	713.6	3339.9	2232.9	48.7	42.4	7.22
102250	114.30	909.3	3517.6	2561.6	35.6	31.1	7.18
102375	118.11	797.4	3432.3	2391.3	33.9	29.0	7.14
102500	121.92	817.2	3462.0	2445.4	31.9	27.3	7.10
103250	114.30	909.5	3515.2	2557.2	36.5	34.3	7.18
103375	118.11	837.5	3467.8	2476.2	33.1	29.0	7.13
103500	121.92	898.4	3527.2	2566.5	31.8	28.0	7.11
104250	114.30	702.7	3322.4	2206.8	31.9	27.8	7.18
104375	118.11	742.1	3356.9	2270.2	28.8	26.3	7.21
104500	121.92	846.3	3468.5	2486.6	31.3	27.3	7.18
105000	112.40	917.5	3530.3	2582.0	39.8	37.6	7.17
105125	116.21	818.8	3460.5	2441.6	33.2	28.6	7.12
105250	120.02	782.6	3421.9	2368.8	32.7	27.9	7.13
105375	123.83	921.6	3537.5	2591.8	34.4	28.6	7.14
105500	127.64	942.4	3549.3	2619.6	32.3	27.4	7.15

Table 29. Results for "great" points at the Folsom and Main East building from 6am – 8pm.

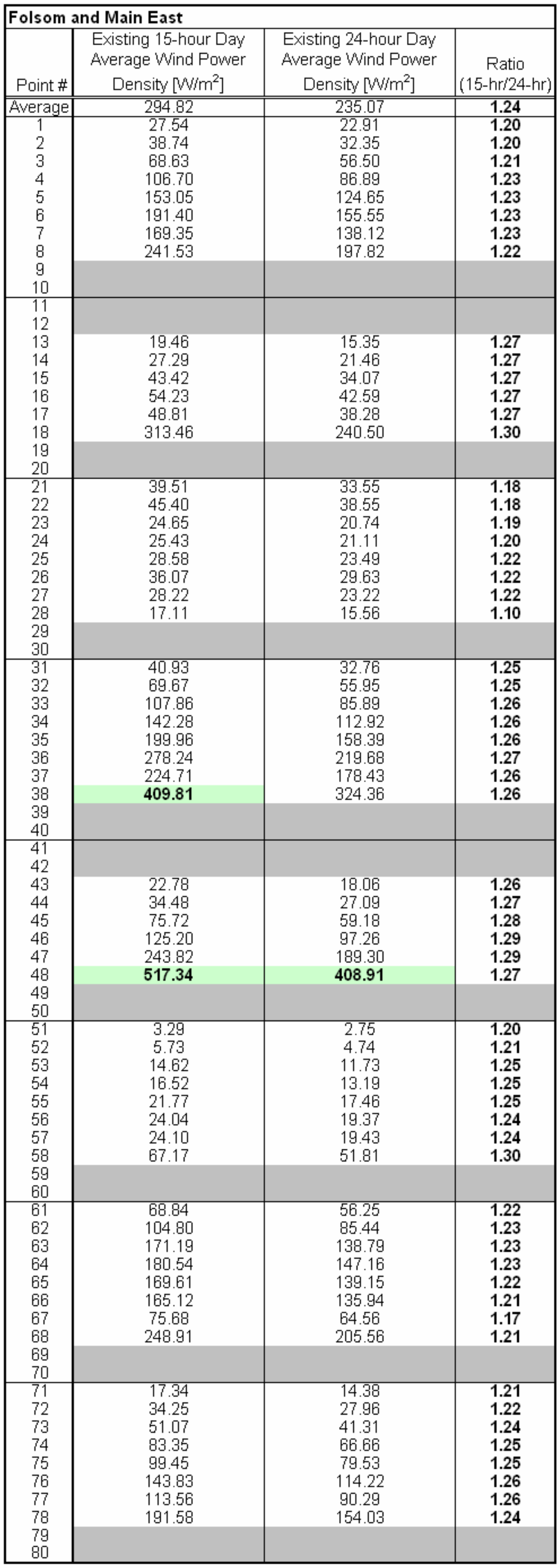

Folsom and Main East			
Point #	Existing 15-hour Day Average Wind Power Density [W/m^2]	Existing 24-hour Day Average Wind Power Density [W/m^2]	Ratio (15-hr/24-hr)
Average	294.82	235.07	**1.24**
1	27.54	22.91	**1.20**
2	38.74	32.35	**1.20**
3	68.63	56.50	**1.21**
4	106.70	86.89	**1.23**
5	153.05	124.65	**1.23**
6	191.40	155.55	**1.23**
7	169.35	138.12	**1.23**
8	241.53	197.82	**1.22**
9			
10			
11			
12			
13	19.46	15.35	**1.27**
14	27.29	21.46	**1.27**
15	43.42	34.07	**1.27**
16	54.23	42.59	**1.27**
17	48.81	38.28	**1.27**
18	313.46	240.50	**1.30**
19			
20			
21	39.51	33.55	**1.18**
22	45.40	38.55	**1.18**
23	24.65	20.74	**1.19**
24	25.43	21.11	**1.20**
25	28.58	23.49	**1.22**
26	36.07	29.63	**1.22**
27	28.22	23.22	**1.22**
28	17.11	15.56	**1.10**
29			
30			
31	40.93	32.76	**1.25**
32	69.67	55.95	**1.25**
33	107.86	85.89	**1.26**
34	142.28	112.92	**1.26**
35	199.96	158.39	**1.26**
36	278.24	219.68	**1.27**
37	224.71	178.43	**1.26**
38	**409.81**	324.36	**1.26**
39			
40			
41			
42			
43	22.78	18.06	**1.26**
44	34.48	27.09	**1.27**
45	75.72	59.18	**1.28**
46	125.20	97.26	**1.29**
47	243.82	189.30	**1.29**
48	**517.34**	**408.91**	**1.27**
49			
50			
51	3.29	2.75	**1.20**
52	5.73	4.74	**1.21**
53	14.62	11.73	**1.25**
54	16.52	13.19	**1.25**
55	21.77	17.46	**1.25**
56	24.04	19.37	**1.24**
57	24.10	19.43	**1.24**
58	67.17	51.81	**1.30**
59			
60			
61	68.84	56.25	**1.22**
62	104.80	85.44	**1.23**
63	171.19	138.79	**1.23**
64	180.54	147.16	**1.23**
65	169.61	139.15	**1.22**
66	165.12	135.94	**1.21**
67	75.68	64.56	**1.17**
68	248.91	205.56	**1.21**
69			
70			
71	17.34	14.38	**1.21**
72	34.25	27.96	**1.22**
73	51.07	41.31	**1.24**
74	83.35	66.66	**1.25**
75	99.45	79.53	**1.25**
76	143.83	114.22	**1.26**
77	113.56	90.29	**1.26**
78	191.58	154.03	**1.24**
79			
80			

Table 30a. Ratio of average wind power densities of the 6am – 8pm case to the 24-hours per day case for the Folsom and Main East building.

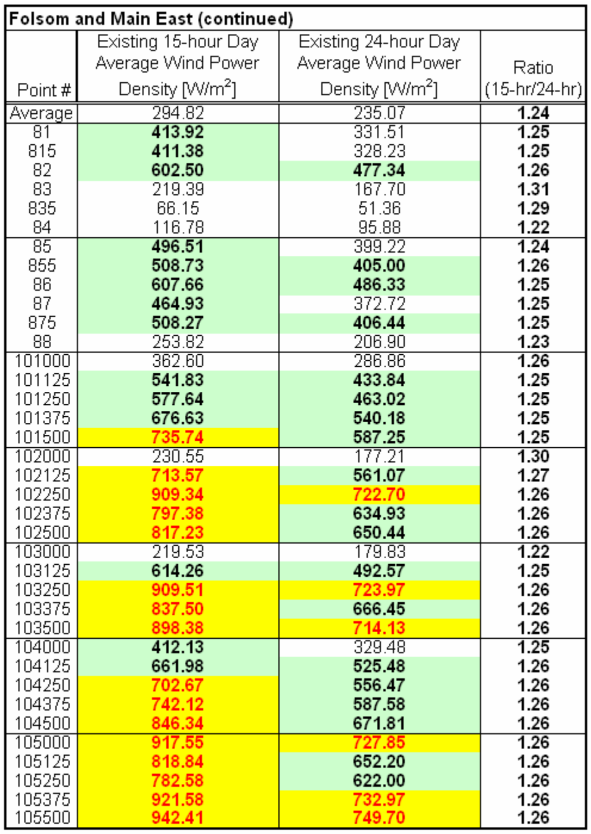

Folsom and Main East (continued)			
Point #	Existing 15-hour Day Average Wind Power Density [W/m^2]	Existing 24-hour Day Average Wind Power Density [W/m^2]	Ratio (15-hr/24-hr)
Average	294.82	235.07	**1.24**
81	**413.92**	331.51	**1.25**
815	**411.38**	328.23	**1.25**
82	**602.50**	**477.34**	**1.26**
83	219.39	167.70	**1.31**
835	66.15	51.36	**1.29**
84	116.78	95.88	**1.22**
85	**496.51**	399.22	**1.24**
855	**508.73**	**405.00**	**1.26**
86	**607.66**	**486.33**	**1.25**
87	**464.93**	372.72	**1.25**
875	**508.27**	**406.44**	**1.25**
88	253.82	206.90	**1.23**
101000	362.60	286.86	**1.26**
101125	**541.83**	**433.84**	**1.25**
101250	**577.64**	**463.02**	**1.25**
101375	**676.63**	**540.18**	**1.25**
101500	**735.74**	**587.25**	**1.25**
102000	230.55	177.21	**1.30**
102125	**713.57**	**561.07**	**1.27**
102250	**909.34**	**722.70**	**1.26**
102375	**797.38**	**634.93**	**1.26**
102500	**817.23**	**650.44**	**1.26**
103000	219.53	179.83	**1.22**
103125	**614.26**	**492.57**	**1.25**
103250	**909.51**	**723.97**	**1.26**
103375	**837.50**	**666.45**	**1.26**
103500	**898.38**	**714.13**	**1.26**
104000	**412.13**	329.48	**1.25**
104125	**661.98**	**525.48**	**1.26**
104250	**702.67**	**556.47**	**1.26**
104375	**742.12**	**587.58**	**1.26**
104500	**846.34**	**671.81**	**1.26**
105000	**917.55**	**727.85**	**1.26**
105125	**818.84**	**652.20**	**1.26**
105250	**782.58**	**622.00**	**1.26**
105375	**921.58**	**732.97**	**1.26**
105500	**942.41**	**749.70**	**1.26**

Table 30b. Ratio of average wind power densities of the 6am – 8pm case to the 24-hours per day case for the Folsom and Main East building (continued from Table 30a).

3.2.2 Folsom and Main West Results

The "good" wind resource points' results of the wind-tunnel testing for the Folsom and Main East building are shown in Table 31, and the "great" wind resource points' results are in Table 32.

Average wind power densities were highest near or above the roof level. The highest average wind power density was 755.5 Watts per square meter at point 105125. The only "great" wind resource sites are located at or above the rooftop level of the building, and the only "good" wind resource sites not on or above roof level are point 40 and 49 with average wind power densities of 485.1 and 450.7 Watts per square meter, respectively.

The highest turbulence intensity for a point with "good" or "great" wind resource was point 104000 with 76.7percent. The average of the measurement locations' average wind power density for Folsom and Main West was 232.73 Watts per square meter.

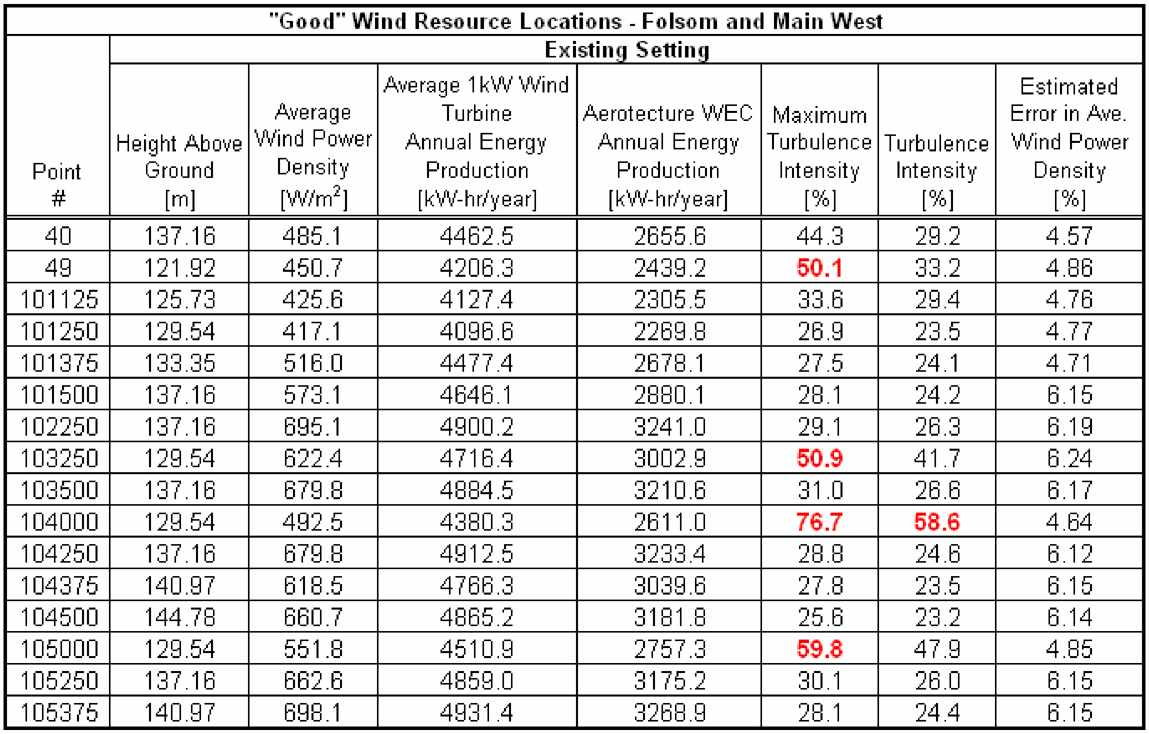

"Good" Wind Resource Locations - Folsom and Main West							
	Existing Setting						
Point #	Height Above Ground [m]	Average Wind Power Density [W/m^2]	Average 1kW Wind Turbine Annual Energy Production [kW-hr/year]	Aerotecture WEC Annual Energy Production [kW-hr/year]	Maximum Turbulence Intensity [%]	Turbulence Intensity [%]	Estimated Error in Ave. Wind Power Density [%]
40	137.16	485.1	4462.5	2655.6	44.3	29.2	4.57
49	121.92	450.7	4206.3	2439.2	**50.1**	33.2	4.86
101125	125.73	425.6	4127.4	2305.5	33.6	29.4	4.76
101250	129.54	417.1	4096.6	2269.8	26.9	23.5	4.77
101375	133.35	516.0	4477.4	2678.1	27.5	24.1	4.71
101500	137.16	573.1	4646.1	2880.1	28.1	24.2	6.15
102250	137.16	695.1	4900.2	3241.0	29.1	26.3	6.19
103250	129.54	622.4	4716.4	3002.9	**50.9**	41.7	6.24
103500	137.16	679.8	4884.5	3210.6	31.0	26.6	6.17
104000	129.54	492.5	4380.3	2611.0	**76.7**	**58.6**	4.64
104250	137.16	679.8	4912.5	3233.4	28.8	24.6	6.12
104375	140.97	618.5	4766.3	3039.6	27.8	23.5	6.15
104500	144.78	660.7	4865.2	3181.8	25.6	23.2	6.14
105000	129.54	551.8	4510.9	2757.3	**59.8**	47.9	4.85
105250	137.16	662.6	4859.0	3175.2	30.1	26.0	6.15
105375	140.97	698.1	4931.4	3268.9	28.1	24.4	6.15

Table 31. Results for "good" points at Folsom and Main West.

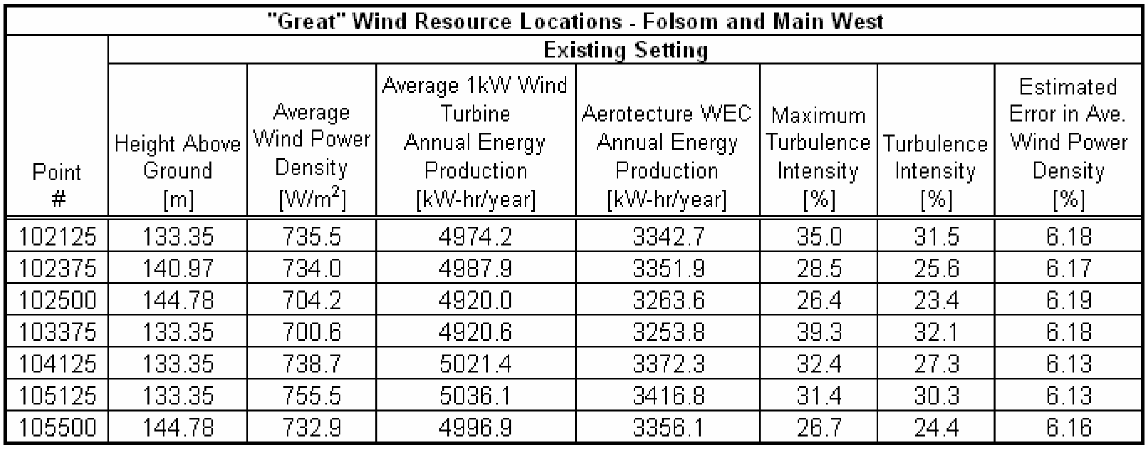

"Great" Wind Resource Locations - Folsom and Main West							
	Existing Setting						
Point #	Height Above Ground [m]	Average Wind Power Density [W/m^2]	Average 1kW Wind Turbine Annual Energy Production [kW-hr/year]	Aerotecture WEC Annual Energy Production [kW-hr/year]	Maximum Turbulence Intensity [%]	Turbulence Intensity [%]	Estimated Error in Ave. Wind Power Density [%]
102125	133.35	735.5	4974.2	3342.7	35.0	31.5	6.18
102375	140.97	734.0	4987.9	3351.9	28.5	25.6	6.17
102500	144.78	704.2	4920.0	3263.6	26.4	23.4	6.19
103375	133.35	700.6	4920.6	3253.8	39.3	32.1	6.18
104125	133.35	738.7	5021.4	3372.3	32.4	27.3	6.13
105125	133.35	755.5	5036.1	3416.8	31.4	30.3	6.13
105500	144.78	732.9	4996.9	3356.1	26.7	24.4	6.16

Table 32. Results for "great" points at Folsom and Main West.

Folsom and Main West Results with Winds from 6am – 8pm

The reduced, full-scale data for Fox Plaza for winds from 6am to 8pm are displayed in the same manner as in the previous section. The "good" wind resource points' results of the wind-tunnel testing for the CSAA Building are shown in Table 33, and the "great" wind resource points' results are in Table 34. Tables 35a and 35b show the ratio of the average wind speed densities of 6am to 8pm case to the all hours' case for each point tested.

The point with the highest average wind power density during the hours of 6am to 8pm (the 15-hour day case) was point 105125 which had a value of 946.55 Watts per square meter. All points showed an increase in average wind power density from the 24-hour day case, demonstrating that the winds are higher during business hours.

"Good" Wind Resource Locations - Folsom and Main West - 6am - 8pm							
	Existing Setting						
Point #	Height Above Ground [m]	Average Wind Power Density [W/m^2]	Average 1kW Wind Turbine Annual Energy Production [kW-hr/year]	Aerotecture WEC Annual Energy Production [kW-hr/year]	Maximum Turbulence Intensity [%]	Turbulence Intensity [%]	Estimated Error in Ave. Wind Power Density [%]
40	137.16	608.2	3229.3	2024.6	44.3	29.3	7.01
49	121.92	567.8	3063.5	1862.1	**50.1**	33.2	7.35
101125	125.73	522.7	3017.4	1791.4	33.6	29.4	7.06
101250	129.54	514.9	2998.0	1766.4	26.9	23.5	7.11
101375	133.35	643.6	3231.0	2072.3	27.5	24.1	7.12
102000	129.54	408.2	2842.9	1494.6	49.9	46.2	7.06
103125	125.73	406.5	2690.6	1423.6	**60.1**	**51.3**	7.18
104000	129.54	615.2	3183.6	2013.9	**76.7**	**58.3**	7.11
105000	129.54	691.4	3244.6	2132.5	**59.8**	47.9	7.30

Table 33. Results for “good” points at the Folsom and Main West building from 6am – 8pm.

"Great" Wind Resource Locations - Folsom and Main West - 6am - 8pm							
	Existing Setting						
Point #	Height Above Ground [m]	Average Wind Power Density [W/m^2]	Average 1kW Wind Turbine Annual Energy Production [kW-hr/year]	Aerotecture WEC Annual Energy Production [kW-hr/year]	Maximum Turbulence Intensity [%]	Turbulence Intensity [%]	Estimated Error in Ave. Wind Power Density [%]
101500	137.16	717.1	3330.0	2223.5	28.1	24.2	7.13
102125	133.35	921.8	3515.9	2568.4	35.0	31.4	7.17
102250	137.16	871.2	3475.3	2493.9	29.1	26.3	7.17
102375	140.97	921.1	3523.6	2576.3	28.5	25.6	7.16
102500	144.78	882.2	3485.8	2510.3	26.4	23.5	7.17
103250	129.54	773.4	3368.5	2300.5	**50.9**	41.7	7.18
103375	133.35	874.8	3485.9	2502.9	39.3	32.1	7.14
103500	137.16	850.5	3467.1	2486.6	31.0	26.6	7.14
104125	133.35	922.8	3541.7	2591.9	32.4	27.3	7.09
104250	137.16	851.1	3485.1	2490.7	28.8	24.6	7.09
104375	140.97	773.1	3403.6	2336.5	27.8	23.5	7.11
104500	144.78	828.1	3458.6	2454.2	25.6	23.2	7.12
105125	133.35	946.6	3552.0	2625.1	31.4	30.3	7.12
105250	137.16	828.2	3454.2	2446.8	30.1	26.0	7.12
105375	140.97	875.7	3494.1	2515.9	28.1	24.5	7.14
105500	144.78	920.0	3528.4	2580.0	26.7	24.4	7.15

Table 34. Results for “great” points at the Folsom and Main West building from 6am – 8pm.

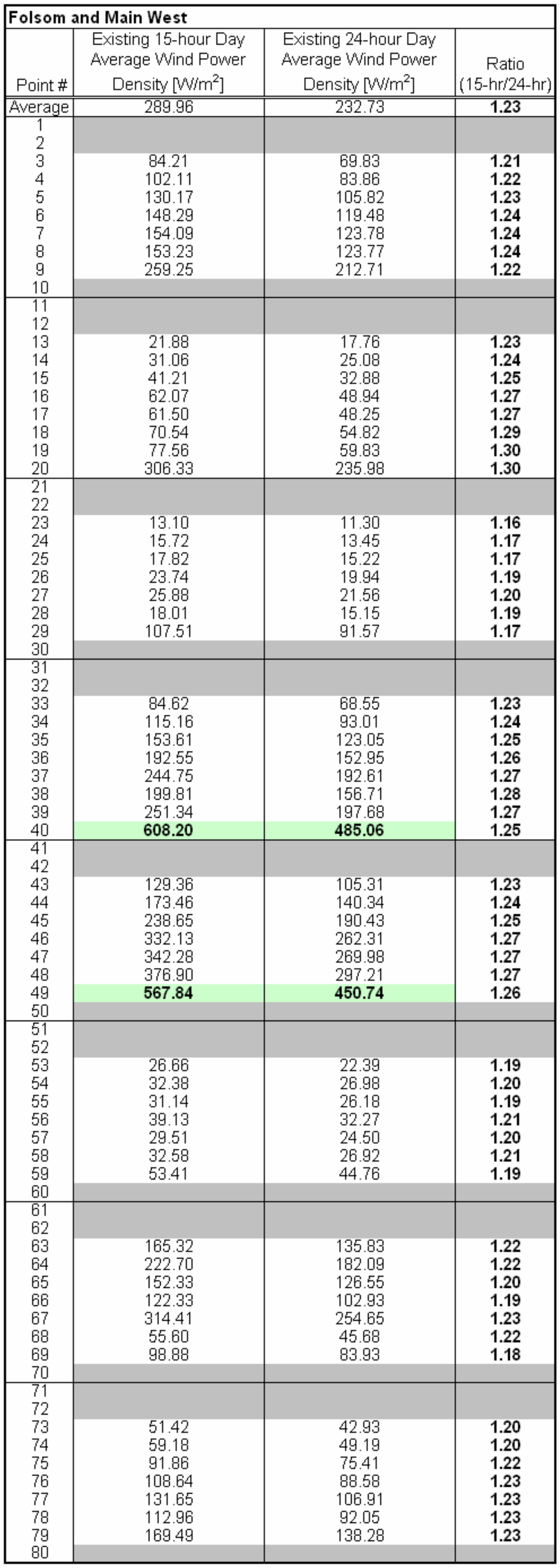

Folsom and Main West

Point #	Existing 15-hour Day Average Wind Power Density [W/m^2]	Existing 24-hour Day Average Wind Power Density [W/m^2]	Ratio (15-hr/24-hr)
Average	289.96	232.73	**1.23**
1			
2			
3	84.21	69.83	**1.21**
4	102.11	83.86	**1.22**
5	130.17	105.82	**1.23**
6	148.29	119.48	**1.24**
7	154.09	123.78	**1.24**
8	153.23	123.77	**1.24**
9	259.25	212.71	**1.22**
10			
11			
12			
13	21.88	17.76	**1.23**
14	31.06	25.08	**1.24**
15	41.21	32.88	**1.25**
16	62.07	48.94	**1.27**
17	61.50	48.25	**1.27**
18	70.54	54.82	**1.29**
19	77.56	59.83	**1.30**
20	306.33	235.98	**1.30**
21			
22			
23	13.10	11.30	**1.16**
24	15.72	13.45	**1.17**
25	17.82	15.22	**1.17**
26	23.74	19.94	**1.19**
27	25.88	21.56	**1.20**
28	18.01	15.15	**1.19**
29	107.51	91.57	**1.17**
30			
31			
32			
33	84.62	68.55	**1.23**
34	115.16	93.01	**1.24**
35	153.61	123.05	**1.25**
36	192.55	152.95	**1.26**
37	244.75	192.61	**1.27**
38	199.81	156.71	**1.28**
39	251.34	197.68	**1.27**
40	**608.20**	**485.06**	**1.25**
41			
42			
43	129.36	105.31	**1.23**
44	173.46	140.34	**1.24**
45	238.65	190.43	**1.25**
46	332.13	262.31	**1.27**
47	342.28	269.98	**1.27**
48	376.90	297.21	**1.27**
49	**567.84**	**450.74**	**1.26**
50			
51			
52			
53	26.66	22.39	**1.19**
54	32.38	26.98	**1.20**
55	31.14	26.18	**1.19**
56	39.13	32.27	**1.21**
57	29.51	24.50	**1.20**
58	32.58	26.92	**1.21**
59	53.41	44.76	**1.19**
60			
61			
62			
63	165.32	135.83	**1.22**
64	222.70	182.09	**1.22**
65	152.33	126.55	**1.20**
66	122.33	102.93	**1.19**
67	314.41	254.65	**1.23**
68	55.60	45.68	**1.22**
69	98.88	83.93	**1.18**
70			
71			
72			
73	51.42	42.93	**1.20**
74	59.18	49.19	**1.20**
75	91.86	75.41	**1.22**
76	108.64	88.58	**1.23**
77	131.65	106.91	**1.23**
78	112.96	92.05	**1.23**
79	169.49	138.28	**1.23**
80			

Table 35a. Ratio of average wind power densities of the 6am – 8pm case to the 24-hours per day case for the Folsom and Main West building.

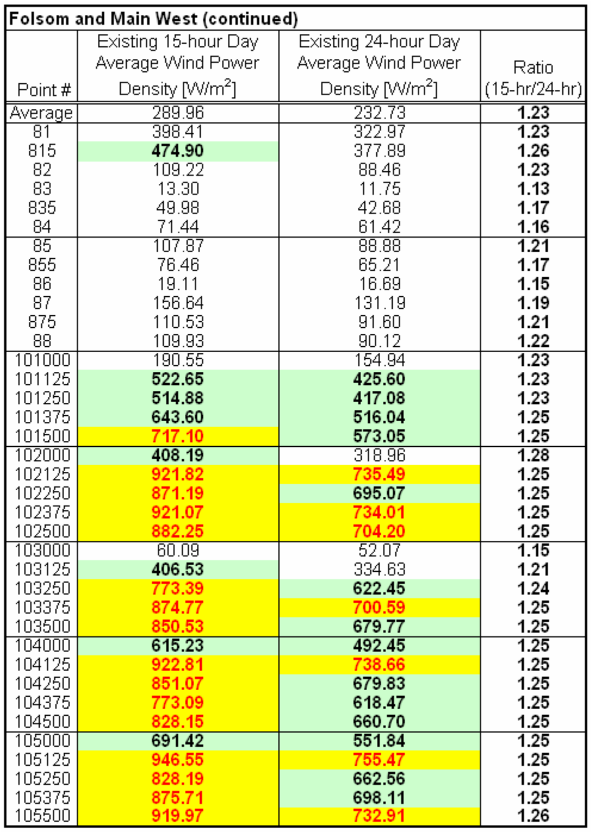

Folsom and Main West (continued)			
Point #	Existing 15-hour Day Average Wind Power Density [W/m^2]	Existing 24-hour Day Average Wind Power Density [W/m^2]	Ratio (15-hr/24-hr)
Average	289.96	232.73	**1.23**
81	398.41	322.97	**1.23**
815	**474.90**	377.89	**1.26**
82	109.22	88.46	**1.23**
83	13.30	11.75	**1.13**
835	49.98	42.68	**1.17**
84	71.44	61.42	**1.16**
85	107.87	88.88	**1.21**
855	76.46	65.21	**1.17**
86	19.11	16.69	**1.15**
87	156.64	131.19	**1.19**
875	110.53	91.60	**1.21**
88	109.93	90.12	**1.22**
101000	190.55	154.94	**1.23**
101125	**522.65**	**425.60**	**1.23**
101250	**514.88**	**417.08**	**1.23**
101375	**643.60**	**516.04**	**1.25**
101500	**717.10**	**573.05**	**1.25**
102000	**408.19**	318.96	**1.28**
102125	**921.82**	**735.49**	**1.25**
102250	**871.19**	**695.07**	**1.25**
102375	**921.07**	**734.01**	**1.25**
102500	**882.25**	**704.20**	**1.25**
103000	60.09	52.07	**1.15**
103125	**406.53**	334.63	**1.21**
103250	**773.39**	**622.45**	**1.24**
103375	**874.77**	**700.59**	**1.25**
103500	**850.53**	**679.77**	**1.25**
104000	**615.23**	**492.45**	**1.25**
104125	**922.81**	**738.66**	**1.25**
104250	**851.07**	**679.83**	**1.25**
104375	**773.09**	**618.47**	**1.25**
104500	**828.15**	**660.70**	**1.25**
105000	**691.42**	**551.84**	**1.25**
105125	**946.55**	**755.47**	**1.25**
105250	**828.19**	**662.56**	**1.25**
105375	**875.71**	**698.11**	**1.25**
105500	**919.97**	**732.91**	**1.26**

Table 35b. Ratio of average wind power densities of the 6am – 8pm case to the 24-hours per day case for the Folsom and Main West building (continued from Table 35a).

3.3 Results in Graphical Form

The following sections present the data, shown in the preceding tables in graphical form. Photos taken of the actual models and local areas used in the wind-tunnel tests are overlaid with color-coded points showing where “great”, “good” and “poor", corresponding to the colors used by the preceding tables: a yellow dot with red text and outline is considered a “great” location, a green dot with black text and outline is considered a “good” location, and a white dot with black text and outline is considered a “poor” location. The numbers shown within the dot corresponds to that point number of that measurement location, which also corresponds to the point numbers in the preceding tables.

It is important to note that the point placements are approximate and are not necessarily to scale. Placements of points on the photos were slightly shifted for some points to give a better view of other points and are therefore presented as a qualitative analysis. A more detailed and precise description of the point locations shown in this section is given in Tables 1 through 5.

3.3.1 Fox Plaza Graphical Results

The results from Tables 15a and 15b are shown in Figures 22 through 25 in graphical form for the Fox Plaza Building. Figure 22 shows the results for the existing setting and Figure 23 shows the results for the cumulative setting, both figures assume the WECs run continuously all day and night; Figure 24 shows graphical results for the existing setting and Figure 25 shows the results for the cumulative setting, and both of these figures assume the WECs run only from 6am to 8pm.

Fox Plaza has a unique architectural feature that includes a slender protruding structure on the north and south faces and the roof, which may aid in flow acceleration, if other surrounding structures do not block the wind. Figures 22 through 25 illustrate how this feature may lead to higher annual average wind power density values on the north or south face, or near the corners of the building.

Figure 22 illustrates that the best locations to place a WEC is above the roof level and on the north face of the building. Since most of the winds come from the northwest, that would place the CSAA building somewhat upwind for many of the wind directions tested, probably creating a region of accelerated flow on the north face of this building.

The south face of the building would not be a good place to locate WECs due to its low annual average wind power density values, potentially due to the same reason the north face sees such good potential: the wind has probably been redirected from the south face of the building to go around the north face. Several other areas of the building see local flow accelerations which yield higher values, such as the upper southwest corner.

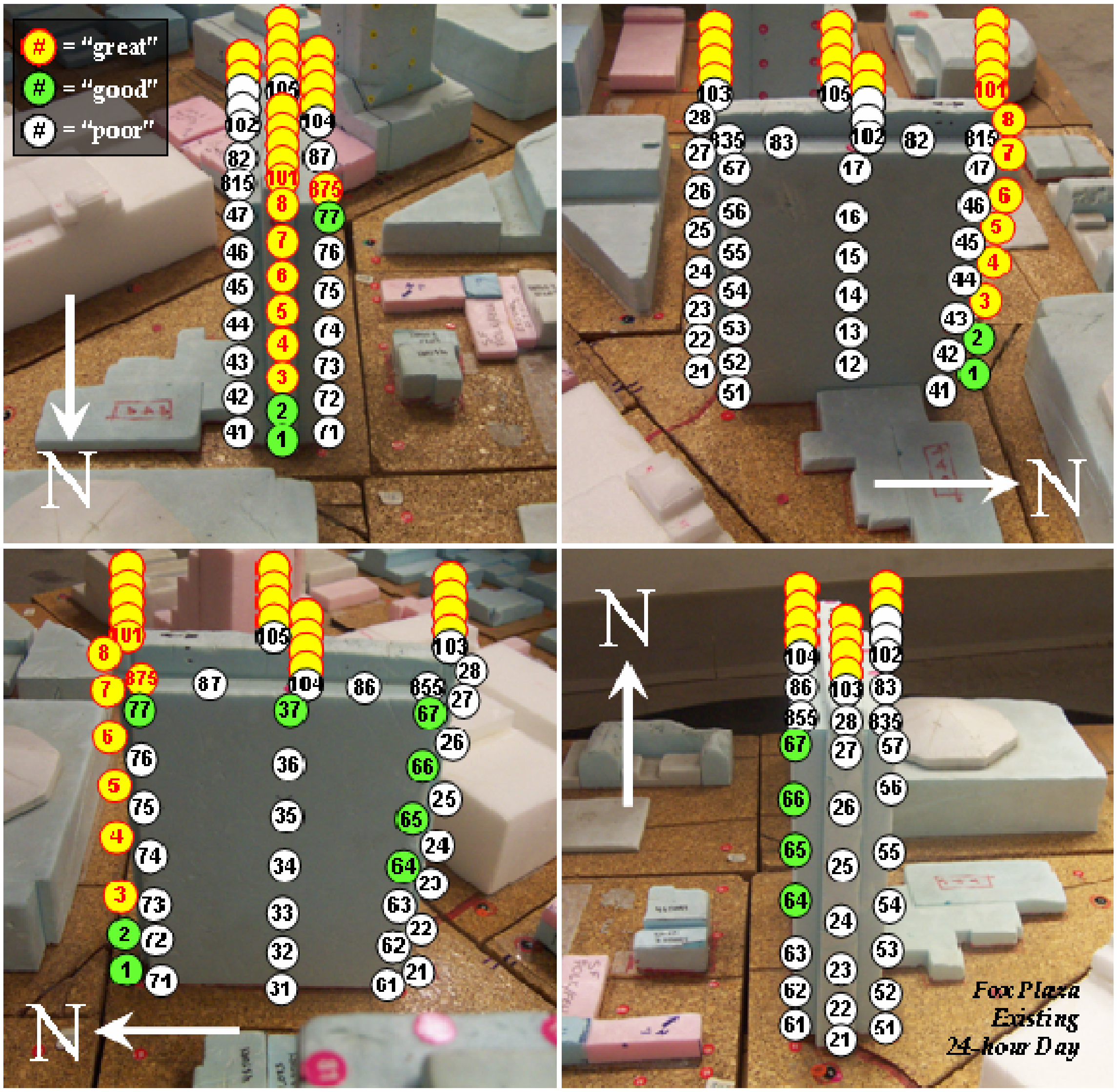

Figure 22. Graphical results for Fox Plaza WECs running 24-hours per day for the existing setting.

Figure 23 illustrates how the annual average wind power densities change from the existing to the cumulative settings. The values have actually dropped slightly due to the area's development. There is a building upwind at One Polk, located directly between the CSAA building and Fox Plaza, and an addition to Fox Plaza that may be blocking some of the wind from accelerating around the building. A large development on 10th Street and Market Street is also located next to Fox Plaza, and while it looks like it should create a wind-tunnel effect down Market Street, it also appears to be disturbing the flow in a manner restricting flow acceleration near the surface of Fox Plaza.

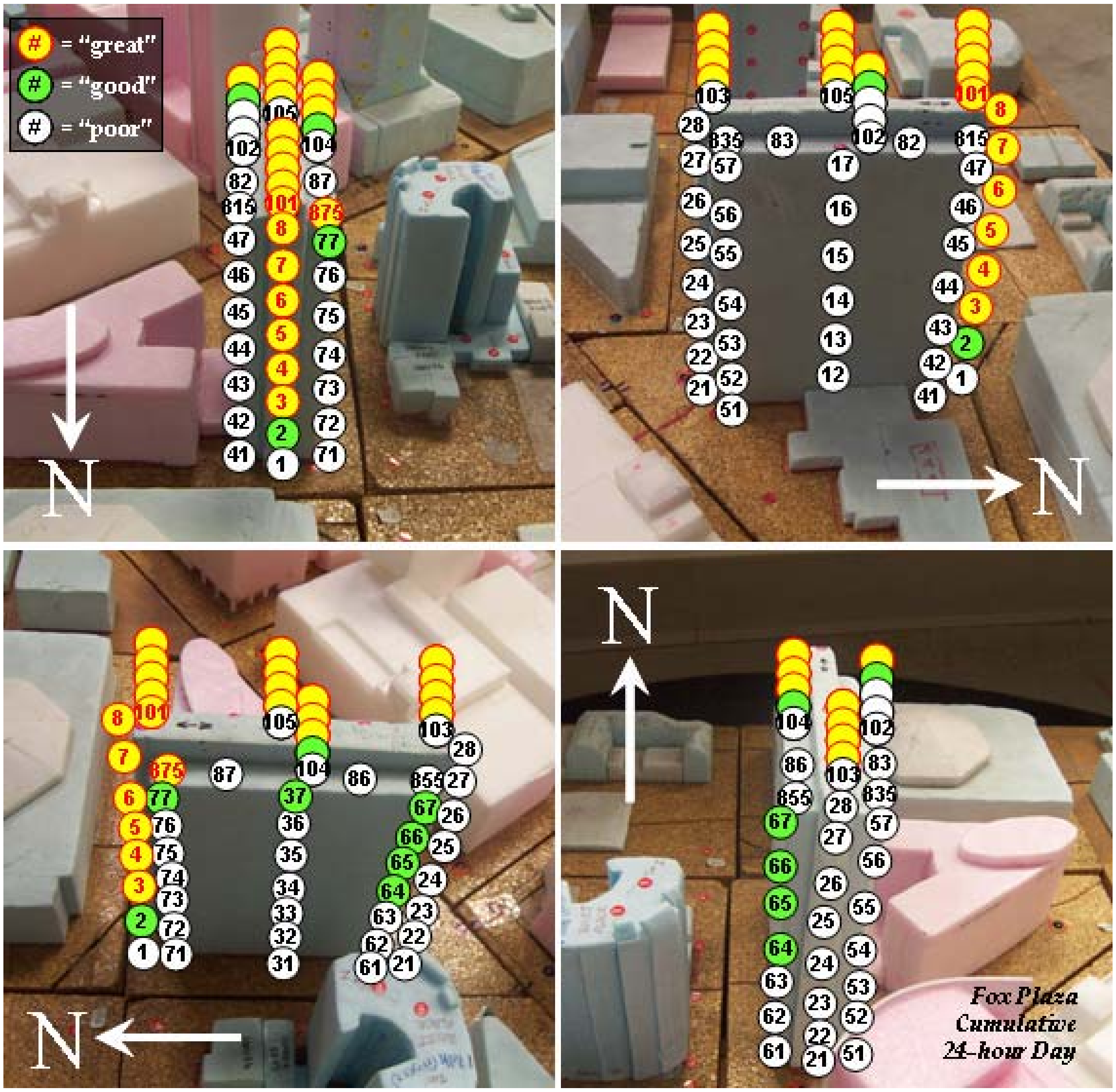

Figure 23. Graphical results for Fox Plaza WECs running 24-hours per day for the cumulative setting.

Figure 24 is similar to Figure 22 except the data is analyzed using only wind data from 6AM to 8PM. Since higher winds typically occur during this time of the day, the values are slightly elevated above those in Figure 22, but the trends are the same. The same is true for Figure 25, which is the cumulative setting analyzed for the same 15-hour day, which is the cumulative setting analyzed for the same 15-hour day has trends similar to Figure 23.

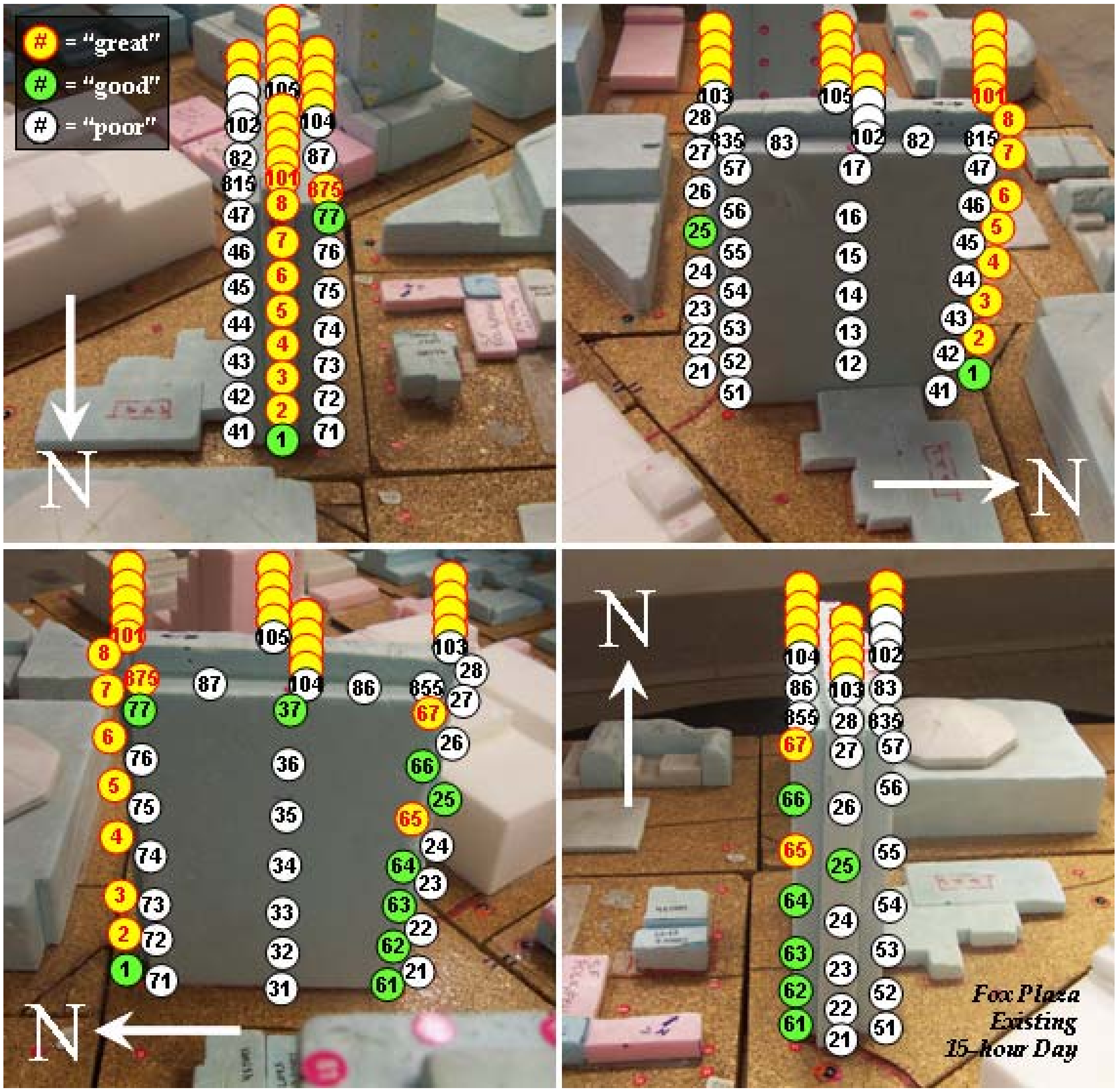

Figure 24. Graphical results for Fox Plaza WECs running 15-hours per day for the existing setting.

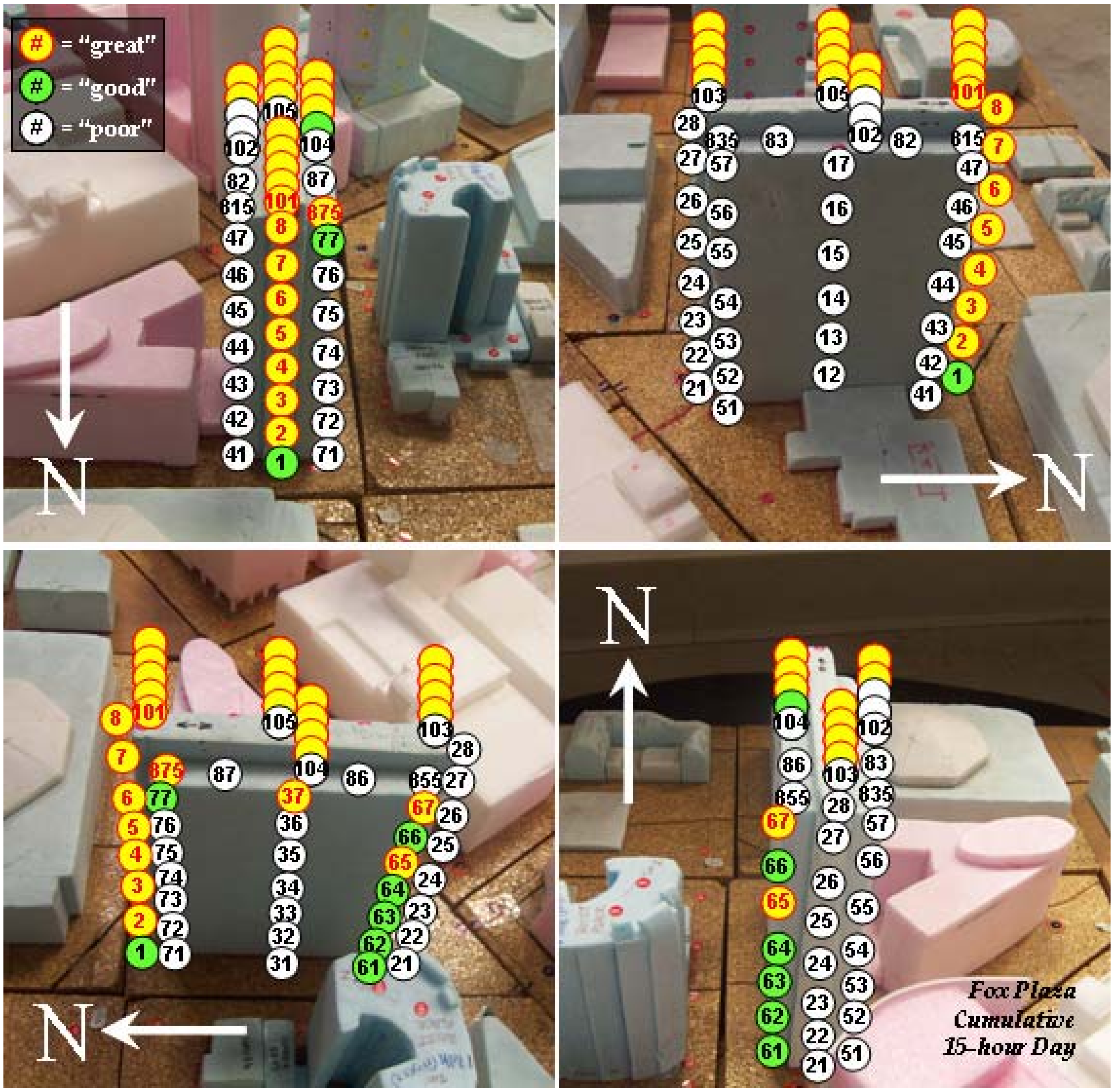

Figure 25. Graphical results for Fox Plaza WECs running 15-hours per day for the cumulative setting.

3.3.2 CSAA Building Graphical Results

The results from Tables 20a and 20b are shown in Figures 26 through 29 in graphical form for the CSAA Building. Figure 26 shows the results for the existing setting and Figure 27 shows the results for the cumulative setting, both figures assume the WECs run continuously all day and night; Figure 28 shows graphical results for the existing setting and Figure 29 shows the results for the cumulative setting, and both of these figures assume the WECs run only from 6AM to 8PM.

The CSAA building has a penthouse feature on the roof that elevates point 105 above the rest of the points, and since there are few upwind structures on the same order of magnitude with respect to height for the most frequently occurring winds in San Francisco, point 105 shows some of the highest annual average wind power densities. This feature also may cause local flow accelerations for other rooftop locations.

Figure 26 illustrates that the best locations for WECs is in fact the rooftop level or above. The northeast and southwest corners are also suitable locations to place WECs. The northeast corner might be seeing local flow acceleration due to wind accelerating over the smaller structure attached to the CSAA building. The southwest corner is relatively unobstructed from tall upwind structures for the most frequently occurring winds.

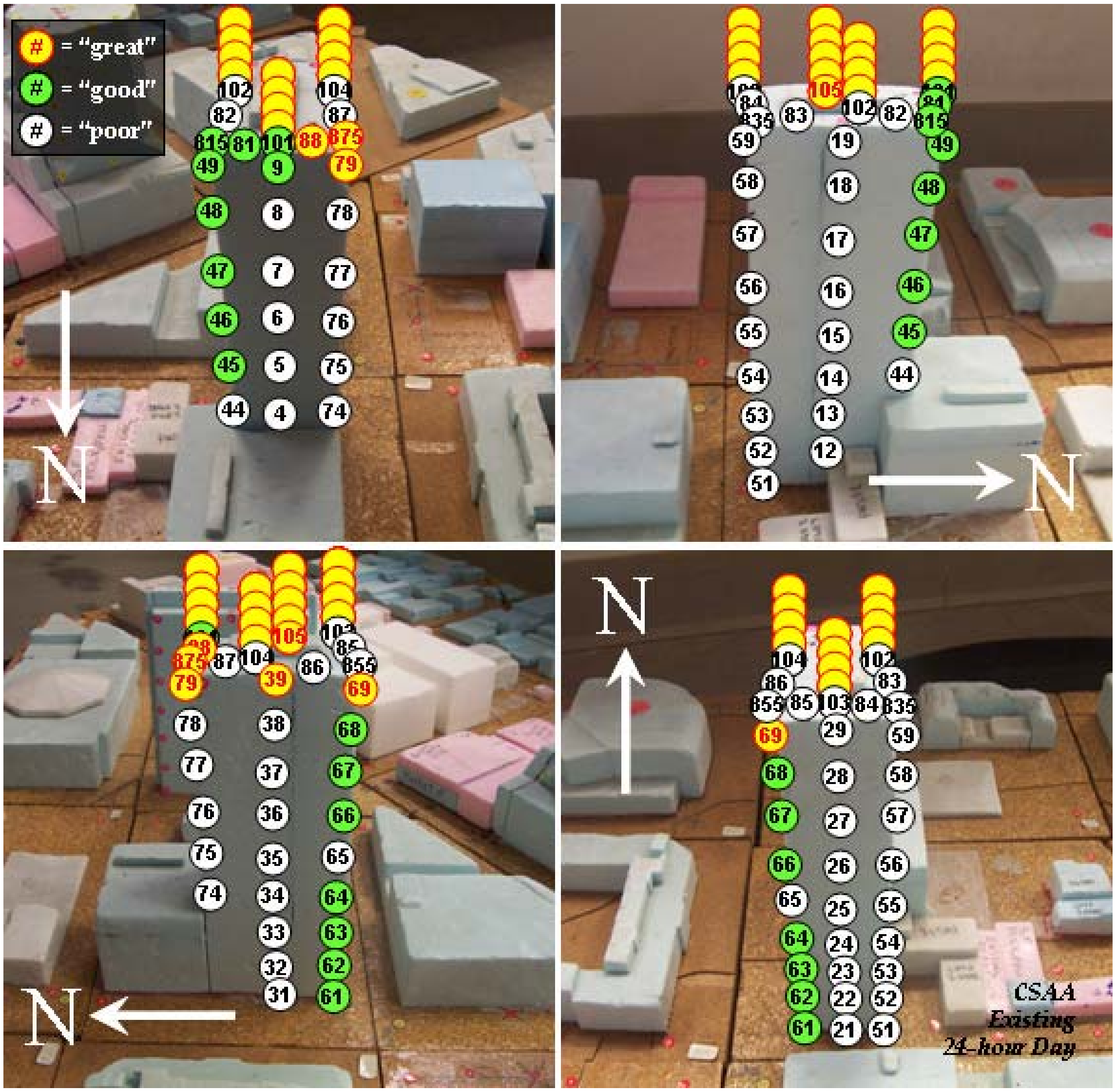

Figure 26. Graphical results CSAA WECs running 24-hours per day for the existing setting.

Figure 27 shows how the annual average wind power densities change due to potential local developments in the area. Overall, the potential developments will cause an increase in the available wind power, with higher annual average wind power densities on the southwest corner of the building and several rooftop locations. While the only upwind development is a small building located across the corner of the intersection at 77 Van Ness, it appears that this structure and the building located at One Polk, as well as other downwind developments, cause more favorable wind conditions at this building's location, even though these same developments caused less favorable conditions at Fox Plaza.

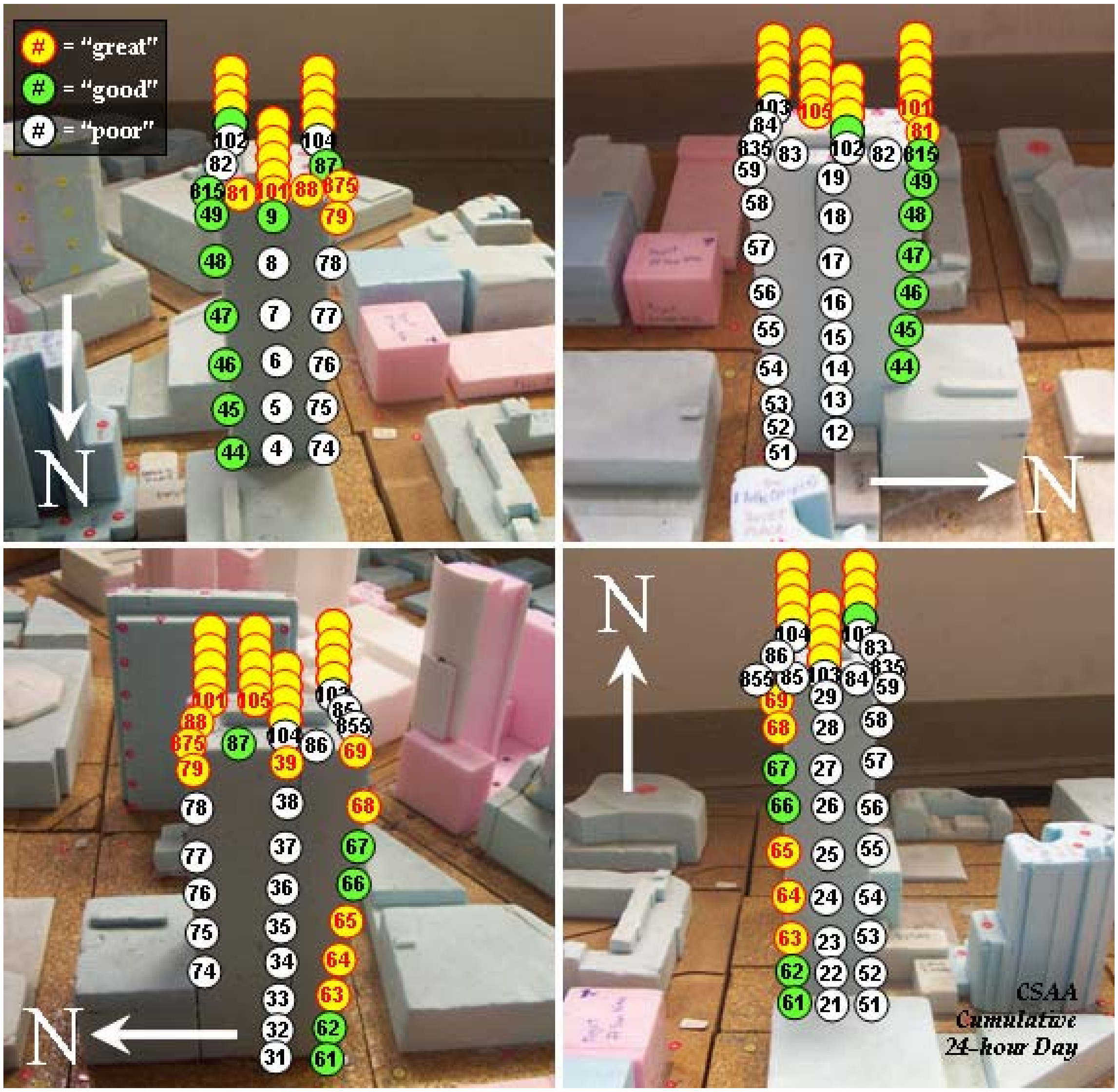

Figure 27. Graphical results for CSAA WECs running 24-hours per day for the cumulative setting.

Figure 28 is similar to Figure 26 except the data is analyzed using only wind data from 6AM to 8PM. Since higher winds typically occur during this time of the day, the values are slightly elevated above those in Figure 26, but the trends are the same. The same is true for Figure 29, which is the cumulative setting analyzed for the same 15-hour day has trends similar to Figure 27.

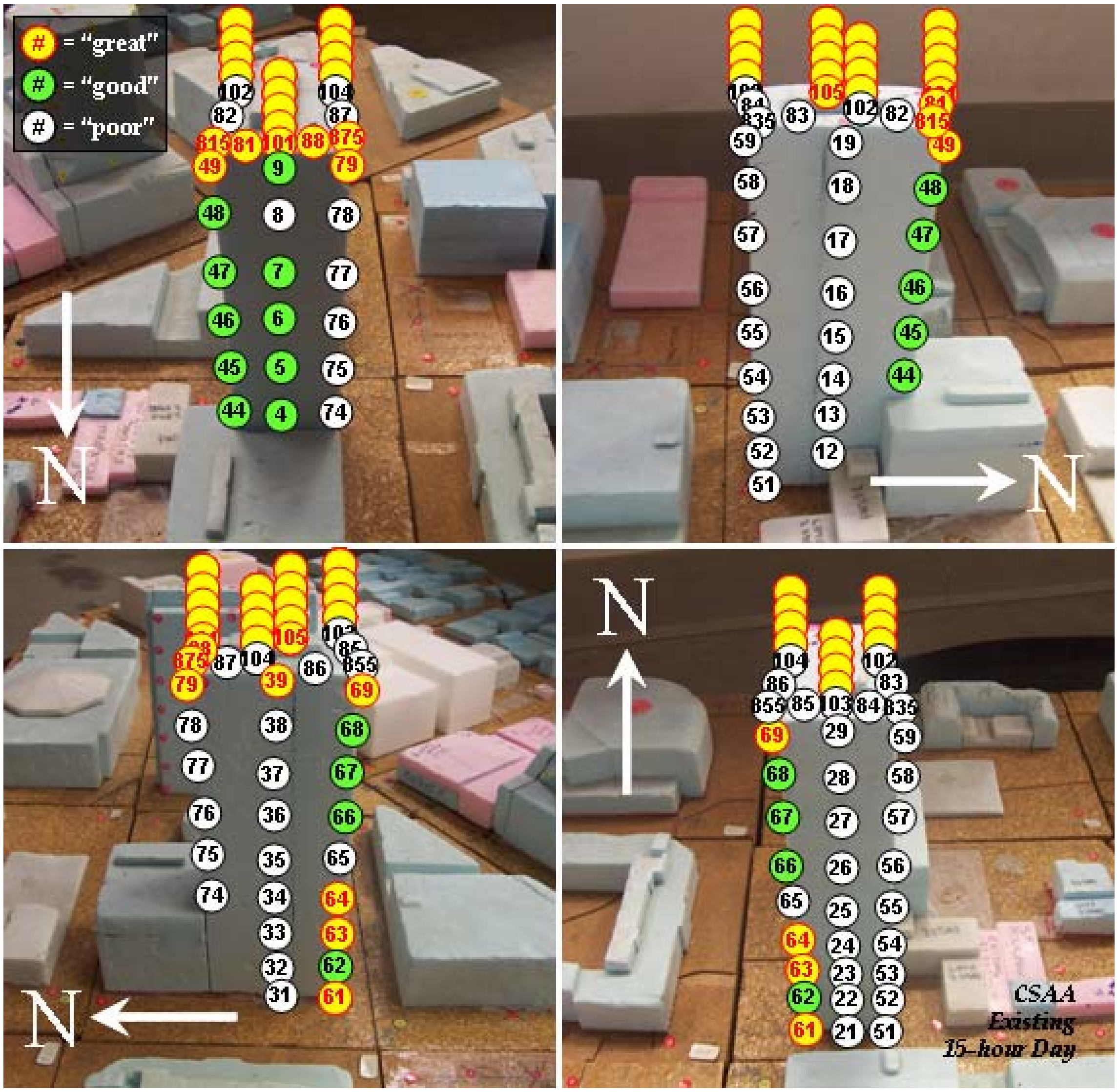

Figure 28. Graphical results for CSAA WECs running 15-hours per day for the existing setting.

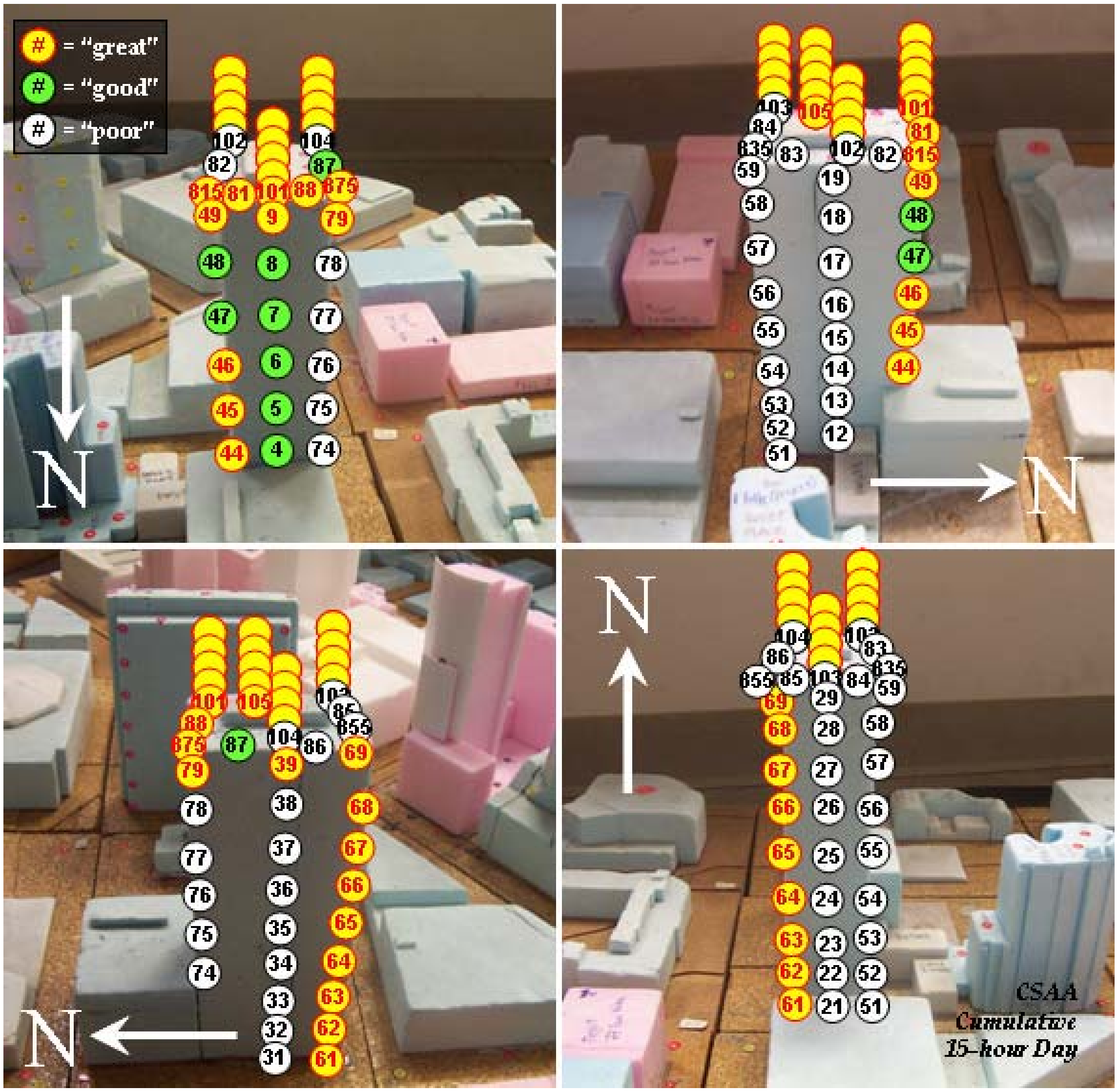

Figure 29. Graphical results for CSAA WECs running 15-hours per day for the cumulative setting.

3.3.3 *Bank of America Building Graphical Results*

The results from the Tables 25a and 25b are shown in Figures 30 through 33 in graphical form for the Bank of America Building. Figure 30 shows the results for the existing setting and Figure 31 shows the results for the cumulative setting, both figures assume the WECs run continuously all day and night; Figure 32 shows graphical results for the existing setting and Figure 33 shows the results for the cumulative setting, and both of these figures assume the WECs run only from 6AM to 8PM.

The Bank of America Building has the unique architecture of having a shorter but thicker octagonal tower with a relatively smooth rooftop on top of a large boxy base. Figure 30 illustrates that the best WEC locations are on or above the rooftop level. Unlike the other buildings studied, however, the other “great” location to place WECs is on the southwest face, a wide, flat faces of the building, where Fox Plaza and the CSAA building have shown that the best locations are either the corners or the slim protruding faces which are quite like corners themselves. While there was no study into the direction of the wind over these buildings, it is possible that the flow is accelerating up and over the building on this face instead of stagnating and wrapping around the corners of this side of the building.

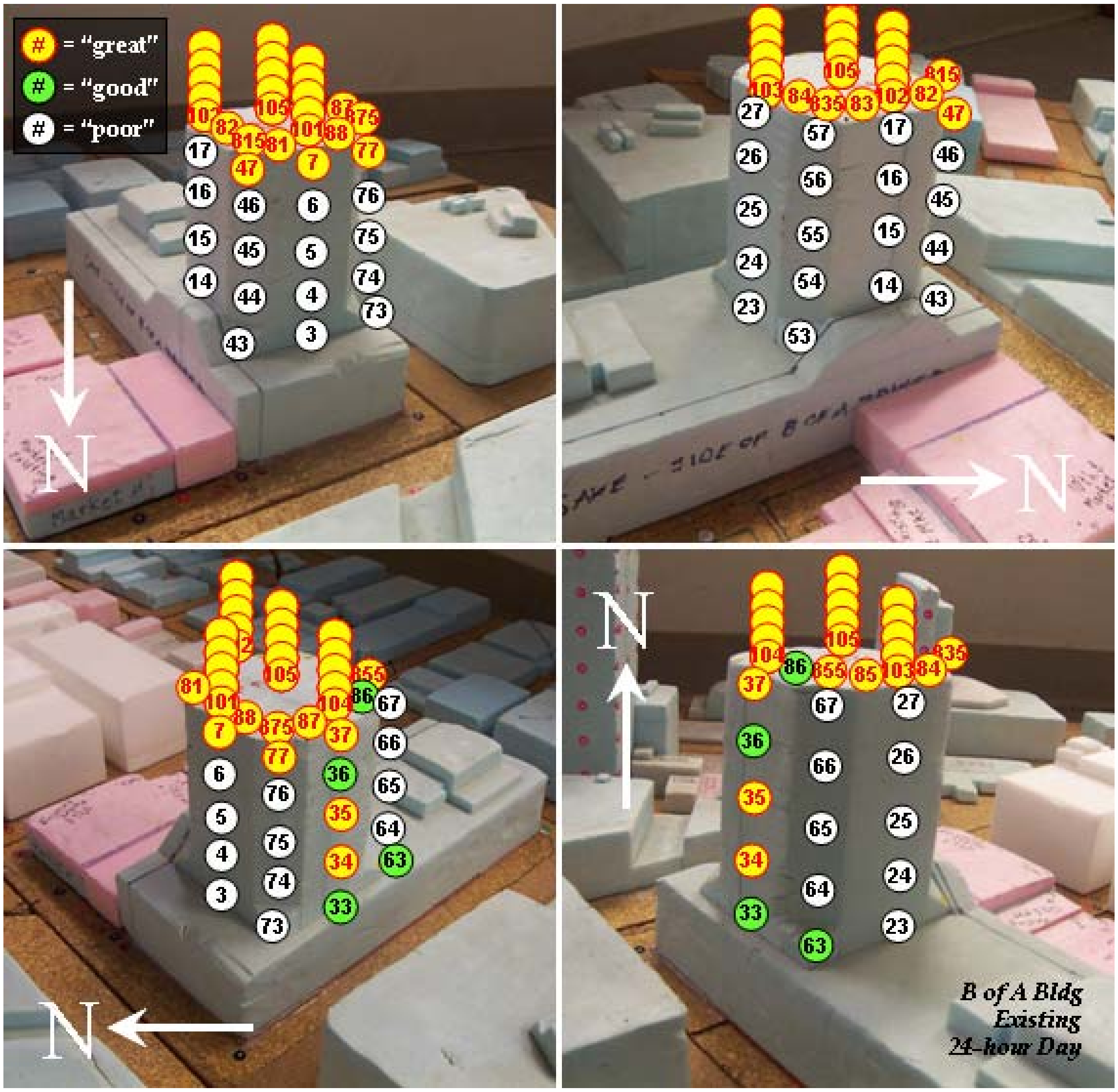

Figure 30. Graphical results Bank of America WECs running 24-hours per day for the existing setting.

Figure 31 shows how the local development changes the wind conditions on the Bank of America building. The flow over the southwest face is decreased, possibly due to the 10th and Market building development located just a few feet away from the Bank of America Building. The winds over the top of the building are increased, however, as well as on the north corner of the building.

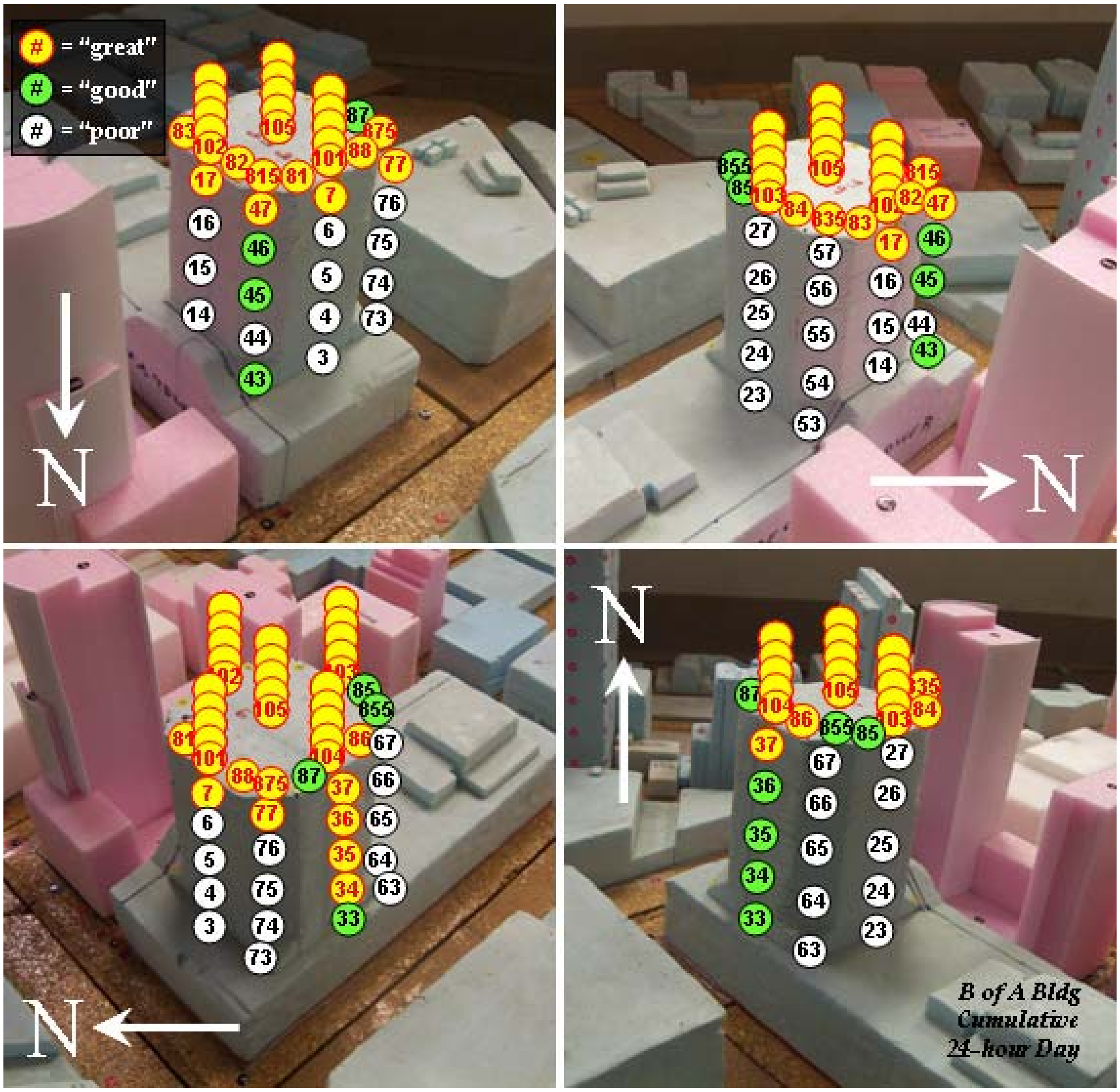

Figure 31. Graphical results for Bank of America WECs running 24-hours per day for the cumulative setting.

Figure 32 is similar to Figure 30 except the data is analyzed using only wind data from 6AM to 8PM. Since higher winds typically occur during this time of the day, the values are slightly elevated above those in Figure 30, but the trends are the same. The same is true for Figure 33, which is the cumulative setting analyzed for the same 15-hour day has trends similar to Figure 31.

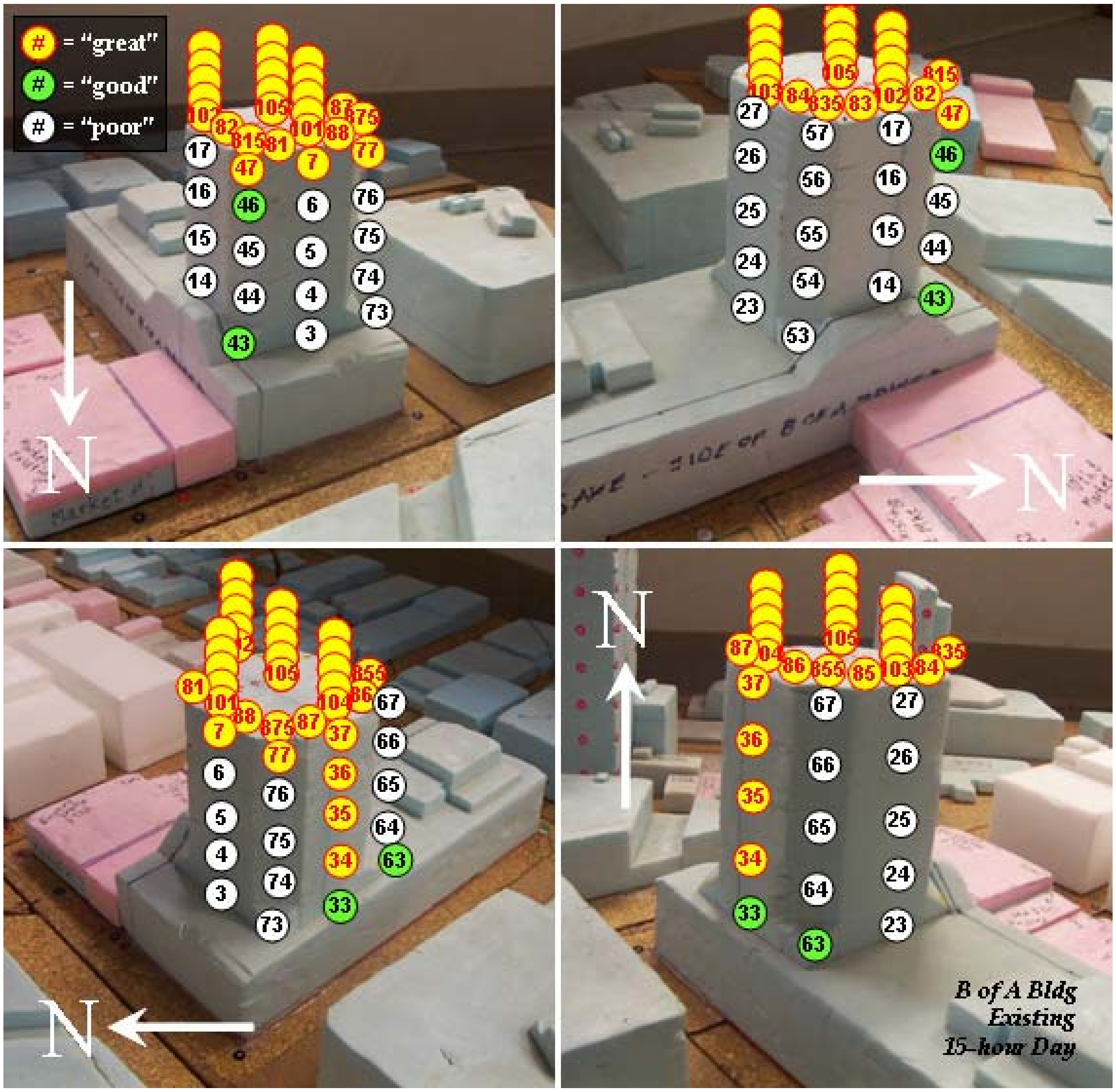

Figure 32. Graphical results for Bank of America WECs running 15-hours per day for the existing setting.

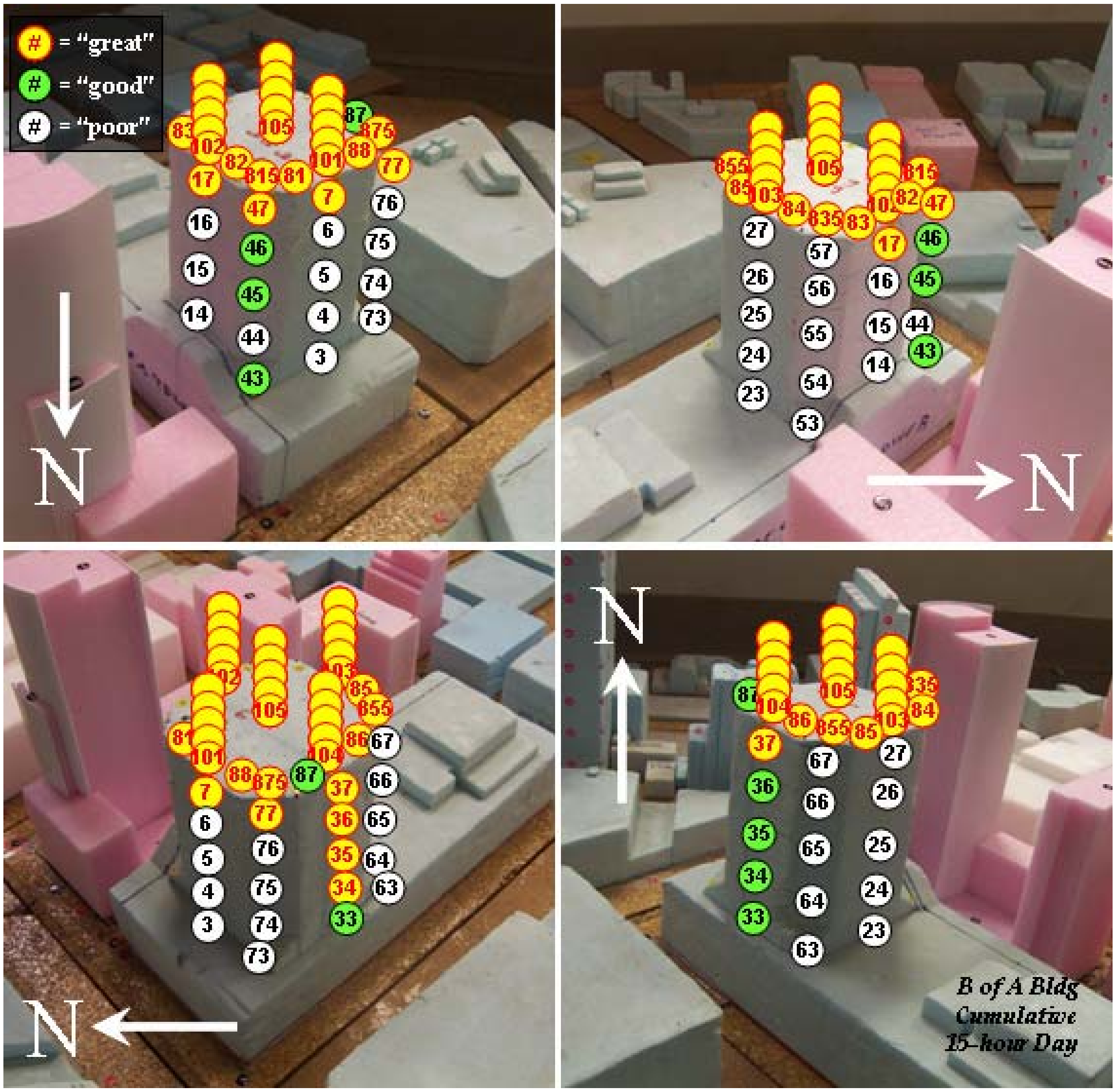

Figure 33. Graphical results for Bank of America WECs running 15-hours per day for the cumulative setting.

3.3.4 Folsom and Main East Building Graphical Results

The results from Tables 30a and 30b are shown in Figures 34 and 35 in graphical form for the Folsom and Main East Building. Figure 34 shows the results for the existing setting assuming the WECs run continuously all day and night; Figure 35 shows graphical results for the existing setting and assumes the WECs run only from 6AM to 8PM.

Figure 34 illustrates that the best places to locate WECs is above the roof level. While this building has a penthouse structure on the small roof, it does not appear to provide a significant flow acceleration over the roof since there are very few “great” annual average wind power density values. Since this area of San Francisco has a less dense skyline (or fewer tall buildings) and is close to the bay, the result appears to be a lack of flow acceleration effects. It is also possible that the few tall buildings that are in the vicinity are so scattered that instead of creating wind accelerations down streets and corridors, they break up and take energy out of the wind.

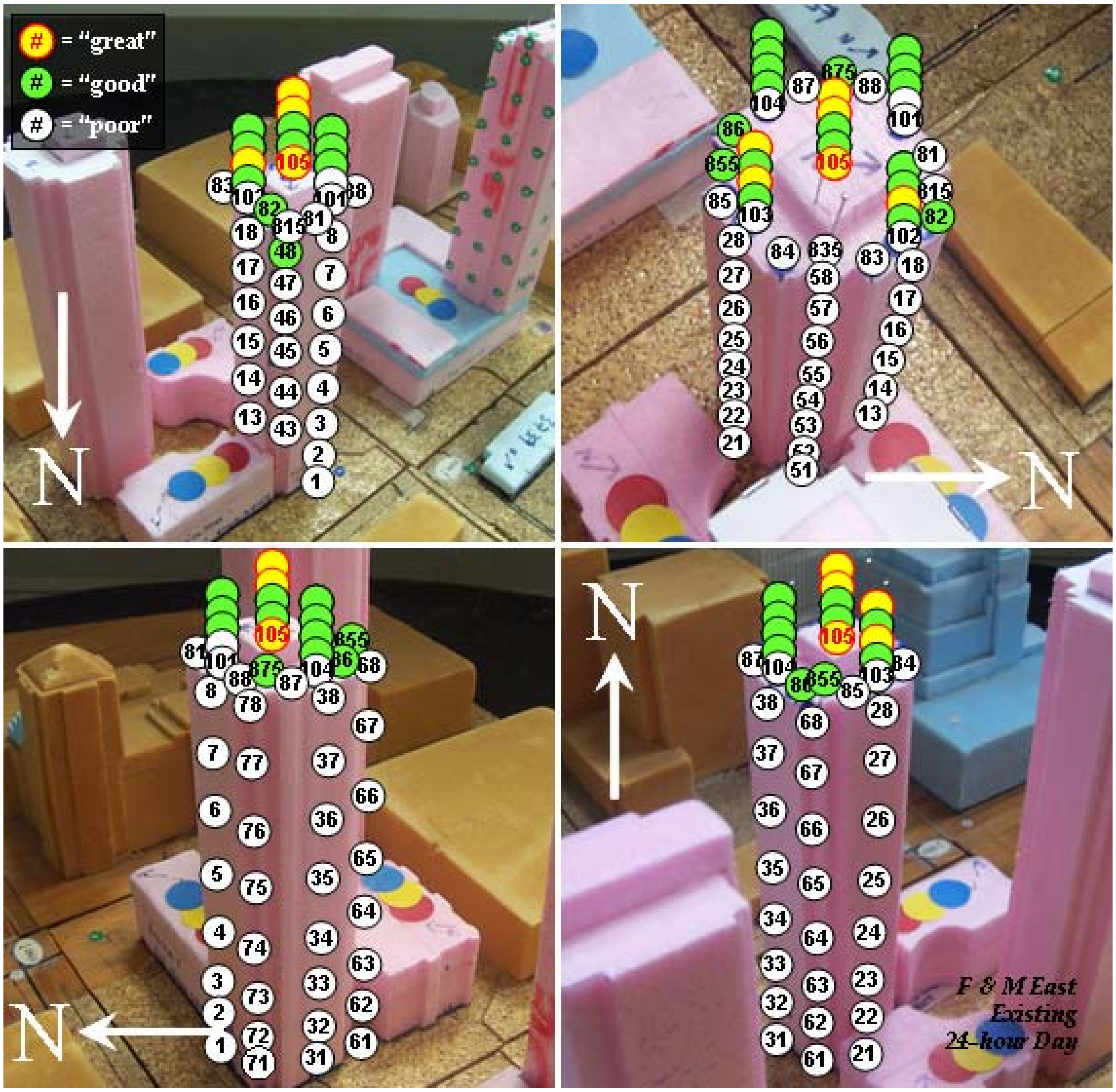

Figure 34. Graphical results Folsom and Main East WECs running 24-hours per day for the existing setting.

Figure 35 is the similar to Figure 34 except the data is analyzed using only wind data from 6AM to 8PM. Since higher winds typically occur during this time of the day, the values are slightly elevated above those in Figure 34, but the trends are the same.

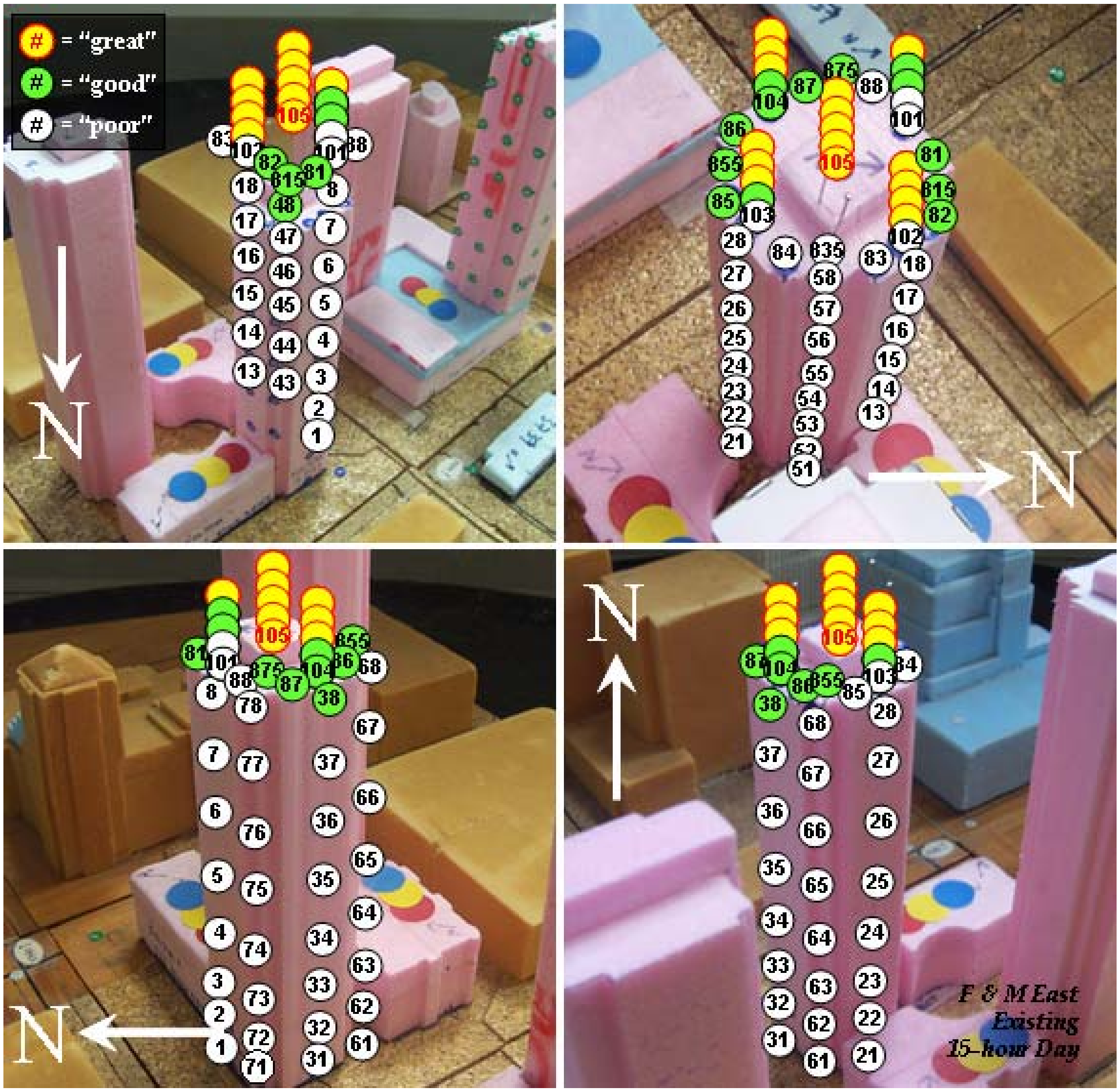

Figure 35. Graphical results for Folsom and Main East WECs running 15-hours per day for the existing setting.

3.3.5 Folsom and Main West Building Graphical Results

The results from Tables 35a and 35b are shown in Figures 36 and 37 in graphical form for the Folsom and Main West Building. Figure 36 shows the results for the existing setting assuming the WECs run continuously all day and night; Figure 37 shows graphical results for the existing setting and assumes the WECs run only from 6AM to 8PM.

Figure 36 shows that there are not many “great” locations to place a WEC on this building. The only “great” locations are above the roof level. As stated previously, this area of San Francisco has a less dense skyline (or fewer tall buildings) and is close to the bay, most likely resulting in fewer local fields of flow accelerations. It is also possible that the few tall buildings that are in the vicinity are so scattered that instead of creating wind accelerations down streets and corridors, they break up and take energy out of the wind.

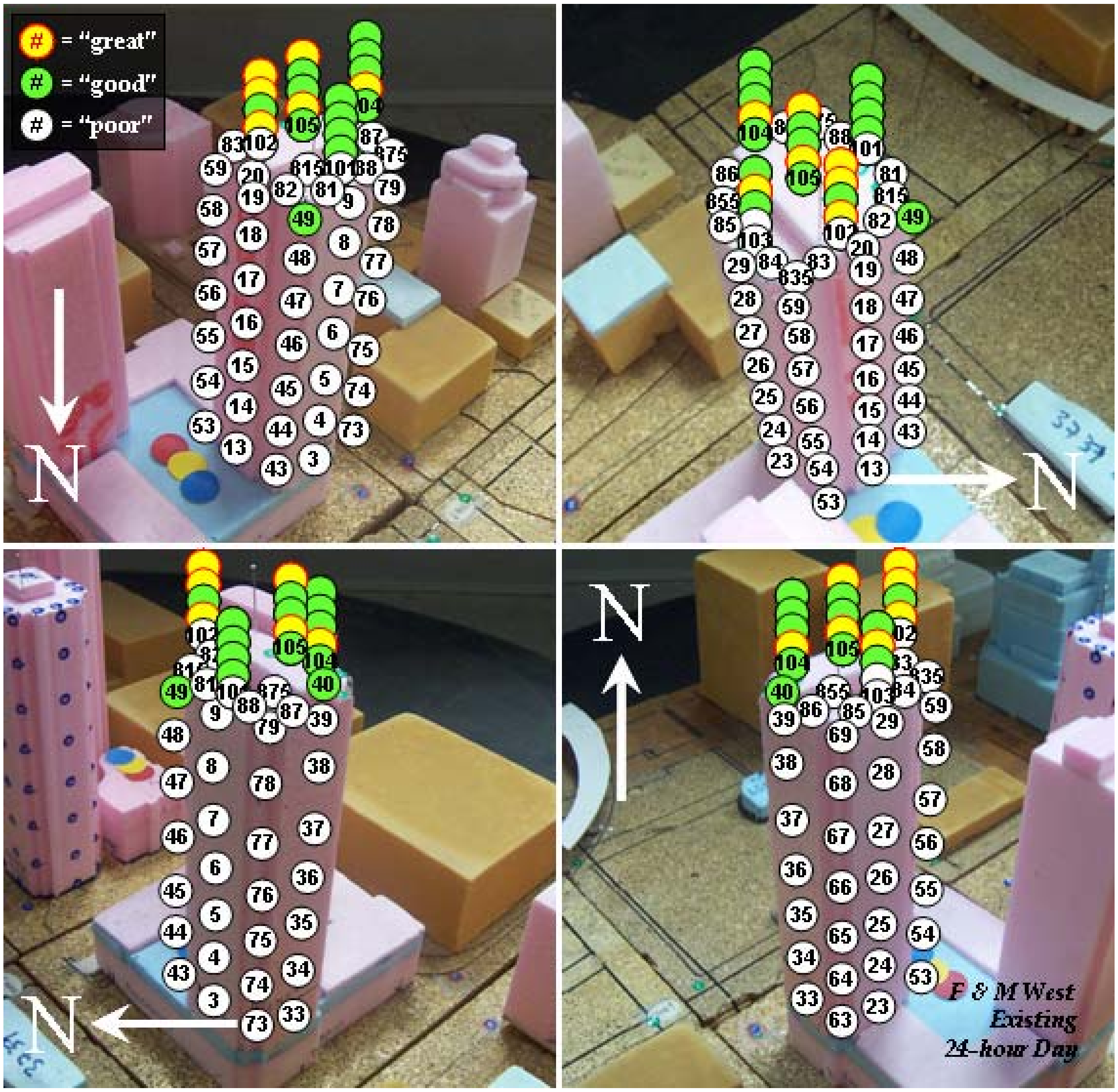

Figure 36. Graphical results Folsom and Main West WECs running 24-hours per day for the existing setting.

Figure 37 is the same as Figure 36 except the data is analyzed using only wind data from 6AM to 8PM. Since higher winds typically occur during this time of the day, the values are slightly elevated above those in Figure 36, but the trends are the same.

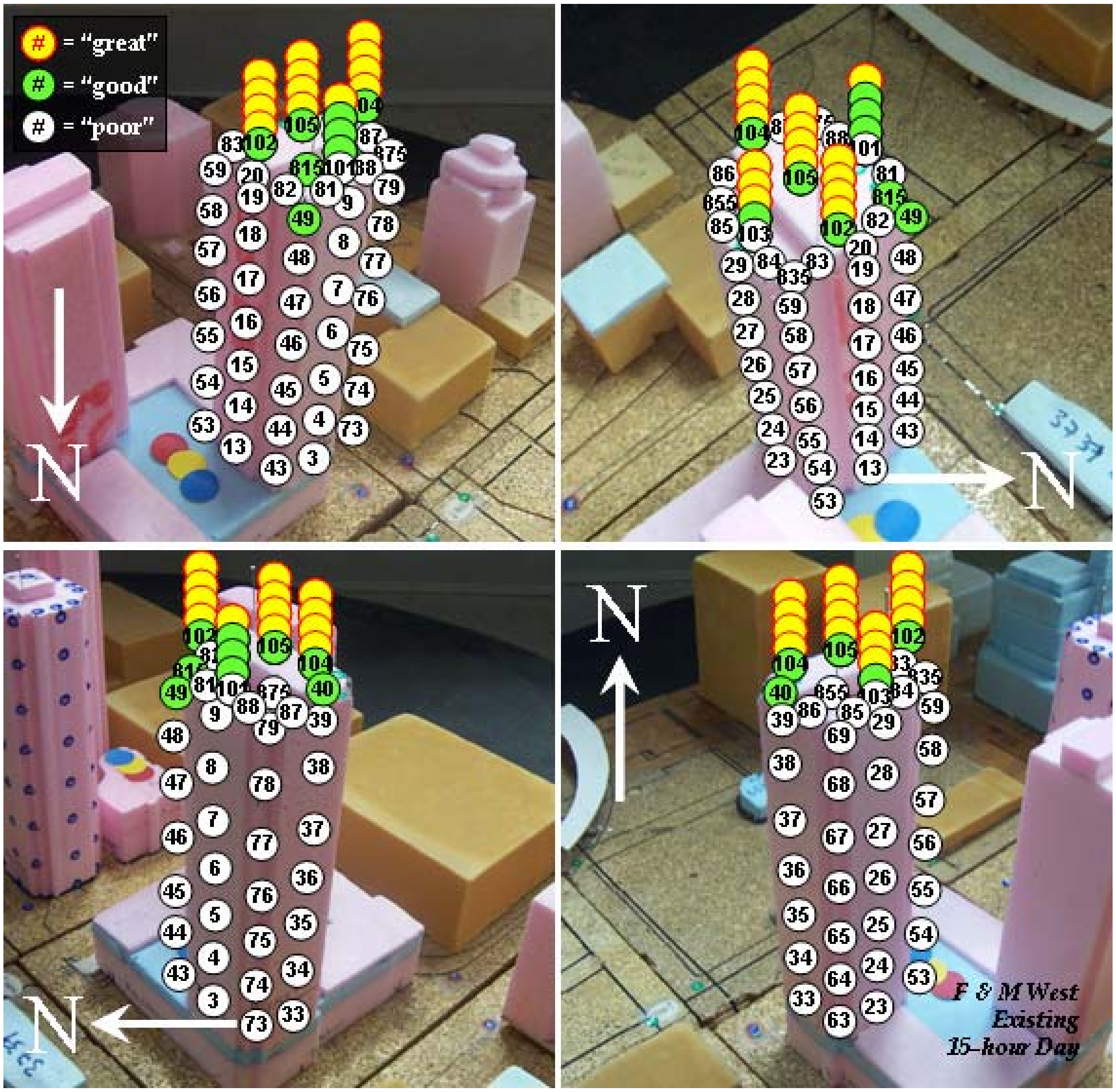

Figure 37. Graphical results for Folsom and Main West WECs running 15-hours per day for the existing setting.

4.0 Conclusions and Recommendations

It was shown through wind-tunnel testing that the highest average wind power densities typically occur at or above the roof level of buildings in an urban environment. In some cases, speed-up is evident over the roof of a building, where the maximum wind speed is greatest closer to the roof than the higher measurement locations, within the measured space above roof level. Sites located near 10th Street and Market Street averaged much higher average wind power densities than the sites located near Folsom Street and Main Street, which are near the Bay, demonstrating site-specific wind characteristics.

One potential advantage of using urban WECs is that they could be designed to run in a turbulent environment without the major losses in efficiency and safety that a traditional WEC, such as a horizontal axis wind turbine, may suffer in such an environment. Knowledge of wind characteristics in an urban environment is necessary to be able to design an effective WEC for urban use. Wind-tunnel testing is an effective way to gather information on the characteristics of wind in an urban environment.

Furthermore, it is unclear how the criteria for “great”, “good” and “poor” annual average wind power densities given by Manwell (2003) were determined, though it is assumed these qualitative evaluations are based on the analysis of a typical horizontal or vertical axis wind turbine since most of the work presented in the source regards these types of wind turbines. It may be the case that these criteria are based on some cost-benefit analyses which may be applicable to only horizontal or vertical axis wind turbines, making further assessment of future WECs necessary. The results presented would still be valid in this case since the qualitative analysis has no bearing on the actual data reduction and the trends would still be the same given different criteria.

Wind-tunnel testing can be used to acquire wind information based to various wind directions and changes in the cityscape (which may affect near-surface wind characteristics of a building where WECs are located), and can simulate annual wind conditions relatively simply and quickly. Wind-tunnel testing was found to be an effective means for determining wind characteristics over the near surface of buildings in an urban environment. While a few general trends were found, it was also shown that each building had its own wind characteristics, leading to the conclusion that testing of specific sites should be recommended if it is desired to incorporate WECs into a building's design.

4.1 Recommendations

In order to gain a more general understanding of wind over the surface of a building in an urban environment, it is recommended that more buildings be wind-tunnel tested to get a better sampling of possible wind conditions. With enough information, it may be possible to find ways to better generalize the wind characteristics of certain types of cityscapes and building configurations. Other urban areas, besides San Francisco, may also be studied in the wind tunnel to further expand knowledge of wind patterns in an urban environment.

The variation of wind characteristics in different locations in the city of San Francisco leads to the recommendation that developers interested in incorporating WECs into a building's design should perform a wind power analysis, such as the ones conducted in this study, on the specific building being developed.

Urban environments have the potential to provide a suitable wind energy resource, provided that turbulence effects, if proven to be a problem with current of future designed WECs, can be mitigated. A closer look into how turbulence can affect urban WECs is advised.

One way to improve the data obtained from wind-tunnel testing in the future is to implement the use of a three-dimensional probe. The current setup employed a single hotwire which only captures components of the wind in a plane perpendicular to the wire. Wind-tunnel testing with a three-dimensional probe takes a serious investment in time and money due to the complexity of calibrating and operating the probe. It is recommended that a cost-benefit analysis be performed before testing with a three-dimensional probe is more seriously considered. Testing may also be conducted utilizing tufts to gain a qualitative understanding of the general direction of the flow over the near surfaces of buildings in urban environments, since many WECs are highly dependent on the direction of the wind.

5.0 References

Aerotecture International, Inc. http://www.aerotecture.com. Accessed July 9, 2006.

AeroVironment Inc. "Architectural Wind". Brochure, 2005.

Arens E., D. Ballanti, C. Bennett, S. Guldman and B. White. "Developing the San Francisco Wind Ordinance and its Guidelines of Compliance". Building and Environment, 24 (4), 297-303, 1989.

Coquilla, R., B. Kuspa, J. Phoreman, B. White. "Air-Quality Evaluation of Stacks: Building No. 3 Chiron Corporation, Emeryville: A Wind-Tunnel Study". Laboratory Report. Davis, California, 2002.

Department of City Planning. City and County of San Francisco Municipal Code: *Planning Code Volume I*. Section 148, Ordinance 414-85, Approved September 17, 1985.

ESA: Environmental Science Associates, Brocure. San Francisco, California, 2006.

Gifford, F. A. Turbulent diffusion typing schemes: a review. *Nuclear Safety*, 17(1):71, 1976.

Grauthoff, Manfred. Utilization of Wind Energy in Urban Areas – Chance or Utopian Dream? Netherlands: Elsevier Sequoia, 1991.

"Industry News: New Turbine Stirs Interest". ASHRAE Journal, pg 8, June 2003.

Manwell, J. F., J. G. McGowan, A. L. Rogers. Wind Energy Explained: Theory, Design and Application. San Francisco: John Wiley & Sons Ltd, 2003.

Pasquill, F. "Effects of Buildings on the Local Wind". Phil. Trans. Roy. Soc. London, 439-456, 1971.

Snyder, William H., Guideline for Fluid Modeling of Atmospheric Diffusion, U.S. Environmantal Protection agency, Research Triangle Park, North Carolina, 1981.

Sutton,O.G. Atmospheric Turbulence, Methuen, London, 1949.

Tyler, Derek. Research Information: Using Buildings to Harvest Wind Energy. Buckinghamshire, UK: EBSCO Publishing, 2002.

Witcher, D., Garrad Hassan and Partners Ltd. *Seismic Analysis of Wind Turbines in the Time Domain*. Bristol, UK: John Wiley & Sons Ltd, 2004.

White, Bruce R. "Analysis and Wind-Tunnel Simulation of Pedestrian-Level Winds in San Francisco". Journal of Wind Engineering and Industrial Aerodynamics, 41-44 (1992) 2353-2364.

White, Bruce R. 2006 Private Communication.

6.0 APPENDIX A: THE ATMOSPHERIC BOUNDARY LAYER WIND TUNNEL AT UNIVERSITY OF CALIFORNIA, DAVIS

In the present investigation, the Atmospheric Boundary Layer Wind Tunnel (ABLWT) located at University of California, Davis was used (Figure A-1). Built in 1979 the wind tunnel was originally designed to simulate turbulent boundary layers comparable to wind flow near the surface of the earth. In order to achieve this effect, the tunnel requires a long flow-development section such that a mature boundary-layer flow is produced at the test section. The wind tunnel is an open-return type with an overall length of 21.3 m and is composed of five sections: the entrance, the flow-development section, the test section, the diffuser section, and the fan and motor.

The entrance section is elliptical in shape with a smooth contraction area that minimizes the free-stream turbulence of the incoming flow. Following the contraction area is a commercially available air filter that reduces large-scale pressure fluctuations of the flow and filters larger-size particles out of the incoming flow. Behind the filter, a honeycomb flow straightener is used to reduce large-scale turbulence.

The flow development section is 12.2 m long with an adjustable ceiling for longitudinal pressure-gradient control. For the present study, the ceiling was diverged ceiling so that a zero-pressure-gradient condition is formed in the stream wise direction. At the leading edge of the section immediately following the honeycomb flow straightener, four triangularly shaped spires are stationed on the wind tunnel floor to provide favorable turbulent characteristics in the boundary-layer flow. Roughness elements are then placed all over the floor of this section to artificially thicken the boundary layer. For a free-stream wind speed of 4.0 m/s, the wind tunnel boundary layer grows to a height of one meter at the test section. With a thick boundary layer, larger models could be tested and thus measurements could be made at higher resolution.

Dimensions of the test section are 2.44 m in stream wise length, 1.66 m high, and 1.18 m wide. Similar to the flow-development section, the test section ceiling can also be adjusted to obtain the desired stream wise pressure gradient. Experiments can be observed from both sides of the test section through framed Plexiglas windows. One of the windows is also a sliding door that allows access into the test section. When closed twelve clamps distributed over the top and lower edges are used to seal the door. Inside the test section, a three-dimensional probe-positioning system is installed at the ceiling to provide fast and accurate sensor placement. The traversing system scissor-type extensions, which provide vertical probe motion, are also made of aerodynamically shaped struts to minimize flow disturbances.

The diffuser section is 2.37 m long and has an expansion area that provides a continuous transition from the rectangular cross-section of the test section to the circular cross-sectional area of the fan. To eliminate upstream swirl effects from the fan and avoid flow separation in the diffuser section, fiberboard and honeycomb flow straighteners are placed between the fan and diffuser sections.

The fan consists of eight constant-pitch blades 1.83 m in diameter and is powered by a 56 kW (75 hp) variable-speed DC motor. A dual belt and pulley drive system is used to couple the motor and the fan.

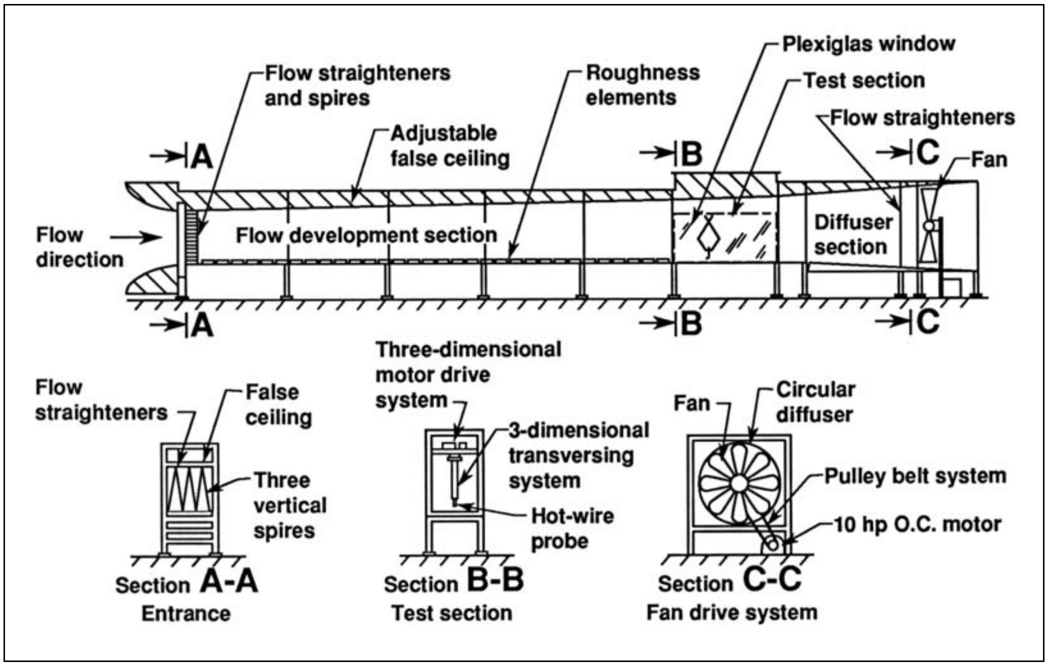

Figure A-1. Schematic diagram of the UC Davis Atmospheric Boundary Layer Wind Tunnel.

7.0 APPENDIX B: INSTRUMENTATION AND MEASUREMENT SYSTEMS

Wind tunnel measurements of the mean velocity and turbulence characteristics were performed using hot-wire anemometry. A standard Thermo Systems Inc. (TSI) single hot-wire sensor model 1210-60 was used to measure the wind quantities. The sensor was installed at the end of a TSI model 1150 50-cm probe support, which was secured onto the support plate of the three-dimensional sensor positioning system in the U.C. Davis Atmospheric Boundary Layer Wind Tunnel (ABLWT) test section. A 10-m shielded tri-axial cable was then used to connect the probe support and sensor arrangement to a TSI model IFA 100 constant temperature thermal-anemometry unit with signal conditioner.

Hot-wire sensor calibrations were conducted in the ABLWT test section over the range of common velocities measured in the wind tunnel boundary layer. Signal-conditioned voltage readings of the hot-wire sensor were then matched against the velocity measurements from a Pitot-static tube connected to a Meriam model 34FB2 oil micro-manometer, which had a resolution of 25.4 μm of oil level. The specific gravity of the oil was 0.934. The Pitot-static tube was secured to an aerodynamically shaped stand and was positioned so that its flow-sensing tip is normal to the flow and situated near the volumetric center of the test section. Normal to the flow, the end of the hot-wire sensor was then traversed to a position 10 cm next to the tip of the Pitot-static tube.

Raw voltage data sets of hot-wire velocity measurements were digitally collected using a LabVIEW data acquisition system, which was installed in a personal computer with a Pentium 166Mhz processor. Hot wire voltages were obtained from the signal conditioner output of the IFA 100 anemometer. The output was connected to a multi-channel daughter board linked to a United Electronics Inc. (UEI) analog-to-digital (A/D) data acquisition board, which is installed in one of the ISA motherboard slots of the PC. LabVIEW software was used to develop virtual instruments (VI) that would initiate and configure the A/D board, then collect the voltage data given by the measurement equipment, display appropriately converted results on the computer screen, and finally save the raw voltage data into a designated filename.

For the hot-wire acquisition, the converted velocity data and its histogram is displayed along with the mean voltages, mean velocity, root-mean-square velocity, and turbulence intensity, and data acquisition included 30,000 samples that were collected at a sampling rate of 1000 Hz. This acquisition setting greatly satisfies the Nyquist sampling theorem such that the average tunnel turbulence signal was 300 Hz.

8.0 APPENDIX C: WIND TUNNEL ATMOSPHERIC FLOW SIMILARITY PARAMETERS

Wind tunnel models of a particular test site are typically several orders of magnitude smaller than the full-scale size. In order to appropriately simulate atmospheric winds in the U.C. Davis Atmospheric Boundary Layer Wind Tunnel (ABLWT), certain flow parameters must be satisfied between a model and its corresponding full-scale equivalent. Similitude parameters can be obtained by non-dimensionalizing the equations of motion, which build the starting point for the similarity analysis. Fluid motion can be described by the following time-averaged equations.

Conservation of mass:

$$\frac{\partial \overline{U}_i}{\partial t_i} = 0 \text{ and } \frac{\partial \rho}{\partial t} + \frac{\partial (\rho \overline{U}_i)}{\partial x_i} = 0 \qquad \text{(C-1)}$$

Conservation of momentum:

$$\frac{\partial \overline{U}_i}{\partial t} + \overline{u}\,\frac{\partial \overline{U}_i}{\partial x_j} + 2\varepsilon_{ijk}\Omega_j \overline{U}_k = -\frac{1}{\rho_0}\frac{\partial \overline{\delta P}}{\partial x_i} - \frac{\overline{\delta T}}{T_0} g\delta_{i3} + \nu_0 \frac{\partial^2 \overline{U}_i}{\partial x_j} + \frac{\partial(\overline{-u_j u_i})}{\partial x_j} \qquad \text{(C-2)}$$

Conservation of energy:

$$\frac{\partial \overline{\delta T}}{\partial t} + \overline{U}_i \frac{\partial \overline{\delta T}}{\partial x_i} = \left[\frac{\kappa_0}{\rho_0 c_{p_0}}\right] \frac{\partial^2 \overline{\delta T}}{\partial x_k \partial x_k} + \frac{\partial(\overline{-\theta u_i})}{\partial x_i} + \frac{\overline{\phi}}{\rho_0 c_{p_0}} \qquad \text{(C-3)}$$

Here, the mean quantities are represented by capital letters while the fluctuating values by small letters. δP is the deviation of pressure in a neutral atmosphere. ρ_0 and T_0 are the density and temperature of a neutral atmosphere and ν_0 is the kinematic viscosity. In the equation for the conservation of energy, ϕ is the dissipation function, $\overline{\delta T}$ is the deviation of temperature from the temperature of a neutral atmosphere, κ_0 is the thermal diffusivity, and c_{p_o} is the heat capacity.

Applying the Boussinesq density approximation, application of the equations is then restricted to fluid flows where $\overline{\delta T} << T_0$. Defining the following non-dimensional quantities and then substituting into the above equations.

$$\overline{U}_i' = \overline{U}_i' \big/ U_0 \;;\; u_i' = u_i \big/ U_0 \;;\; x_i' = x_i \big/ L_0 \;;\; t' = tU_0 \big/ L_0 \;;\; \Omega_j' = \Omega_j \big/ \Omega_0 \;;\; \overline{\delta P}' = \overline{\delta P} \big/ \rho_0 U_0^2 \;;$$
$$\overline{\delta T}' = \overline{\delta T} \big/ \delta T_0 \;;\; g' = g \big/ g_0 \;;\; \overline{\varphi}' = \overline{\varphi} \big/ \varphi_0 \qquad \text{(C-4)}$$

The equations of motion can be presented in the following dimensionless forms.

Continuity Equation:

$$\frac{\partial u_i'}{\partial k_i'} = 0 \text{ and } \frac{\partial \rho'}{\partial t'} + \frac{\partial (\rho' u_i')}{\partial x_i'} = 0 \qquad \text{(C-5)}$$

Momentum Equation:

$$\frac{\partial \overline{U}'_i}{\partial t'} + \overline{U}'_j \frac{\partial \overline{U}'_i}{\partial x'_j} + \frac{2}{Ro} \varepsilon_{ijk} \overline{U}'_k \Omega'_j = -\frac{\partial \overline{\delta P}'}{\partial x'_i} + \frac{1}{Fr^2} \overline{\delta T}' \delta_{3i} + \frac{1}{Re} \frac{\partial^2 \overline{U_i}'}{\partial x'_j \partial x'_j} + \frac{\partial (-\overline{u'_j u'_i})}{\partial x'_j} \tag{C-6}$$

Turbulent Energy Equation:

$$\frac{\partial \overline{\delta T}'}{\partial t'} + \overline{U}'_i \frac{\partial \overline{\delta T}'}{\partial x'_i} = Pr \cdot \frac{1}{Re} \frac{\partial^2 \overline{\delta T}'}{\partial x'_k \partial x'_k} + \frac{\partial (-\overline{\theta' u'_i})}{\partial x'_i} + \frac{1}{Re} \cdot Ec \cdot \overline{\varphi}' \tag{C-7}$$

Although the continuity equation gives no similarity parameters, coefficients from both other equations do provide the following desired similarity parameters.

Rossby number: $R_0 \equiv {}^{U_0}\!/_{L_0 \Omega_0}$

Densimetric Froude number: $Fr \equiv {}^{U_0}\!/_{(g L_0 \delta T_0 / T_0)^{1/2}}$

Prandtl number: $Pr \equiv {}^{\rho_0 c_{p_0} \nu_0}\!/_{\kappa_0}$

Eckert number: $Ec \equiv {}^{U_0^2}\!/_{c_{p_0} \delta T_0}$

Reynolds number: $Re \equiv {}^{U_0 L_0}\!/_{\nu_0}$

In the dimensionless momentum equation, the Rossby number is extracted from the denominator of the third term on the left hand side. The Rossby number represents the ratio of advective acceleration to Coriolis acceleration due to the rotation of the earth.

If the Rossby number is large, Coriolis accelerations are small. Since UC Davis ABLWT is not rotating, the Rossby number is infinite allowing the corresponding term in the dimensionless momentum equation to approach zero. In nature, however, the rotation of the earth influences the upper layers of the atmosphere; thus, the Rossby number is small and becomes important to match, and the corresponding term in the momentum equation is sustained.

Most modelers have assumed the Rossby number to be large, thus, neglecting the respective term in the equations of motion and ignoring the Rossby number as a criterion for modeling. Snyder (1981) showed that the characteristic length scale, L_0, must be smaller than 5 km in order to simulate diffusion under neutral or stable conditions in relatively flat terrain. Other researchers discovered similar findings. Since UC Davis ABLWT produces a boundary layer with a height of about one meter, the surface layer vertically extends 10 to 15 cm above the ground. In this region the velocity spectrum would be accurately modeled. The Rossby number can then be ignored in this region. Since testing is limited to the lower 10% to 15% of the boundary layer, the length in longitudinal direction, which can be modeled, has to be no more than a few kilometers.

Derived from the denominator of the second term on the right hand side of the dimensionless momentum equation, the square of the Froude number represents the ratio of inertial forces to buoyancy forces. High values of the Froude number infer that the inertial forces are dominant. For values equal or less than unity, thermal effects become important. Since the conditions inside the UC Davis ABLWT are inherently isothermal, the wind tunnel generates a neutrally stable boundary layer; hence, the

Froude number is infinitely large allowing the respective term in the momentum equation to approach zero.

The third parameter is the Prandtl number, which is automatically matched between the wind tunnel flow and full-scale winds if the same fluid is been used. The Eckert number criterion is important only in compressible flow, which is not of interest for a low-speed wind tunnel.

Reynolds number represents the ratio of inertial to viscous forces. The reduced scale of a wind tunnel model results in a Reynolds number several orders of magnitude smaller than in full-scale. Thus, viscous forces are more dominant in the model than in nature. No atmospheric flow could be modeled, if strict adherence to the Reynolds number criterion was required. However, several arguments have been made to justify the use of a smaller Reynolds number in a model. These arguments include laminar flow analogy, Reynolds number independence, and dissipation scaling. With the absence of thermal and Coriolis effects, several test results have shown that the scaled model flow will be dynamically similar to the full-scale case if a critical Reynolds number is larger than a minimum independence value. The gross structure of turbulence is similar over a wide range of Reynolds numbers. Nearly all modelers use this approach today.

9.0 APPENDIX D: WIND TUNNEL ATMOSPHERIC BOUNDARY-LAYER SIMILARITY

Wind tunnel simulation of the atmospheric boundary layer under neutrally stable conditions must also meet non-dimensional boundary-layer similarity parameters between the scaled-model flow and its full-scale counterpart. The most important conditions are:

- The normalized mean velocity, turbulence intensity, and turbulent energy profiles.
- The roughness Reynolds number, $\mathrm{Re}_z = z_0 u_* / \nu$.
- Jensen’s length-scale criterion of z_0/H.
- The ratio of H/δ for H greater than H/δ > 0.2.

In the turbulent core of a neutrally stable atmospheric boundary layer, the relationship between the local flow velocity, U, versus its corresponding height, H, may be represented by the following velocity-profile equation.

$$\frac{U}{U_\infty} = \left(\frac{H}{\delta}\right)^{\alpha} \tag{D-1}$$

Here, U_∞ is the mean velocity of the inviscid flow above the boundary layer, δ is the height of the boundary layer, and α is the power-law exponent, which represents the upwind surface conditions. Wind tunnel flow can be shaped such that the exponent α will closely match its corresponding full-scale value, which can be determined from field measurements of the local winds. The required power-law exponent, α, can then be obtained by choosing the appropriate type and distribution of roughness elements over the wind tunnel flow-development section.

Full-scale wind data suggest that the atmospheric wind profile at the sites analyzed in San Francisco yields a nominal value of $\alpha = 0.3$. This condition was closely matched in the UC Davis Atmospheric Boundary Layer Wind Tunnel by systematically arranging an pattern of 2″ x 4″ wooden blocks of 12″ in length along the entire surface of the flow-development section. The pattern generally consisted of alternating sets of four and five blocks in one row. A typical velocity profile is presented in Figure D-1, where the simulated power-law exponent is $\alpha = 0.33$.

In the lower 20% of the boundary layer height, the flow is then governed by a rough-wall or "law-of-the-wall" logarithmic velocity profile.

$$\frac{U}{u_*} = \frac{1}{\kappa} \ln\left(\frac{z}{z_o}\right) \tag{D-2}$$

Here, u_* is the surface friction velocity, κ is von Karman's constant, and z_o is the roughness height. This region of the atmospheric boundary layer is relatively unaffected by the Coriolis force, the only region that can be modeled accurately by the wind tunnel (i.e., the lowest 100 m of the atmospheric boundary layer under neutral stability conditions). Thus, it is desirable to have the scaled-model buildings and its surroundings contained within this layer.

The geometric scale of the model should be determined by the size of the wind tunnel, the roughness height, z_o, and the power-law index, α. With a boundary-layer height of 1 m in the test section, the surface layer would be 0.2 m deep for the U.C. Davis ABLWT. For the current study, this boundary layer corresponds to a full-scale height of the order of 800 m (0.2mWT=120mFS?). Fortunately, due to the tall buildings' obstruction of the Ekman spiral, it is possible to obtain good data for a measurement height above 20 centimeters.

Due to scaling effects, full-scale agreement of simulated boundary-layer profiles can only be attained in wind tunnels with long flow-development sections. For full-scale matching of the normalized mean velocity profile, an upwind fetch of approximately 10 to 25 boundary-layer heights can be easily constructed. To fully simulate the normalized turbulence intensity and energy spectra profiles, the flow-development section needs to be extended to about 50 and 100 to 500 times the boundary-layer height, respectively. These profiles must at least meet full-scale similarities in the surface layer region. However, with the addition of spires and other flow tripping devices, the flow development length can be reduced to less than 20 boundary layer heights for most engineering applications.

In the U.C. Davis Atmospheric Boundary Layer Wind Tunnel, the maximum values of turbulence intensity near the surface range from 35% to 40%, similar to that in full-scale. Thus, the turbulent intensity profile, u' / u versus z, should agree reasonably with the full-scale, particularly in the region where testing is performed. Figure D-2 displays a typical turbulence intensity profile of the boundary layer in the ABLWT test section.

The second boundary-layer condition involves the roughness Reynolds number, Re_z. According to the criterion given by Sutton (1949), Reynolds number independence is attained when the roughness Reynolds number is defined as follows.

$$Re_z = \frac{u_* z_0}{\nu} \geq 2.5 \qquad \text{(D-3)}$$

Here, u_* is the friction speed, z_0 is the surface roughness length and ν is the kinematic viscosity. Re_z larger than 2.5 ensures that the flow is aerodynamically rough. Therefore, wind tunnels with a high enough roughness Reynolds numbers simulate full-scale aerodynamically rough flows exactly. To generate a rough surface in the wind tunnel, roughness elements are placed on the wind tunnel floor. The height of the elements must be larger than the height of the viscous sub-layer in order to trip the flow. The UC Davis ABLWT satisfies this condition, since the roughness Reynolds number is about 40, when the wind tunnel free stream velocity, U_∞, is equal 3.8 m/s, the friction speed, u_*, is 0.24 m/s, and the roughness height, z_o, is 0.0025 m. Thus, the flow setting satisfies the Re number independence criterion and dynamically simulates the flow.

To simulate the pressure distribution on objects in the atmospheric wind, Jensen (1958) found that the surface roughness to object-height ratio in the wind tunnel must be equal to that of the atmospheric boundary layer, i.e., z_o/H in the wind tunnel must match the full-scale value. Thus, the geometric scaling should be accurately modeled.

The last condition for the boundary layer is the characteristic scale height to boundary layer ratio, H/δ. There are two possibilities for the value of the ratio. If $H/\delta \geq 0.2$, then the ratios must be matched. If $(H/\delta)_{F.S.} < 0.2$, then only the general inequality of $(H/\delta)_{W.T.} < 0.2$ must be met (F.S. stands for full-scale and W.T. stands for wind tunnel). Using the law-of-the-wall logarithmic profile equation, instead of the power-law velocity profile, this principle would constrain the physical model to the 10% to 15% of the wind tunnel boundary layer height.

Along with these conditions, two other constraints have to be met. First, the mean stream wise pressure gradient in the wind tunnel must be zero. Even if high- and low-pressure systems drive atmospheric boundary layer flows, the magnitude of the pressure gradient in the flow direction is negligible compared to the dynamic pressure variation caused by the boundary layer. The other constraint is that the model should not take up more than 5% to 15% of the cross-sectional area at any down wind location. This assures that local flow acceleration affecting the stream wise pressure gradient will not distort the simulation flow.

Simulations in the U.C. Davis ABLWT were not capable of producing stable or unstable boundary layer flows. In fact, proper simulation of unstable boundary layer flows could be a disadvantage in any wind tunnel due to the artificial secondary flows generated by the heating that dominate and distort the longitudinal mean-flow properties, thus, invalidating the similitude criteria. However, this is not considered as a major constraint, since the winds that produce annual an average dispersion are sufficiently strong, such that for flow over a complex terrain, the primary source of turbulence is due to mechanical shear and not due to diurnal or heating and cooling effects in the atmosphere.

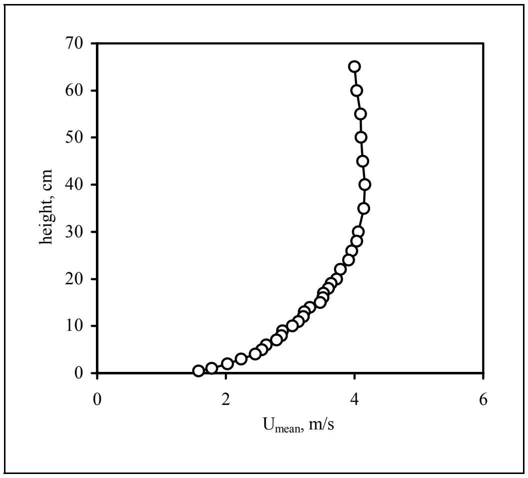

Figure D-1: Mean velocity profile for a typical wind direction in the wind tunnel. The power law exponent α is 0.33. The reference velocity at 65 cm height is 3.55 m/s.

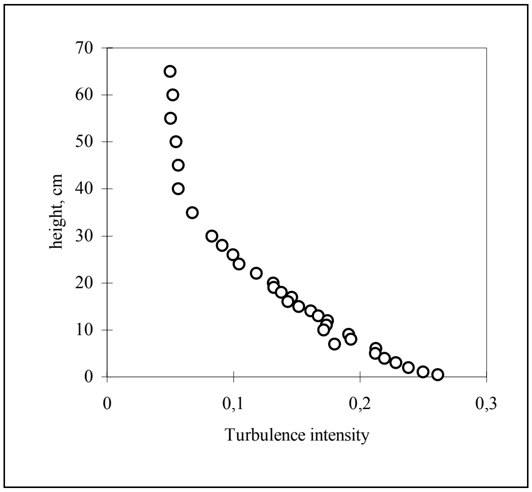

Figure D-2: Turbulence intensity profile for a typical wind direction in the wind tunnel.